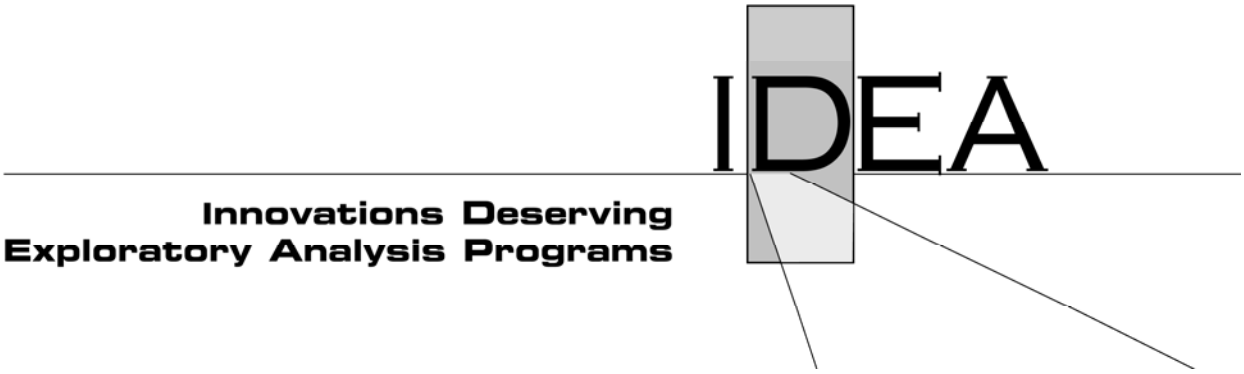

Highway IDEA Program

Geocomposite Capillary Barrier Drain for Limiting Moisture Changes in Pavements: Product Application

Final Report for Highway IDEA Project 113

Prepared by:
John Stormont, R. Eric Pease, University of New Mexico;
Karen Henry, United States Air Force Academy; and
Lynette Barna and Deb Solano, US Army Cold Regions and Research Engineering Laboratory.

April 2009

TRANSPORTATION RESEARCH BOARD
OF THE NATIONAL ACADEMIES

INNOVATIONS DESERVING EXPLORATORY ANALYSIS (IDEA) PROGRAMS
MANAGED BY THE TRANSPORTATION RESEARCH BOARD (TRB)

This NCHRP-IDEA investigation was completed as part of the National Cooperative Highway Research Program (NCHRP). The NCHRP-IDEA program is one of the four IDEA programs managed by the Transportation Research Board (TRB) to foster innovations in highway and intermodal surface transportation systems. The other three IDEA program areas are Transit-IDEA, which focuses on products and results for transit practice, in support of the Transit Cooperative Research Program (TCRP), Safety-IDEA, which focuses on motor carrier safety practice, in support of the Federal Motor Carrier Safety Administration and Federal Railroad Administration, and High Speed Rail-IDEA (HSR), which focuses on products and results for high speed rail practice, in support of the Federal Railroad Administration. The four IDEA program areas are integrated to promote the development and testing of nontraditional and innovative concepts, methods, and technologies for surface transportation systems.

For information on the IDEA Program contact IDEA Program, Transportation Research Board, 500 5th Street, N.W., Washington, D.C. 20001 (phone: 202/334-1461, fax: 202/334-3471, http://www.nationalacademies.org/trb/idea)

Final Report

Contract No. NCHRP-113

"Geocomposite Capillary Barrier Drain for Limiting Moisture Changes in Pavements: Product Application"

March 13, 2009

submitted to:

National Academy of Sciences

IDEA Program

Inam Jawed, Program Officer

submitted by:

John Stormont, R. Eric Pease

Department of Civil Engineering

University of New Mexico

Karen Henry

United States Air Force Academy

Lynette Barna and Deb Solano

US Army Cold Regions and Research Engineering Laboratory.

Executive Summary

The overall purpose of this project is to facilitate the transfer of the GCBD technology to engineering practice through demonstration and documentation of GCBD fabrication, field installation and performance, and the development of the capability to incorporate the GCBD in subsequent designs. The project is organized into three stages. Each successive stage is built upon the product of the previous stage. The first stage involves selecting materials for the GCBD field test, developing a method to terminate the GCBD in an edgedrain trench, and provide specifications and details for field installation. The second stage involves construction and installation of the field test at MnDOT's test facility, including installing numerous measurement systems to quantify the GCBD performance. A parallel effort of this project is to contact geosynthetics and other manufacturers to advise them of the possibility of licensing this technology for commercial applications. The third phase of the project is to develop design guidance for the use of the GCBD.

The transport layer is the key element of the GCBD, and a material referred to as TGLASS was selected as the best available transport layer material. This material was used in the MnROAD field test. There has been discussion with a geosynthetic manufacturer regarding the production of a lower cost transport layer. A method to connect the GCBD to the edgedrain pipe system was developed in the laboratory and used in the MnROAD demonstration. Details and specifications regarding the field installation of the GCBD system were developed and implemented at MnROAD.

Construction of the field test took place between June 19, 2006 and August 16, 2006. Activities included removal of existing pavement, preparing the subgrade, installation of the GCBD, placement of base course, and paving. In addition, measurement systems were installaed to monitor water content, suction, temperature, electrical conductivity, water table depth and drainage. The water content data indicate that the base course layer in the pavement section with the GCBD is substantially drier than the base course in the control section. The GCBD appears to be limiting upward flow from the subgrade into the base course. FWD data suggest the base course in the pavement section with the GCBD has a greater modulus than the base course in the control section.

Design calculations reveal the benefit of the GCBD in terms of reducing the saturation of the base course and the subgrade for a wide range of base course and subgrade materials. The calculations indicate that although the GCBD performance is a function of the climate, a GCBD has benefits in terms of lower saturations in all climates.

The laboratory testing, field measurements and design calculations conducted during this project indicate that the GCBD provides specific benefits, including:

- Reduced equilibrium water content in base course
- Positive pressures are prevented in base course
- Wetting of underlying subgrade due to infiltration is greatly reduced
- Capillary rise of water from subgrade into base is prevented

Table of Contents

1. Introduction

1.1 IDEA Concept and Product

Conventional drainage is designed for saturated flow, even though the positive pore water pressures required for saturated flow reduce strength and lead to rutting, heaving, and failure of pavement systems.The new invention, the Geocomposite Capillary Barrier Drain (GCBD) provides drainage while the soil is unsaturated--it is a method to suck water out of soil. When placed between a base and subgrade, it can drain the unsaturated base and reduce its water content as well as prevent water from reaching the subgrade. The work described in this report shows that the base course layer above a GCBD remains drier than the base course layer in an identical test cell that does not contain one.

The geocomposite capillary barrier drain (GCBD) comprises three layers that are, from top to bottom: a *transport layer* (a specially designed geotextile), a *capillary barrier* (a geonet), and a *separator* (geotextile). The principal function of the GCBD is illustrated in Figure 1.1. Water infiltrating through the base is enters the transport layer, but the capillary barrier formed by the geonet prevents it from entering the underlying subgrade.. As it becomes wetting, the transport layer (a special geotextile) becomes increasingly hydraulically conductive. If the GCBD is placed to dip from horizontal, water flows along the slope in the transport layer. If the transport layer does not become saturated, no breaks through into the capillary barrier. The bottom separator geotextile protects the geonet from becoming filled with subgrade soil. The GCBD also cuts off capillary rise of water in the underlying soil, and if the overlying base and transport layer become saturated due to an extraordinary infiltration event, it provides saturated drainage in the geonet. The GCBD can be configured so that the transport layer (and geonet) can deliver water to a drain pipe for proper drainage.

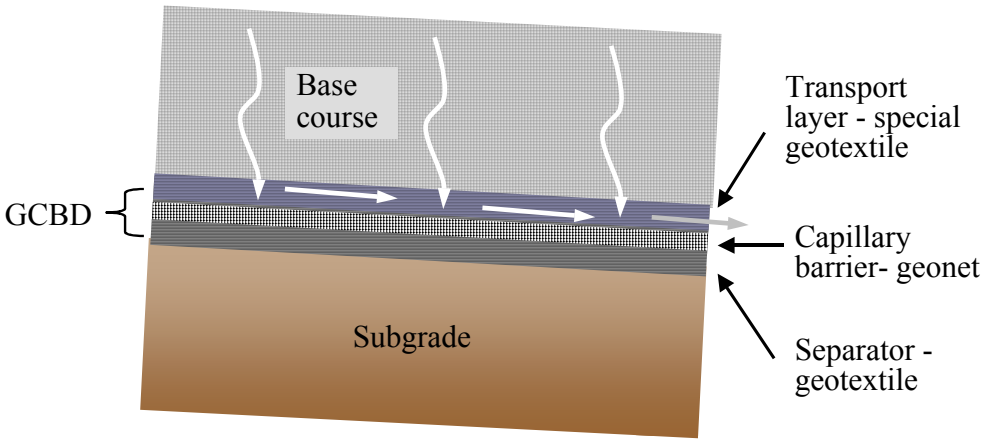

Figure 1.1 – GCBD between base course and subgrade illustrating how water laterally drains in transport layer.

1.2 Economic value of the GCBD

The GCBD is intended to provide improved drainage of pavement sections. Depending on the particular application, it is expected to result in lower water contents in the base course and/or the subgrade. The value of the GCBD, then, depends on the extent that the lower water contents result in a longer service life or permit a less expensive design compared to a design without a GCBD.

The benefit of any drainage (not just the GCBD approach) to pavement life has been difficult to quantify, and is presently the subject of ongoing investigation in the pavement design community. Of the few long-term field studies of the impact of drainage, most have yielded inconclusive results. In a conceptual sense it is well-known that lower water contents result in greater strength and higher modulus of pavement layer materials; however, the precise impact of moisture on the strength and modulus of pavement layers is not easy to measure, and can only be estimated for most materials. Further, the amount of moisture in a pavement section with or without a particular drainage design is very difficult to accurately measure or predict, especially over the decade-long design life of pavements. Because environmental conditions (amount and timing of precipitation) are different at every location, the amount water contents are lowered from a drainage scheme will be location dependent.

The other side of the value equation is cost. The cost of the prototype GCBD discussed in this report is on the order of $\$20/m^2$. Whether this cost is economically viable depends on the value of the improved drainage that is achieved.

The prototype GCBD is approximately 4 times more costly than the cost of a conventional geocomposite drainage product. Even though there are advantages in terms of improved drainage compared to a conventional geocomposite drainage layer, the cost difference is substantial and represents an impediment to implementation of the technology. The increased cost of the GCBD compared to a conventional geocomposite is a consequence of the cost of the transport layer – this material is a specialty insulation product and not produced on a scale comparable to most geosynthetics. Discussions with the manufacturer suggest that some cost reduction would be possible if large quantities were produced, although it is not likely that the cost would be lowered to approach that of a conventional geocomposite. Consequently, there has been and continues to be an ongoing effort to identify alternative materials and manufacturers for a less expensive transport layer.

1.3 Organization of report

Following an Introduction, data from the MnROAD demonstration project is given in Chapter 2. These data include water content data, tipping bucket data and falling weight deflectometer results. In Chapter 3, calculations are presented that show the expected performance of pavement sections with and without the GCBD. Calculations are performed for infiltration through the pavement surface as well as upward and lateral flow. These calculations utilize various base courses, subgrades, and climates. Chapter 4 includes Conclusions and Recommendations for further advancement of the GCBD technology.

The first two reports produced from this effort, from Stage 1 and Stage 2, provide additional information and details regarding the properties of the GCBD, laboratory test performance, and field construction details and specifications. These reports are included as appendices.

2. MnROAD demonstration

2.1 Summary of field demonstration

Pavement test sections were constructed between June 19, 2006 and August 16, 2006. Complete details of the test construction are in the construction report prepared by MnROAD personnel, and is included as part of Appendix 2. A principal objective of the project was accomplished with this installation; namely, to demonstrate that a full-size GCBD can be installed and tied into a drainage collection system.

There were two MnROAD cells that were constructed in this project (Figure 2.1): one with a GCBD system (cell 27) and one without (the control, cell 28). The design and construction of these cells were identical except for the presence of the GCBD and edge drains in cell 27. Sub-surface instrumentation was placed in the base course and subgrade to monitor water content, suction, and temperature. Tipping buckets were installed to measure water flow from the edge of the drains in cell 27, and pressure transducers were installed to measure groundwater level. These sensors are grouped together in vertical arrays (Figure 2.2). The locations of the arrays were selected using a random block design to account for the spatial variability within the test and control sections.

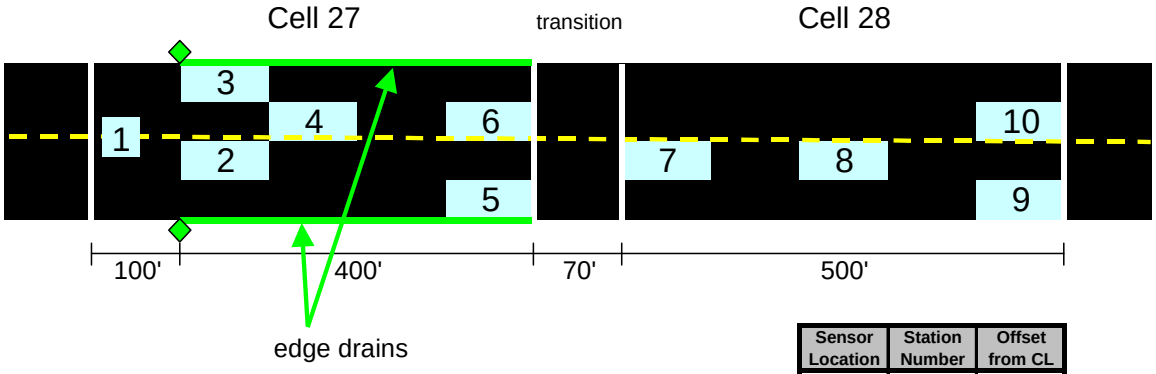

Sensor Location	Station Number	Offset from CL
1	175+70	0"
2	176+80	3.25'
3	176+80	-9.27'
4	177+80	-3.25'
5	179+80	9.75'
6	179+80	-3.25'
7	181+50	3.25'
8	183+50	3.25'
9	185+50	9.75'
10	185+50	-3.25'

Figure 2.1 – Plan view of MnROAD test cells and station locations.

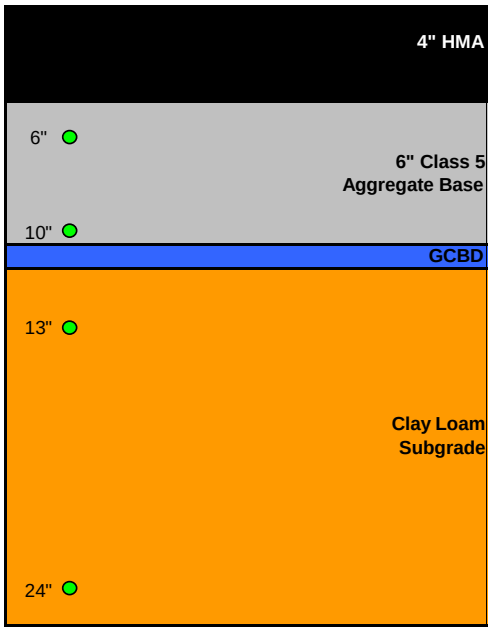

Figure 2.2 – Cross-section showing instrumentation depth in typical vertical section through cell 27.

Data were produced two ways in the field test: periodic, discrete measurements and sensors connected to data loggers. Falling weight deflectometer measurements, crack surveys, and frost heave surveys were to be done periodically. Crack surveys have not revealed any cracks (except in a small section of cell 28 that failed). Frost heave measurements indicate very little heave (Appendix 3).

2.2 Data from field test

Temperature, water content, suction and drainage sensors were monitored with data loggers. These data are then downloaded from the data loggers and imported into a database. There were numerous issues with these data. First, the pressure transducers to measure the groundwater level did not survive construction. Consequently, there are no groundwater level data. The ECHO water content probes used a factory-supplied calibration, and a large portion of the results had to be discounted because they did not make physical sense. The data produced from the heat dissipation sensors were difficult to interpret; it is believed that the calibration procedure for these measurements yielded non-representative calibration curves. The tipping buckets were hand-made units constructed by MnROAD personnel, and the calibration that relates number of tips to quantity of flow is considered only approximate. The time-domain reflectometers (TDRs)

produced the most consistent, reliable and robust field data, and thus data presented here focuses principally on the TDR water content values.

2.2.1 Calibration of TDRs

The TDRs (model CS 616 manufactured by Campbell Scientific, Inc., Logan, Utah) output a measured period in microseconds (μs). To relate the period to the water content, Campbell Scientific provides linear and quadratic equations of the form:

$\theta_v = C_0 + C_1 \cdot P$
and $\theta_v = C_0 + C_1 \cdot P_1 + C_2 \cdot P^2$
where: θ_v = volumetric moisture content
C_0, C_1, C_2 = coefficients
P = period (μs)

Campbell Scientific provides fitting coefficients for a limited number of soils of different density and electrical conductivity at saturation.

Previous analyses of some the data from both the base course and subgrade from cells 27 and 28 (Roberson, 2007) used the quadratic calibration equation and coefficients for a sandy clay loam supplied by Campbell Scientific. These coefficients are not applicable to the soils in cell 27 and 28 because (1) the dry density of subgrade and base course soils were approximately 1.75 and 1.88 g/cm^3, respectively, well in excess of that of the calibration soil; and (2) the calibration soil type was different than the silty clay subgrade and the granular base materials.

Alternative calibration coefficients for the quadratic calibration equation was developed using limited field water content measurements. MnROADS personnel advanced two boreholes, one through cell 27 and one through cell 28, on October 3, 2007. The boreholes were advanced adjacent to sensor profiles 3 and 8, respectively. Soil samples were extracted at depths of approximately 5, 10, 13, and 20 inches (12.7, 25.4, 33.02, 50.8 cm) from top of pavement, from each borehole, and tested for gravimetric moisture content. Table 2.1 summarizes the results.

Table 2.1. Summary of field extracted moisture contents.

Sample ID	Cell/Profile	Depth (inches)	Material	Gravimetric Moisture
CL 5 #1	27/3	5	class 5 base course	3.2
CL 5 #2	27/3	10	class 5 base course	3.7
CL 5 #3	28/8	5	class 5 base course	4.1
CL 5 #4	28/8	10	class 5 base course	3.2
CB #1	27/3	13	compacted borrow	13.7
CB #2	28/8	13	compacted borrow	14.6
SG #1	27/3	20	subgrade	14.4
SG #2	28/8	20	subgrade	11.3

Roberson (2007) reported average dry density values for the MnROADS class 5 base course and subgrade materials as 1.88 and 1.79 g/cm^3, respectively. The average value of all dry density values reported for the subgrade of cells 27 and 28 in a MnROADS geotechnical profile report yielded values of 1.76 and 1.74 g/cm^3, respectively.

Using the dry density values reported by Roberson, the gravimetric moisture contents reported in table were converted to volumetric moisture contents, using the formula:

$\theta_v = w \cdot (\rho_{soil}/\rho_{water})$

where: θ_v = volumetric moisture content
w = gravimetric moisture content
ρ_{soil} = dry density* of the soil (gf/cm^3)
ρ_{water} = density of water (gf/cm^3)

Volumetric moisture contents are reported in Table 2.2.

Table 2.2. Summary of field extracted moisture contents.

Sample ID	Cell/Profile	Depth (inches)	Material	Volumetric Moisture
CL 5 #1	27/3	5	class 5 base course	0.06016
CL 5 #2	27/3	10	class 5 base course	0.06956
CL 5 #3	28/8	5	class 5 base course	0.07708
CL 5 #4	28/8	10	class 5 base course	0.06016
CB #1	27/3	13	compacted borrow	0.24523
CB #2	28/8	13	compacted borrow	0.26134
SG #1	27/3	20	subgrade	0.25776
SG #2	28/8	20	subgrade	0.20227

Three points were needed for each quadratic curve developed. The lowest period of the sensors was estimated at 14 μs, which is the minimum reading as supplied by the manufacturer. This period was correlated to a volumetric moisture content of zero. A period value of 40 μs, the maximum value according to the manufacturer, was correlated to the saturated volumetric moisture content of the soils; which was 0.36 and 0.29 for the subgrade and base course soils, respectively. The third point was a correlation between the moisture content reported for the seven field samples, and the TDR period value measurement from the same day that the field samples were collected. The best fit of a quadratic equation to these data yielded the following coefficients: $C_0 = 0.00051$, C_1=-0.014, and C_2=0.0956 for the subgrade and C_0=0.00012, C_1=0.0045, and C_2=-0.085 for the base course. Figure 2.3 and 2.4 illustrate the final calibration functions for the subgrade and base course materials.

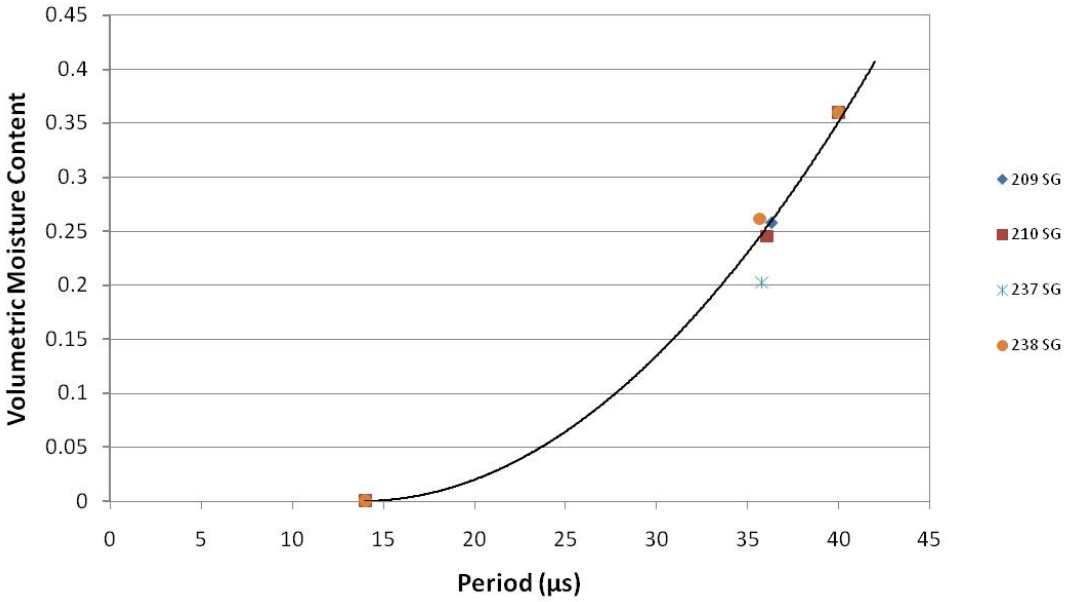

Figure 2.3. Calibration of subgrade (SG) TDR sensors. Solid line is calibration curve. Discrete points are data from different sensors.

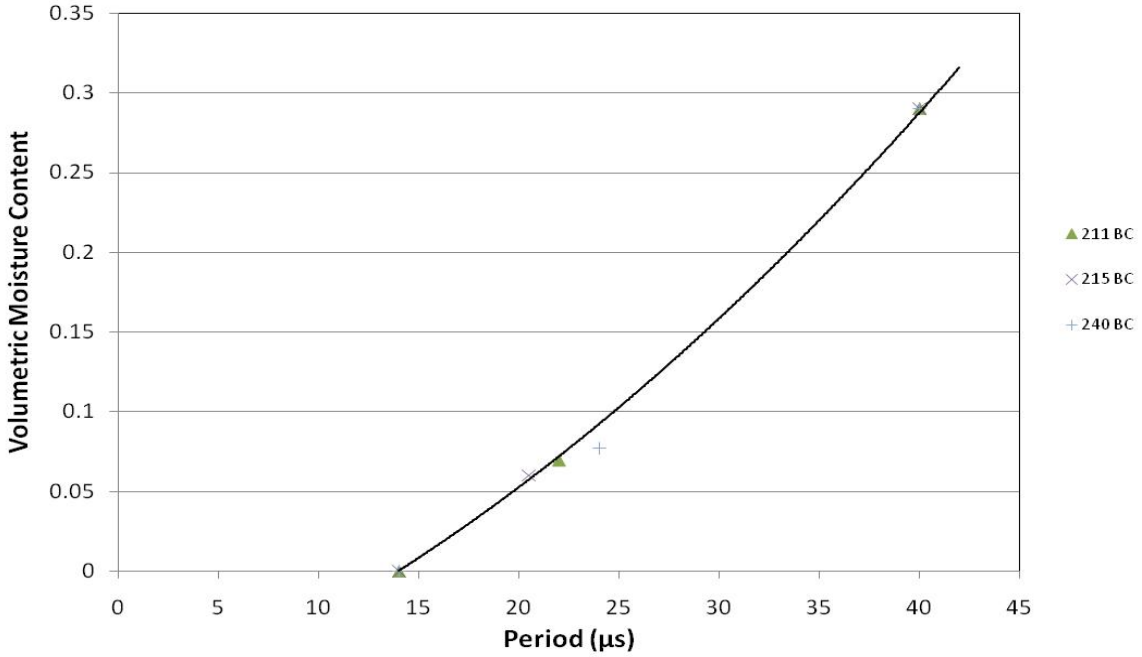

Figure 2.4. Calibration of base course (BC) TDR sensors. Solid line is calibration curve. Discrete points are data from different sensors.

Campbell Scientific provides the following equation to apply a correction for temperatre:

$T_{corrected}(T_{soil}) = \tau_{uncorrected} + (20\text{-}T_{soil})\cdot(0.526 - 0.052 \cdot \tau_{uncorrected} + 0.00136 \cdot \tau_{uncorrected}^2)$

where: $T_{corrected}$ = period reading corrected for temperature (μs)

$T_{uncorrected}$ = uncorrected period value (μs)

T_{soil} = temperature of the soil (·C)

The temperature corrections were applied to the measured sensor values, but the effects were negligible.

2.2.2 Water content data

Water content data from the TDR probes are shown in Figure 2.5 and 2.6 for measurements made in the base course, and Figures 2.7 and 2.8 for measurements in the subgrade. All of the measurements at a single depth are given in each figure. The legend indicates the cell (27 or 28) the measurement was made.

The results are provided over a 28-month period, and include two winter seasons. During the winter (approximately November to March – refer to Figures 2.21 and 2.22 for temperature data that indicates when base course and subgrade temperatures increased above 0º C during 2007), the soil freezes and the TDR data is not a measure of "free" water content in the soils.

Data from the non-frozen portion of the year reveal a remarkably consistent result: the water contents in base course of cell 27 with the GCBD are always lower than that in cell 28. (Note that the bright red line, RE 27 204 represents a sensor in the transition portion of cell 27 where there is no GCBD present.) Further, the pattern is the same for every sensor in the base course of cell 28: water contents rise during the spring, reach a peak value during the summer and then decline. In contrast, a different response is observed in the base course of cell 27: after the spring thaw, the water contents decrease, reaching a minimum in the summer, and then gradually increase in the fall.

The subgrade water contents rise in the spring, peak, in the summer, and decline in the fall. The values are not substantially different for cell 27 and 28.

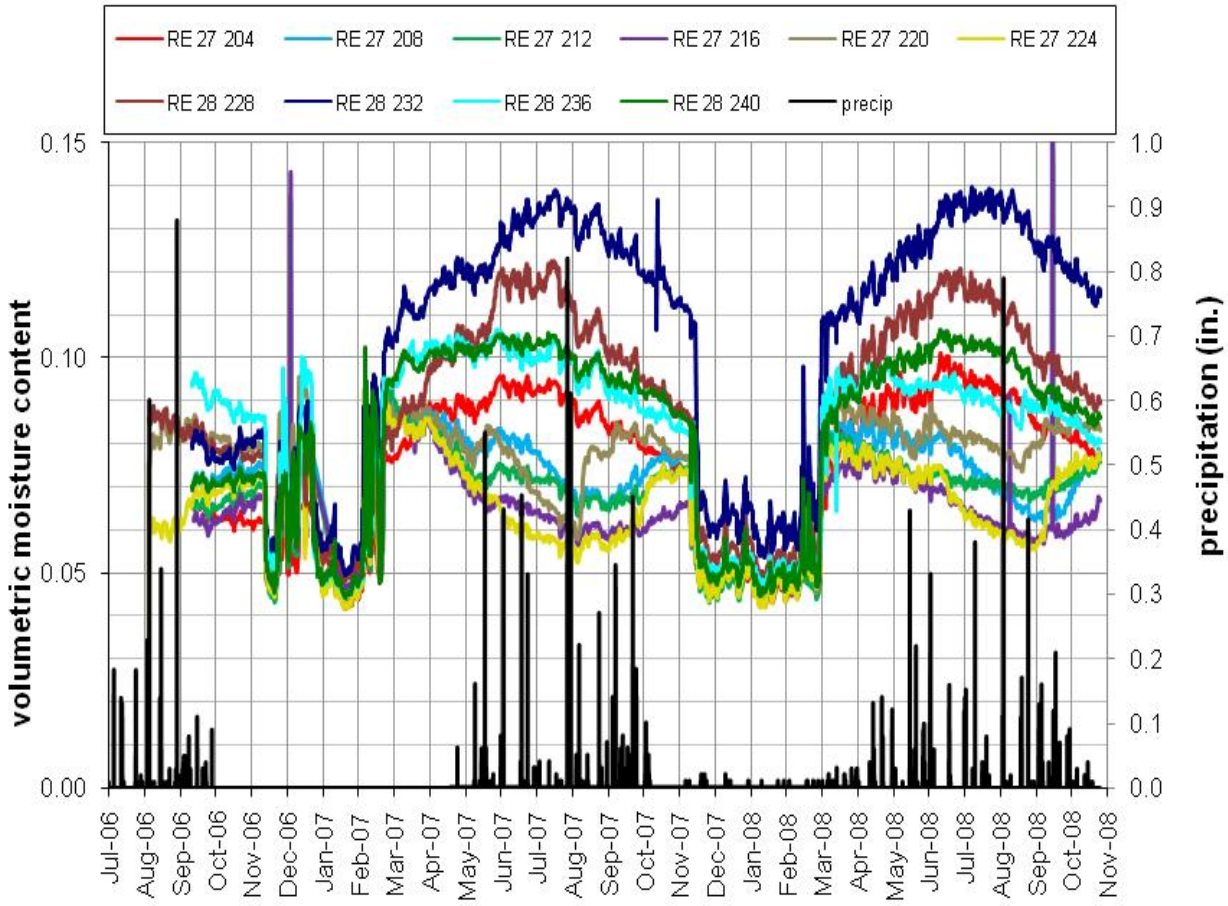

Figure 2.5 – Water content data from TDR probes at 15.2 cm depth in base course. The bars indicate precipitation events.

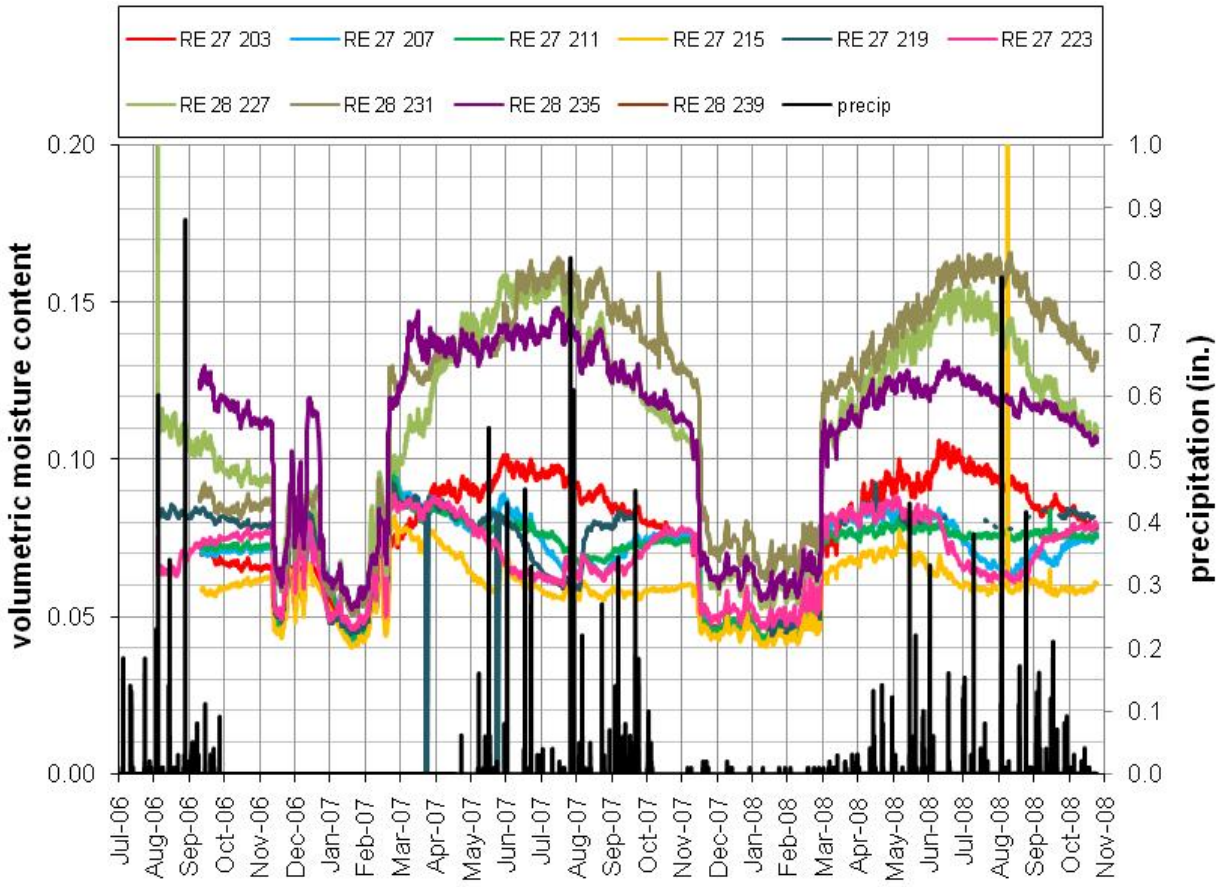

Figure 2.6 – Water content data from TDR probes at 25.4 cm depth in base course. The bars indicate precipitation events.

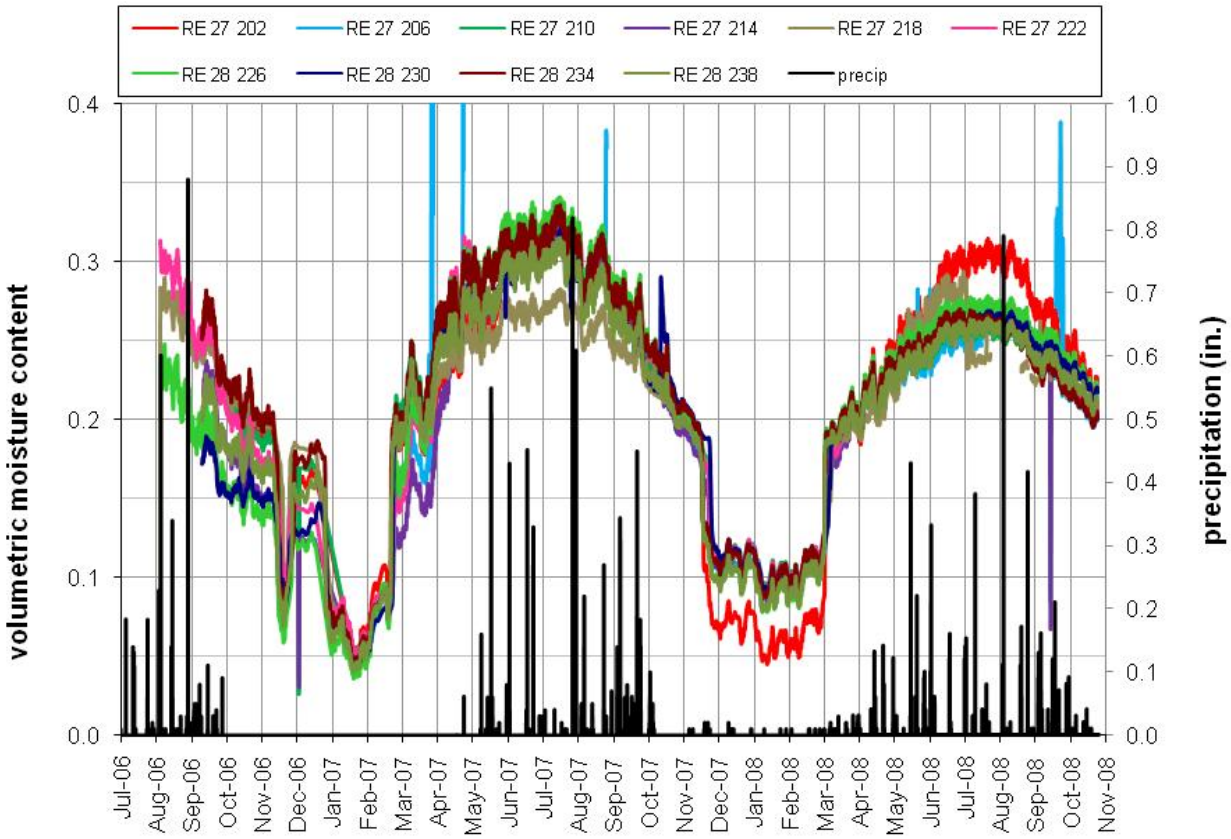

Figure 2.7 – Water content data from TDR probes at 33 cm depth in subgrade. The bars indicate precipitation events.

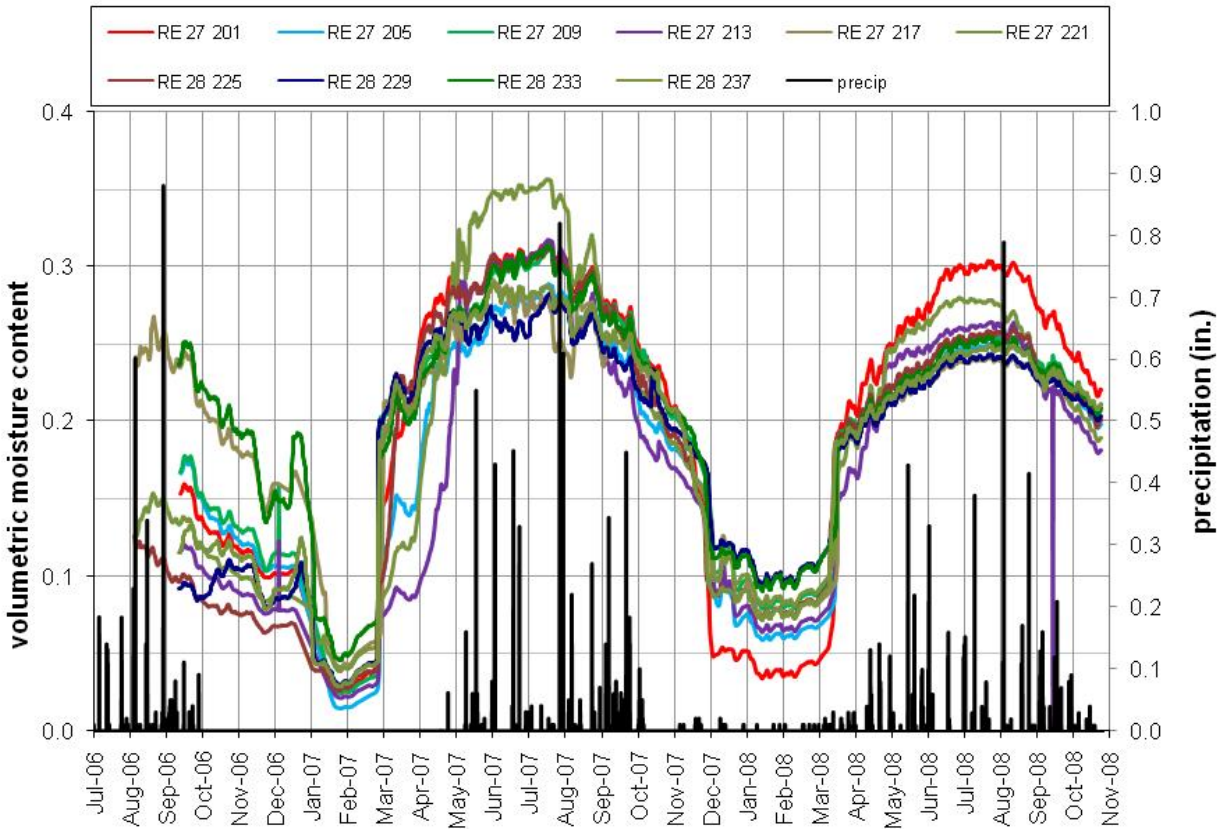

Figure 2.8 – Water content data from TDR at 61 cm in subgrade. The bars indicate precipitation events.

Water content data for three days during 2007 are shown in Figures 2.9, 2.10, and 2.11. These figures include both base course and subgrade water contents, and are shown as a function of position (station). The cell 27 values are on the left (from station 17530 to 18030) and the cell 28 data is on the right of these figures (from station 18100 to 18600). The legend indicates which data is from the upper and lower portions of the base course and subgrade.

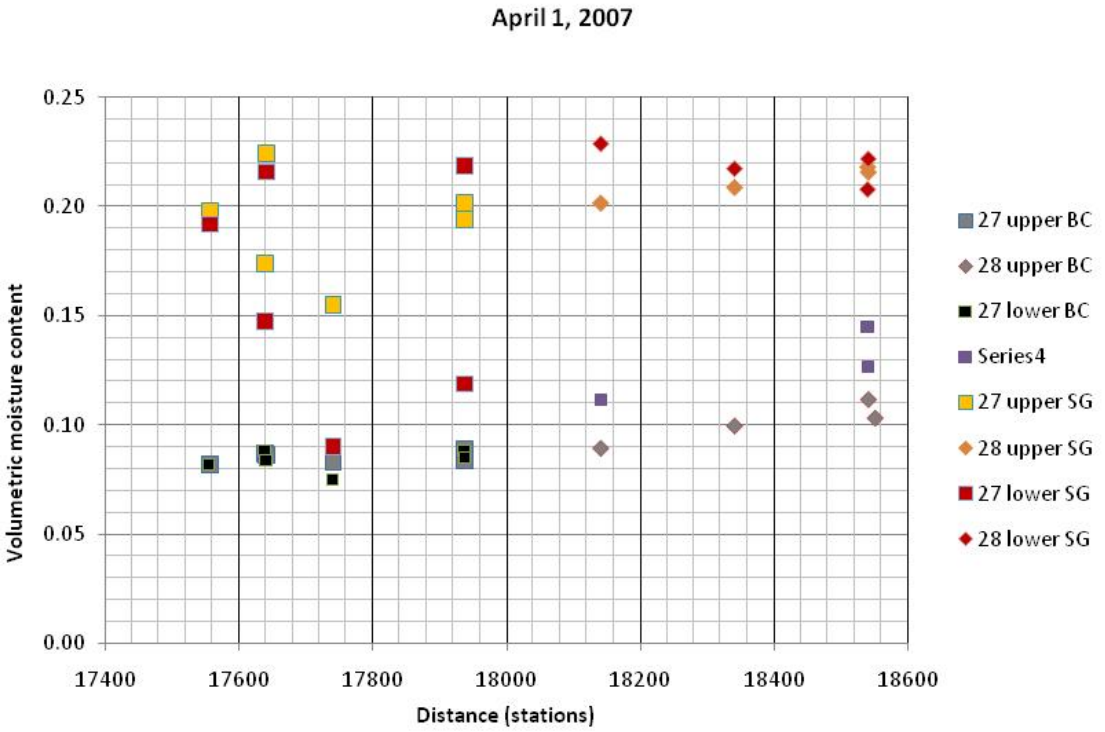

Figure 2.9 – Water contents in base course and subgrade as a function of position (station) for April 1, 2007.

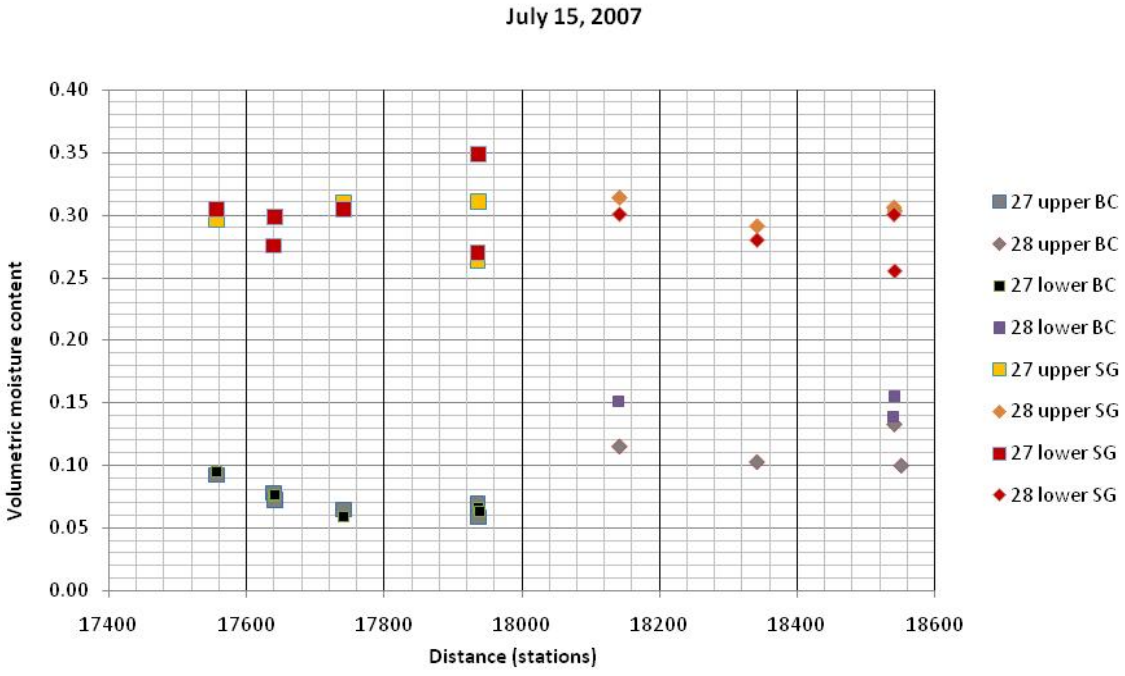

Figure 2.10 – Water contents in base course and subgrade as a function of position (station) for July 15, 2007.

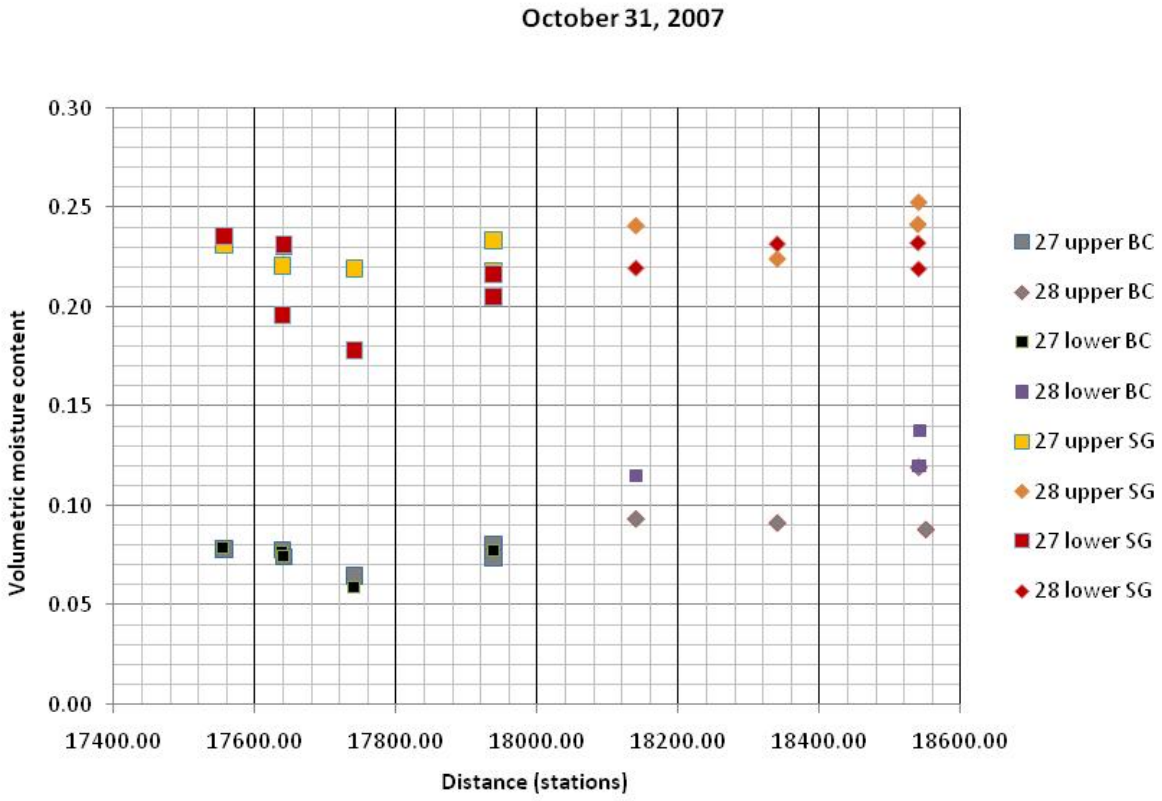

Figure 2.11 – Water contents in base course and subgrade as a function of position (station) for October 31, 2007.

The results in Figures 2.5 through 2.11 indicate that the base course in the cell with the GCBD becomes substantially drier over time than the base course without a GCBD. This result is consistent with water from below or to the side of the GCBDbeing prevented from entering the base course by the capillary. The biggest difference between base course water contents occurs during the summer months, which is typically when the groundwater level is the highest. The best estimate of water table depths at the cell 27 and 28 are in the range of 1 to 3 m, with shallower depths expected during the summer.

The hypothesis that the water is entering the base from below or the side is based on the assumption that the pavement isin good condition and has a low hydraulic conductivity, as would be expected only about a year after construction, and not allowing much if any infiltration.

2.2.3 Tipping bucket data

Tipping bucket data are given in Figure 2.12. There were two tipping buckets, one on the north side and one on the south side of cell 27. Precipitation is also shown on the figure. It is important to consider that the source of water collected by the tipping bucket cannot be discerned. The water can be from the GCBD (which is tied into the collector pipes) or from infiltration into the trench from pavement run-off.

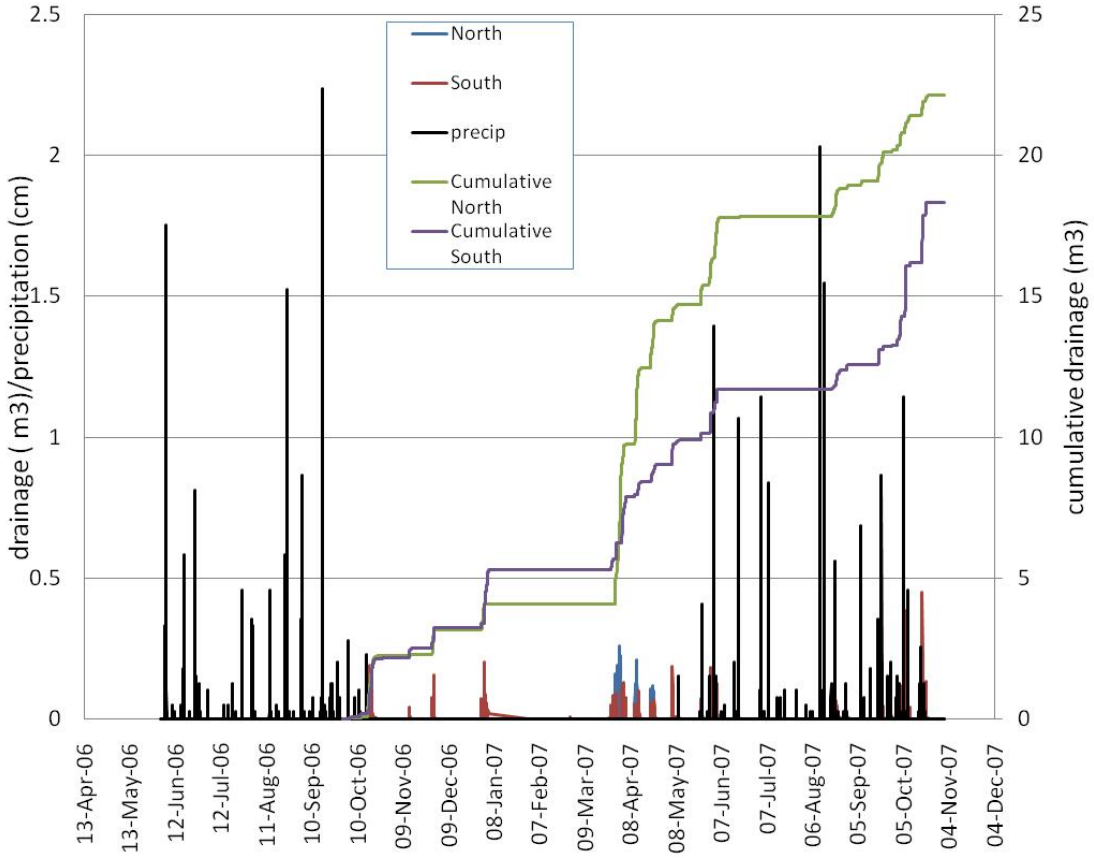

Figure 2.12 – Tipping bucket and precipitation data.

Substantial collection is observed during the spring of 2007, coincident with the spring snowmelt. During the summer of 2007, in spite of substantial precipitation, there was no water collected in the system. This is likely because a lot of precipitation will evaporate during the summer months. The tipping bucket data does not allow for a direct evaluation of the performance of the GCBD. Continued data collection may allow such an evaluation.

2.2.4 FWD data

Falling Weight Deflectometers (FWDs) are used to non-destructively test pavements in order to estimate the modulus values of the pavement layers. Circular plate loads are dropped on the pavement surface and a series of geophones spaced linearly from the center of the load plate measure vertical deflection. The vertical deflections of the geophones closest to the load are used to estimate the modulus of shallow layers and the outermost deflections are related to the subgrade behavior.

MnDOT personnel conducted FWD tests on the cells 27 and 28 periodically from September 18, 2006 to August 27, 2007. Although MnDOT did some preliminary data reduction, CRREL reduced the data reported in this section. Detailed reporting of the FWD test data is being summarized in a report to MnROAD by Barna, et al., (in review).

Schematics showing the locations of the FWD tests are shown in Figures 2.13 and 2.14. There were ten locations along the length of each cell. Seven lanes are indicated across the cells, and FWD tests were conducted on Lanes 1, 2, 6 an 7. The truck that applies traffic travels in Lanes 1 and 2 with a 356 kN (80 kip) axle load and in Lanes 6 and 7 with a 454 kN (102 kip) axle load. However, care is taken to apply the same number of 80 kN (18 kip) equivalent single axle loads in each set of lanes for a given time period. Note that lanes 1 and 7 are in the wheel paths, while lanes 2 and 6 are in between the wheel paths of the truck used to apply the traffic.

During the testing period from 2006 to 2007, FWD data was collected in Lanes 1, 2, 6, and 7. Test dates and corresponding lanes are summarized in Table 2.3. The geophones were spaced at distances of 0, 203, 305, 457, 610, 914, 1219, 1524, and 1829 mm (0, 8, 12, 18, 24, 36, 48, 60, and 72 in.) from the center circular load plate. The radius of the circular load plate was 150 mm (6 in.). At each test point, the weights were dropped 3 times each at 3 drop heights (increasing), for a total of 9 readings. The drop weights were 27, 40, and 54 kN (6, 9, and 12 kips). In each of the 4 lanes tested, there were 10 test stations in the GCBD test cell (Figure 4) and the control test cell (Figure 5).

The commercially available software that comes with the Dynatest FWD, Elmod version 5.0, was used to analyze the results. The raw data files collected by the FWD were used as input into Elmod 5.0. The layer thicknesses were fixed with 100 mm (4 in.) for asphalt (layer 1); 150 mm (6 in.) for the base (layer 2); and 180 mm (7 in.) for the subgrade fill (layer 3). The modulus values for the subgrade (layer 4) were also estimated, and the depth to bedrock was not fixed. The elastic modulus ratio between the 3rd and 4th layer was estimated by the software.

The 'Deflection Basin Fit' option of the Elmod 5.0 analysis software was used for back-calculation, and mean modulus values were thus estimated for the following four sections—1) cell 27, 1.5 and 2 –this is the transition portion of cell 27, that contains no GCBD 2) cell 27, 3 to 10—the portion of cell 27 containing the GCBD, 3) cell 28, 1.5 and 2 and 4) cell 28, 3-10. Note that there is no difference in cell construction for cell 28 1.5 and 2 vs. 3-10.

Figures 2.15 through 2.18 show the estimated modulus values as a function of date based on the FWD tests. There were two test dates for which the data appeared to be valid and for which there was matching lane data between cells 27 and 28. These dates were June 20th, 2007 and August

27th, 2007. Bar graphs indicating the estimated modulus values for these dates are shown in Figures 2.19 and 2.20.

Table 2.3 Summary of falling weight deflectometer (FWD) test dates and locations.

Date	Cell 27				Cell 28			
	Lane 1	Lane 2	Lane 6	Lane 7	Lane 1	Lane 2	Lane 6	Lane 7
9.14.2006					X			
9.18.2006	X	X	X			X	X	X
10.19.2006	X				X			X
11.03.2006	X				X			
12.20.2006					X			
02.20.2007				X				X
03.09.2007				X				X
03.12.2007				X				X
03.14.2007								X
3.15.2007				X				X
3.19.2007				X				X
3.20.2007				X				X
3.23.2007				X				X
5.10.2007	X				X			
5.22.2007	X				X			
6.08.2007	X				X	X		
6.20.2007	X	X	X	X	X	X	X	X
6.22.2007	X				X			
7.02.2007				X				X
7.12.2007				X				X
7.26.2007	X			X				
8.01.2007				X				X
8.24.2007	X							
8.27.2007	X			X	X			X

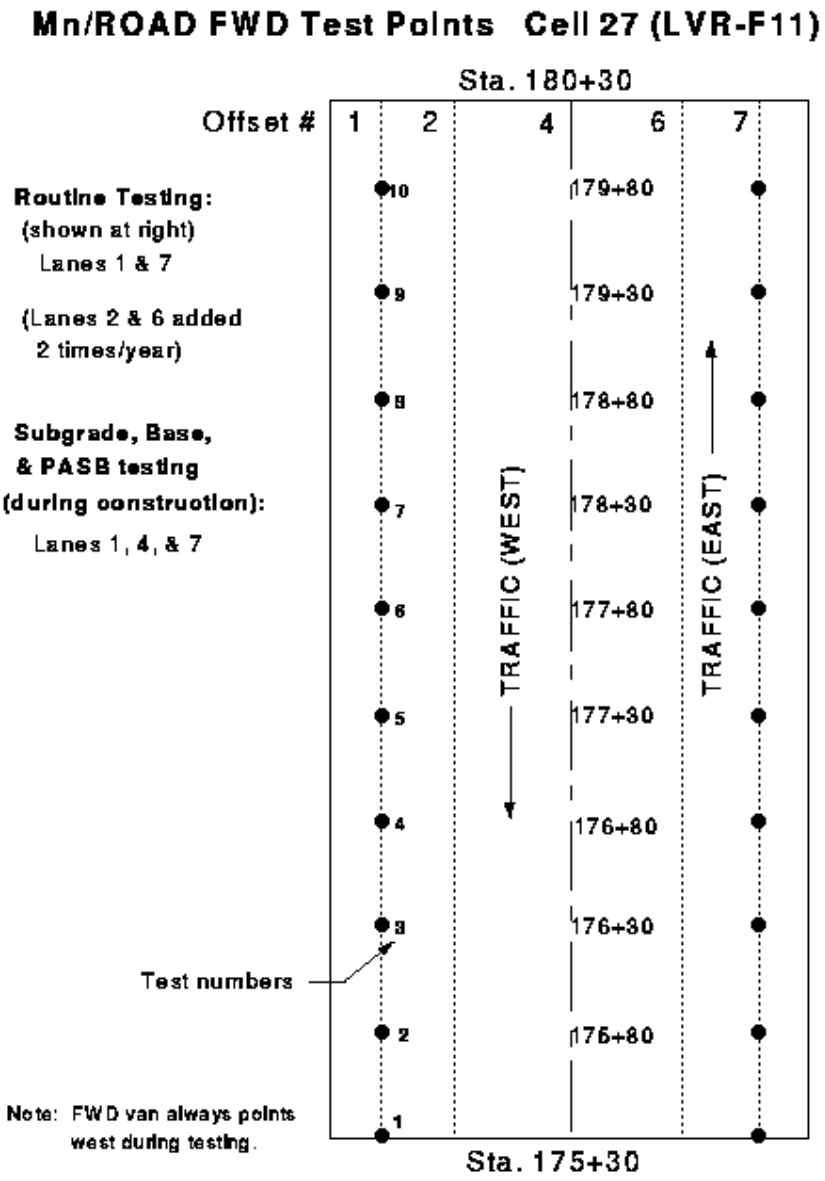

Figure 2.13- FWD measurement locations for cell 27.

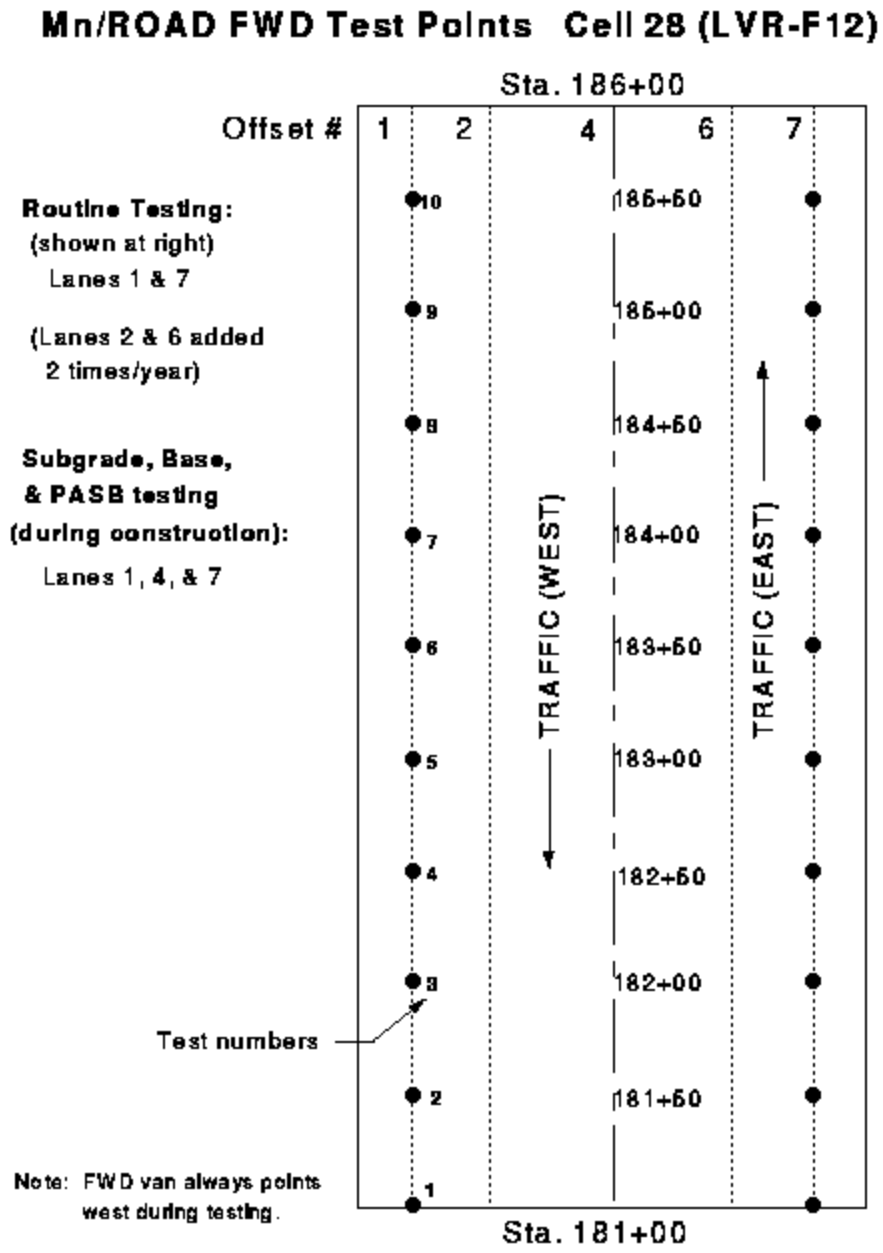

Figure 2.14 – FWD measurement locations in cell 28.

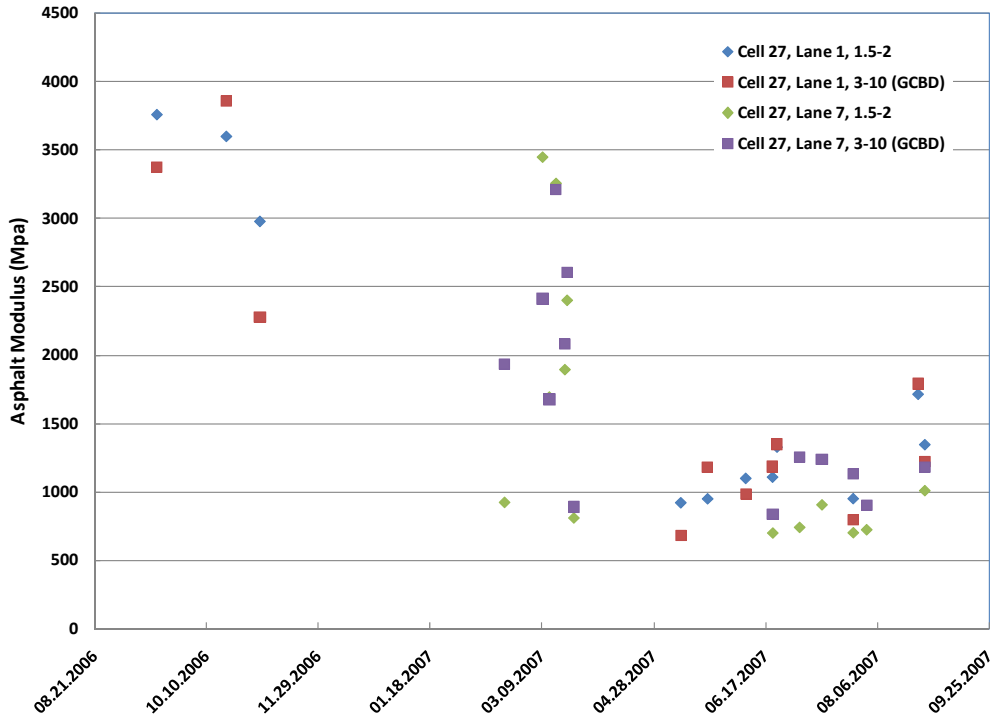

Figure 2.15a – Estimated asphalt modulus values for Cell 27 based on FWD tests.

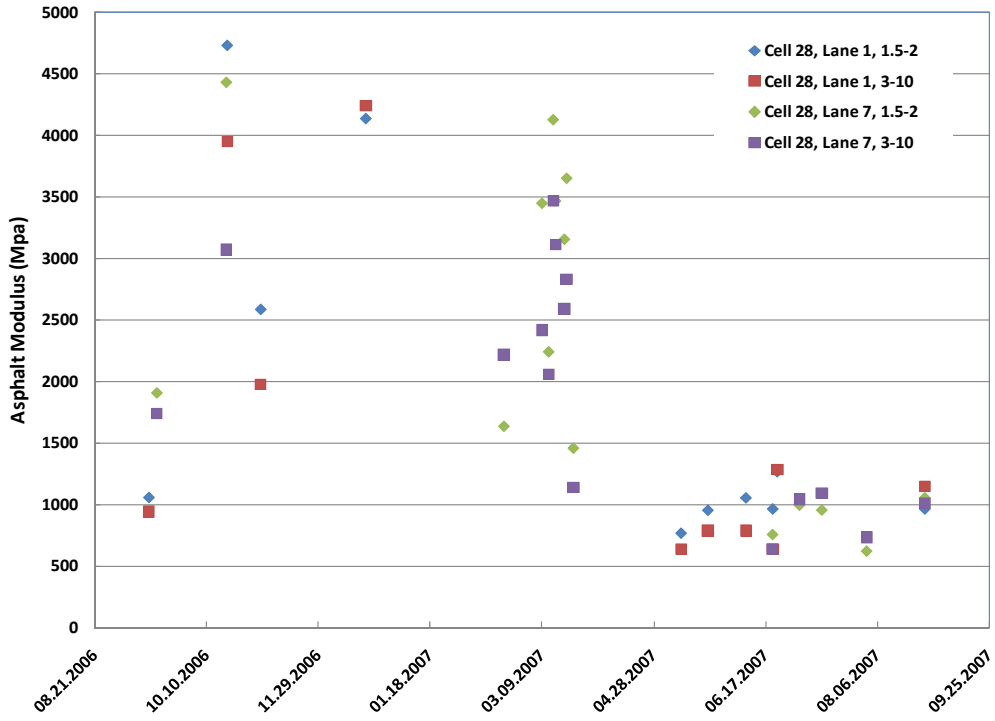

Figure 2.15b – Estimated asphalt modulus values for Cell 28, based on FWD tests.

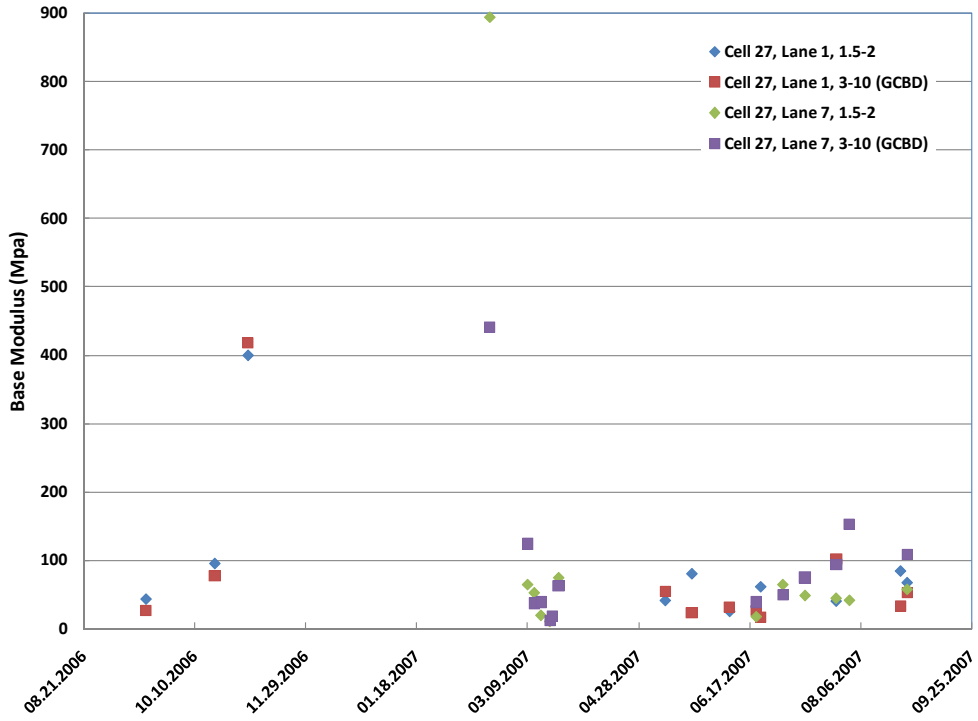

Figure 2.16a – Estimated base modulus values for Cell 27 based on FWD tests.

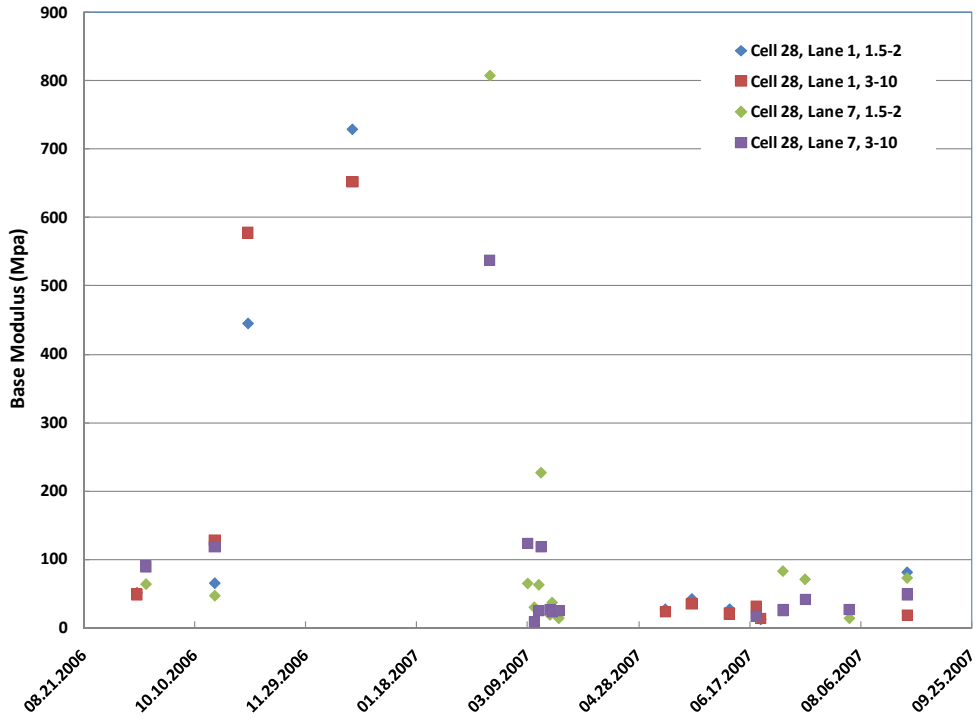

Figure 2.16b – Estimated base modulus values for Cell 28 based on FWD tests.

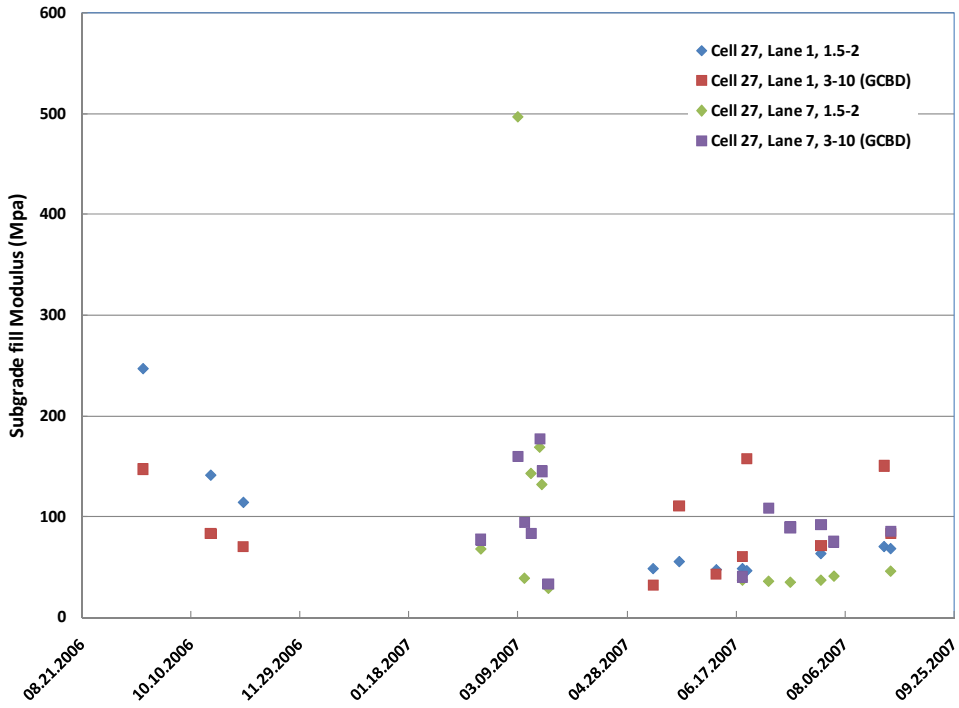

Figure 2.17a – Estimated modulus values of the subgrade fill for Cell 27 based on FWD tests.

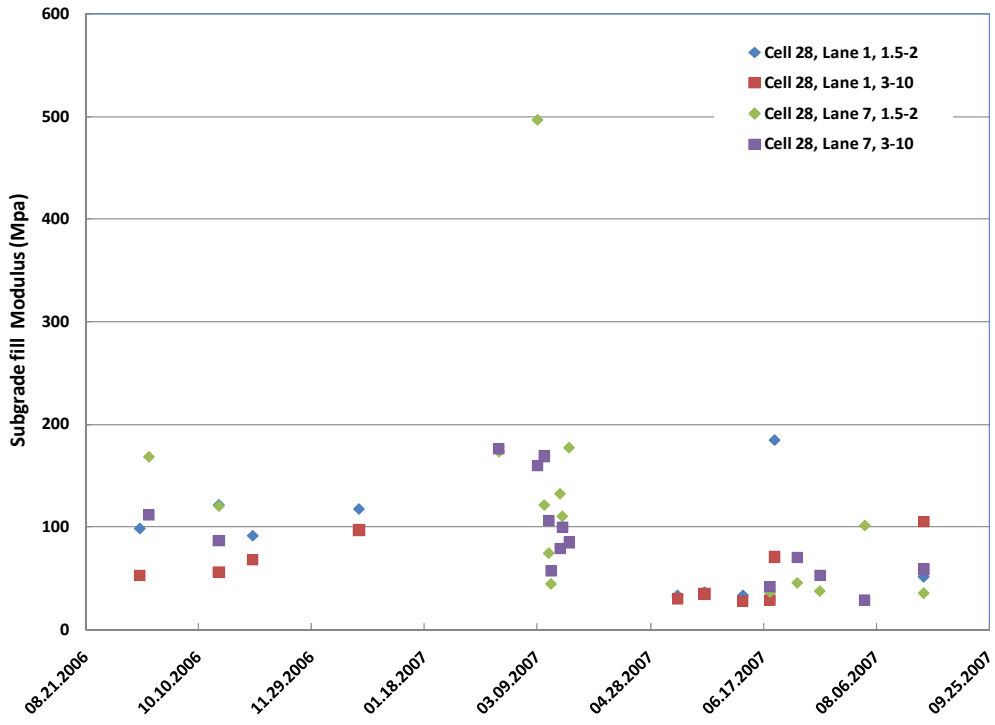

Figure 2.17b – Estimated modulus values of the subgrade fill for Cell 28 based on FWD tests.

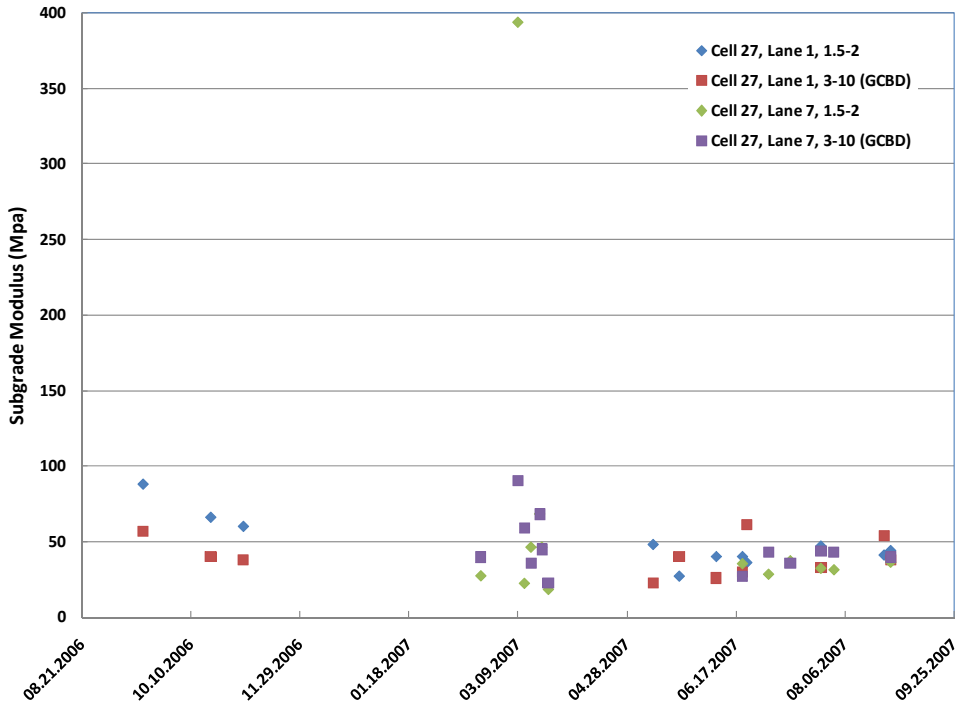

Figure 2.18a – Estimated subgrade modulus values for Cell 27 based on FWD tests.

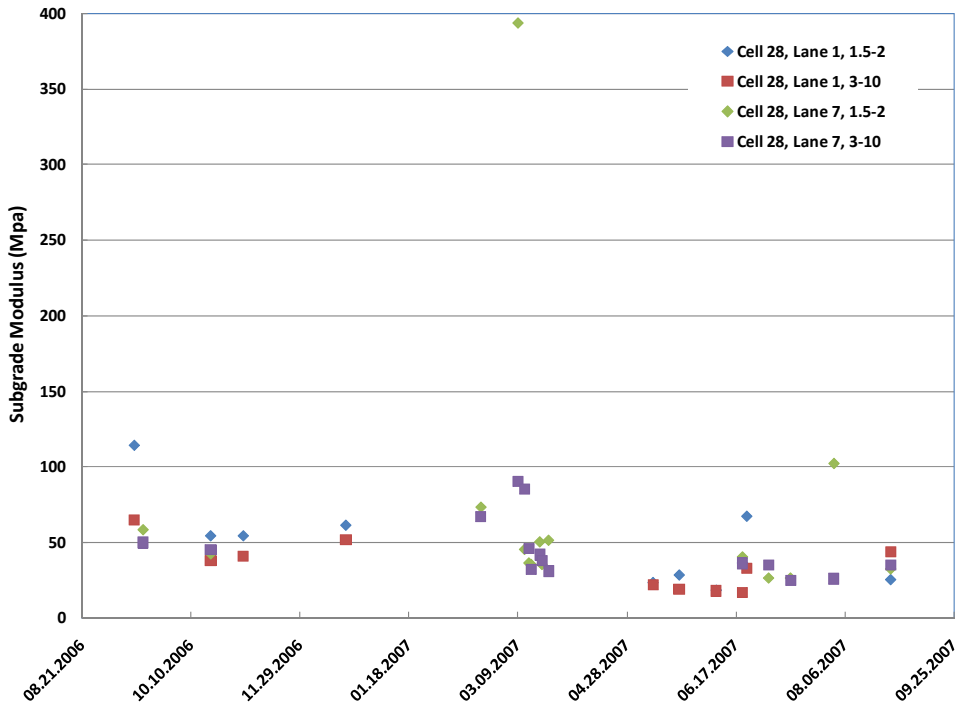

Figure 2.18b – Estimated subgrade modulus values for Cell 28 based on FWD tests.

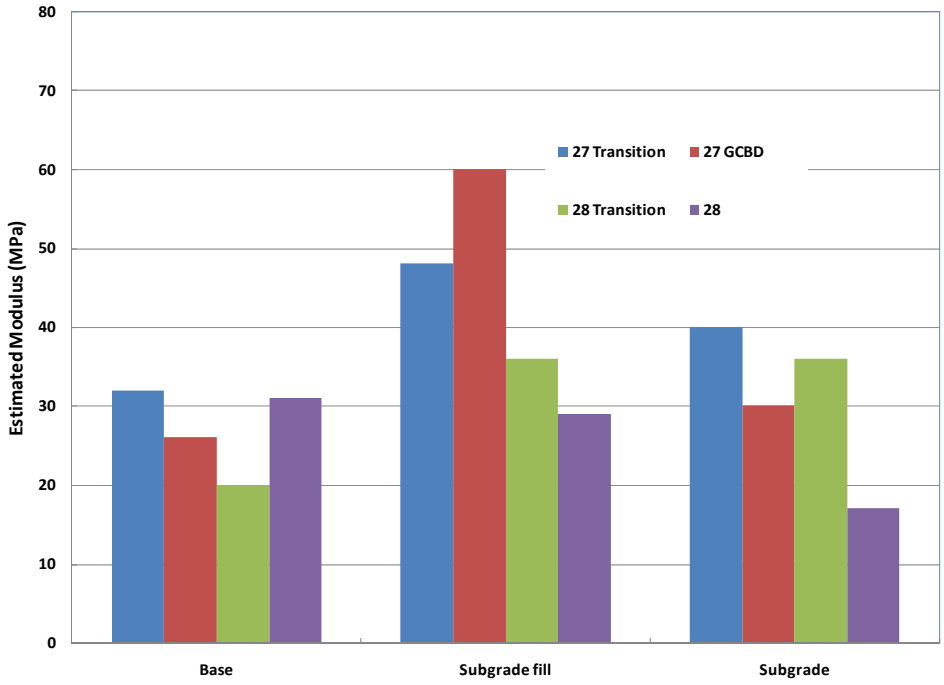

Figure 2.19a – Estimated modulus values based on FWD testing for Lane 1 on June 20, 2007.

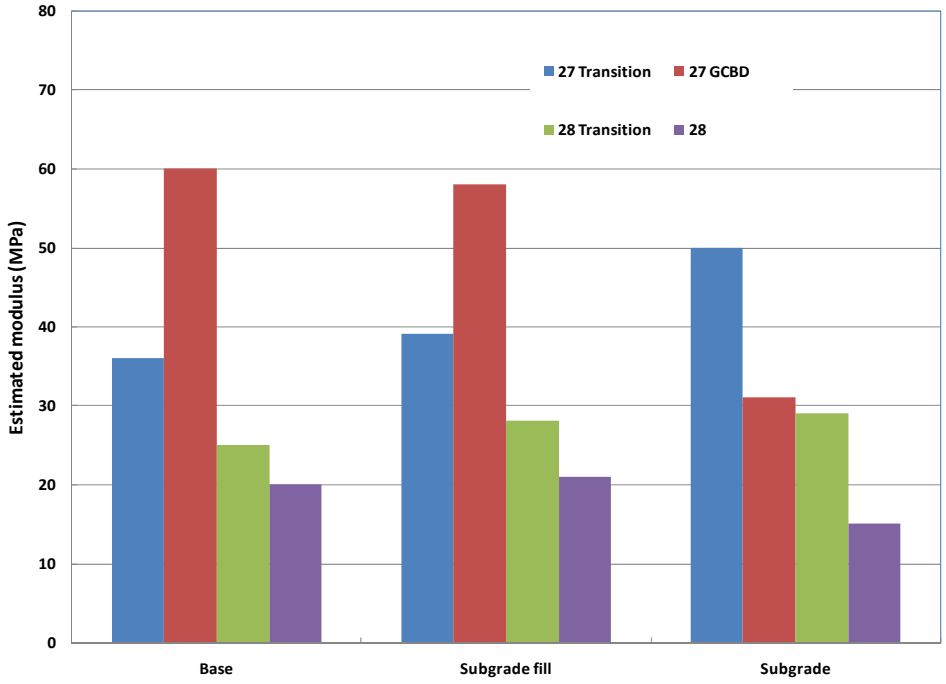

Figure 2.19b – Estimated modulus values based on FWD testing for Lane 2 on June 20, 2007.

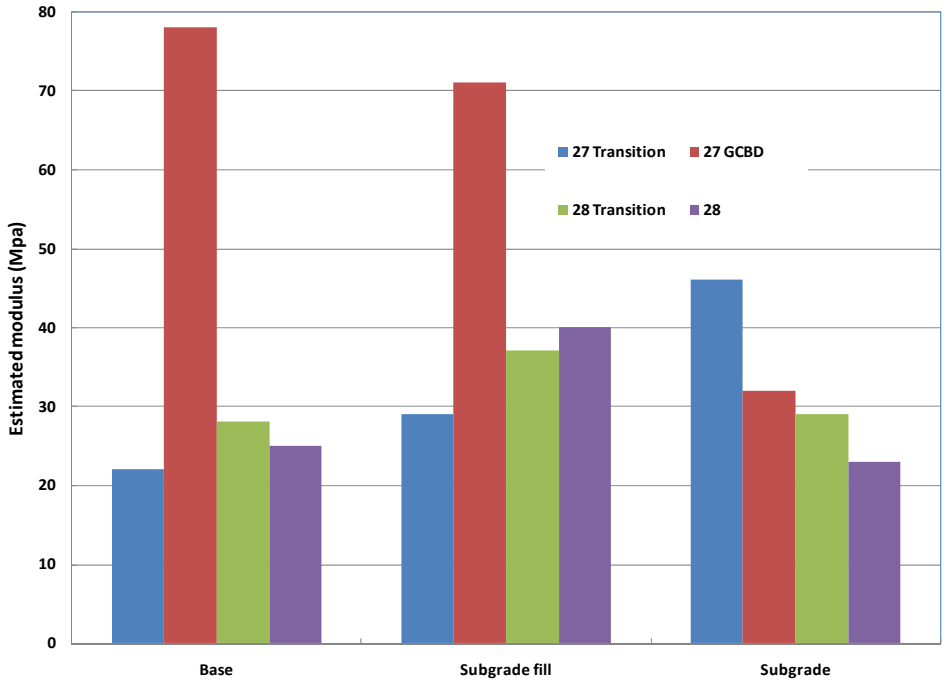

Figure 2.19c – Estimated modulus values based on FWD testing for Lane 6 on June 20, 2007.

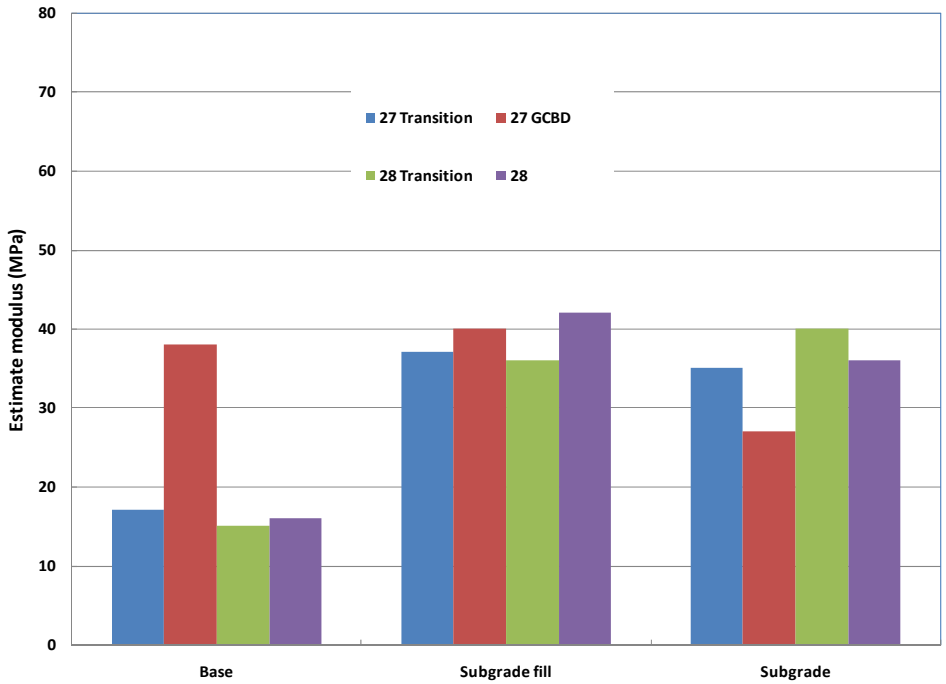

Figure 2.19d – Estimated modulus values based on FWD testing for Lane 7 on June 20, 2007.

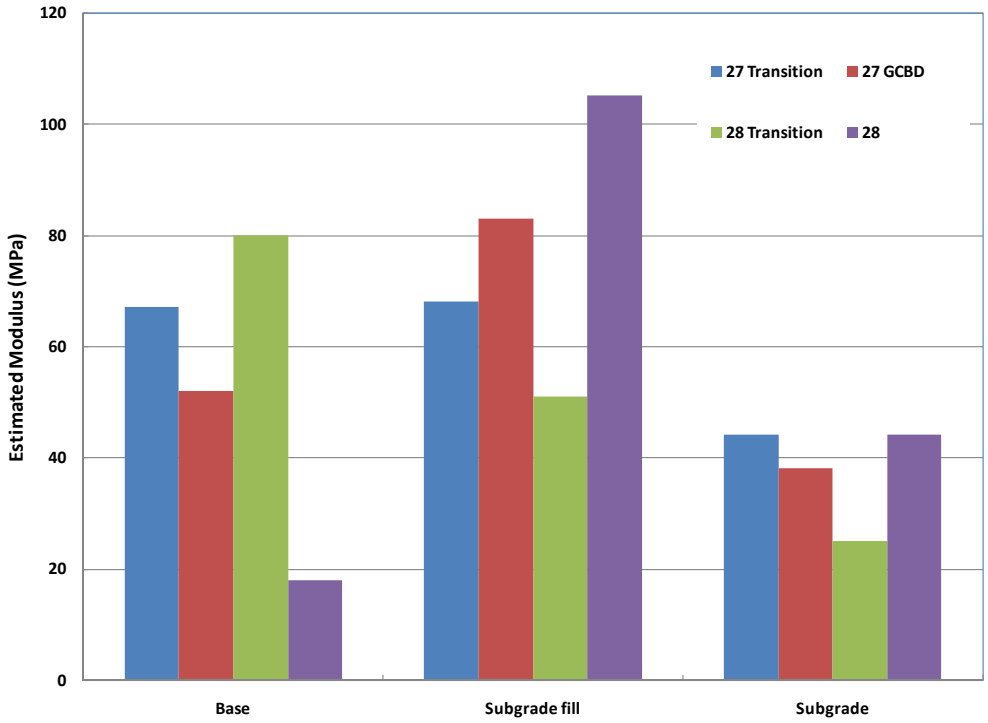

Figure 2.20a – Estimated modulus values based on FWD testing for Lane 1 on August 27, 2007.

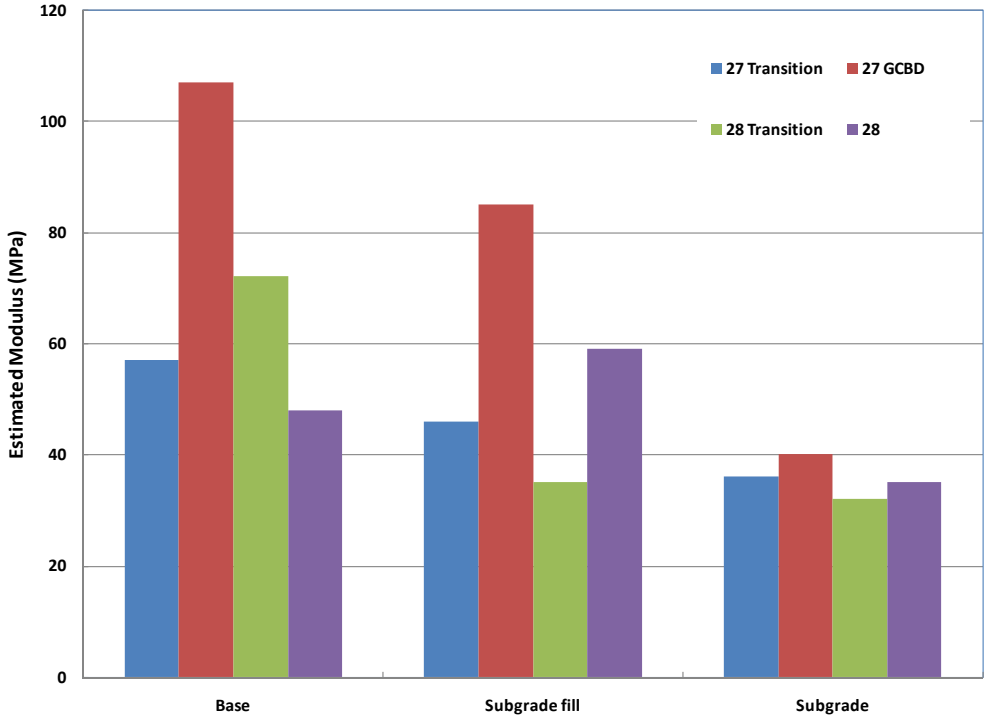

Figure 2.20b – Estimated modulus values based on FWD testing for Lane 7 on August 27, 2007.

The modulus values of all layers decreased from the fall of 2006 (immediately after construction) to the end of summer 2007 (Figs 2.15 through 2.18). Figures 2.21 and 2.22 show temperatures measured by thermocouples in the base and subgrade layers for test cells 27 and 28, respectively. Consideration of the temperature data in conjunction with the estimated modulus values shows that the modulus values of all pavement layers were greater during the winter, when the soil was frozen, than they were after thaw had occurred.

From March 2007 (after spring thaw) until the end of monitoring the following trends are noted:

1) Data suggest that the GCBD portion of cell 27 has higher base modulus values than the other base modulus values (i.e., the transition portion of cell 27 and of cell 28) (Fig. 2.16). Note that the GCBD lies at the bottom of the base layer
2) The soil layer immediately below the GCBD, the subgrade fill, has notably higher modulus values for the GCBD portion of cell 27 than the transition portion of cell 27 and of cell 28 (Fig. 2.17)
3) There are no significant differences in the estimated subgrade modulus values for any of the test sections (Fig. 2.18).

The modulus values estimated for the base layer are generally less than or equal to the underlying subgrade fill and subgrade layers (Fig. 2.16 through 2.20).

On June 20, 2007, it appears that GCBD portion of test cell 27 had a significantly higher base and subgrade modulus values than the non-GCBD portions of the test cells in lanes 2 and 6, while the GCBD appears to have "helped" only the subgrade fill in lane 1 and only the base in lane 7 (Fig. 2.19). On August 27, 2007, both the base and subgrade modulus values of lane 7 were higher in the GCBD portion of the test cells, but there was no significant influence in lane 1 (Fig. 2.20).

Thus, the FWD results generally indicate that the two layers adjacent to the GCBD have greater modulus values than the modulus values of these same two layers in the pavement section without the GCBD. However, there is considerable variability in the data. The results are consistent with the base course being drier in the pavement section that includes the GCBD; however, this is not thought to be the case for the layer below the GCBD—in this case, the GCBD may be providing structural reinforcement. Continued measurements of both water content and modulus values via FWD testing should indicate whether this preliminary conclusion is substantiated with time.

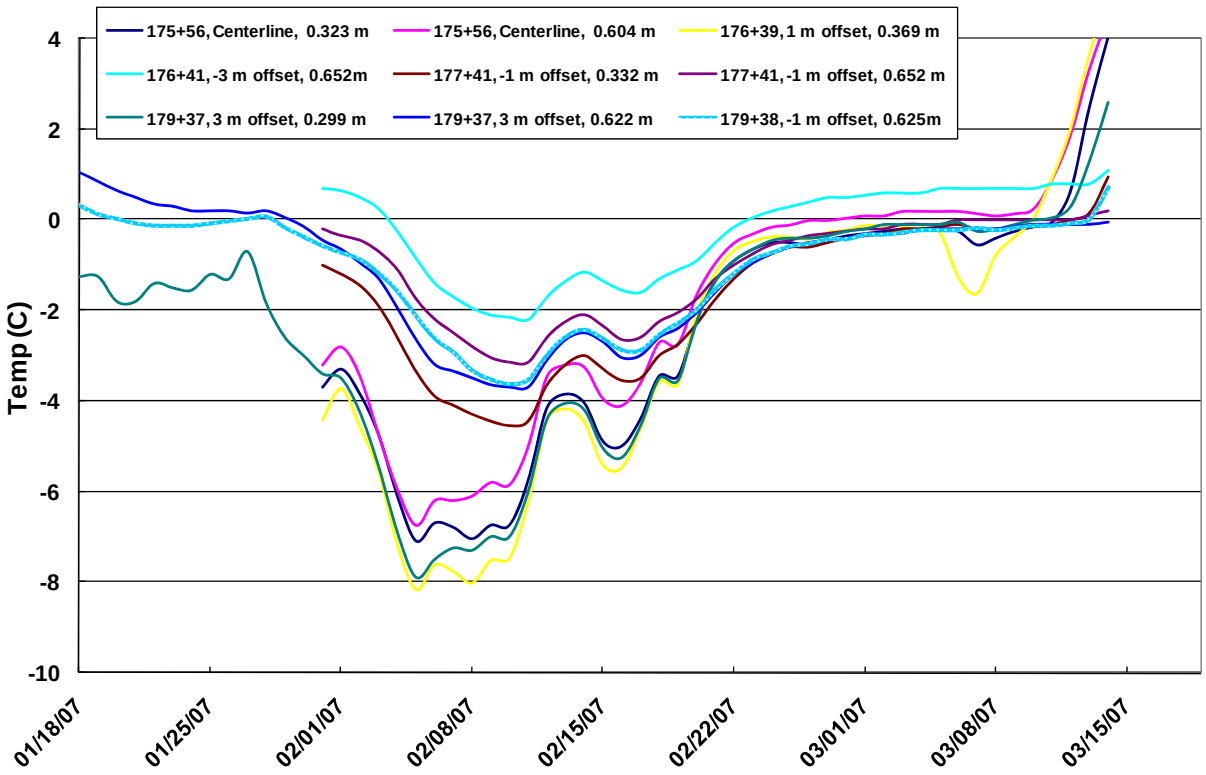

Figure 2.21 – Temperatures recorded in the base and subgrade layers of cell 27. The legend lists the survey station and the offset from the centerline, followed by the depth of the measurement.

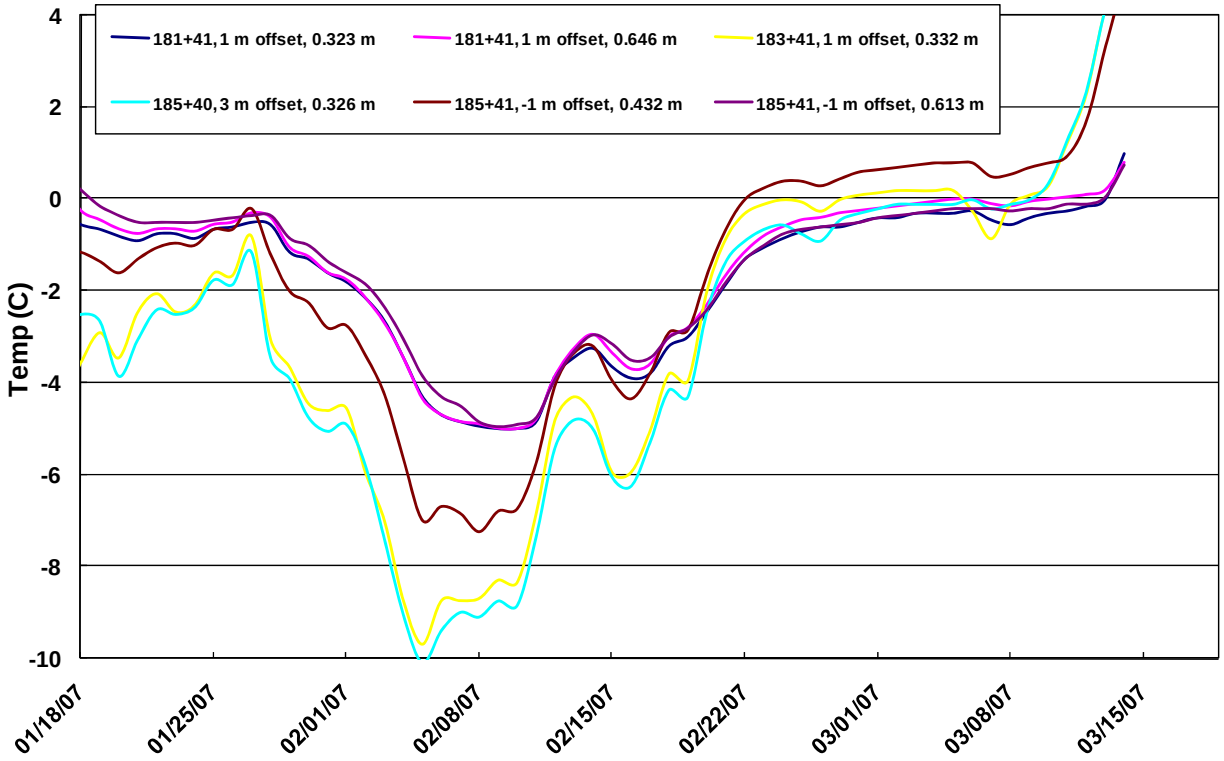

Figure 2.22 – Temperatures recorded in the base and subgrade layers of cell 28. The legend lists the survey station and the offset from the centerline, followed by the depth of the measurement.

2.2.6. Failure of a small portion of cell 28

On June 1, 2007, an approximately 3 m by 6 m portion of the pavement on cell 28 failed (Figure 2.23). The pavement surface was rutted and was broken up. The material was excavated along with the base course and some of the subgrade. The subgrade was described as very wet. The subgrade was replaced at this location with base course material. The pavement surface was subsequently patched. The failure appeared to be related to the very wet conditions in the subgrade, but was localized at this one relatively small location.

Figure 2.23 – Failed pavement in cell 28.

2.3 Conclusions and status from MnROAD demonstration

A principal outcome from the MnROAD demonstration is that the GCBD can be practically installed in a full-scale application. The installation, detailed in the Stage 2 report, required some special attention, but largely because it is a new product. In particular, a means to tie the GCBD into an edgedrain collection system was devised and implemented.

The water content data reveal that the base course in the cell with the GCBD (cell 27) is lower than that in the cell without the GCBD—especially during the summer months. This result is consistent with water from the adjacent soil, likely from below, being blocked from entering the base course due to the capillary barrier effect of the GCBD. In addition, any infiltrating water is likely being diverted in the transport layer.

The FWD data generally indicate higher modulus values of the two layers adjacent to the GCBD—the base layer (overlying) and the subgrade fill layer (underlying)—compared to the test cell portions without the GCBD. This is true for dates after the first seasonal thaw, and are consistent with the base course being drier in the section that includes the GCBD. There is considerable variability in the modulus values estimated based on FWD tests, and more monitoring would help discern any long-term effects of having the GCBD present in the pavement system.

It is unclear the amount, if any, of lateral drainage out of the GCBD at this point in time. With continued deterioration of the pavement over time, more water will enter the base course through the pavement surface, and the lateral diversion capacity of the GCBD would be expected to be utilized. Continued monitoring of the test cells over time will provide more insight into the performance of the GCBD.

3. Design calculations

3.1 Introduction

The impact of the GCBD on a pavement system can be approximated through simple "design calculations." These calculations estimate how the GCBD will change the storage and routing of water in a pavement section for different combinations of base course materials, subgrade materials, water table depths, and climatic conditions (precipitation). From these results, generalizations about GCBD performance can be made, and extrapolation to specific situations can be made.

The design calculations utilize simplified models. They models do not intend to capture the "physics" of water movement within the pavement section; rather, they use water balance approach to approximate the routing and storage of water in pavement systems. While the models produce reasonable results, they should not be considered predictions of drainage quantity and saturation values. Instead, the results provide relative results that serve as a basis for comparison of pavement systems with and without a GCBD. More complete, complex models are available, but the detailed input requirements and numerical issues preclude their use in the parametric simulations for this study.

The direct "measure" of the impact of the GCBD is the change in saturation of the base course and subgrade. The saturation, in turn, affects the strength and deformation characteristics (moduli) of these layers in a pavement system. The results in the following sections are largely presented as saturations; a next step would be to interpret strength and modulus from these saturations.

The layer of concern for a pavement system will depend on the specific conditions. In some cases, the most important consideration for pavement drainage design may be a moisture sensitive subgrade. In this case, it may be crucial that saturation changes in the subgrade be minimized. In other cases, limiting the saturation or preventing complete saturation of a base course layer may be the most important consideration.

3.1.1 Problem description

Water can move into a pavement system from three general sources: through the pavement, laterally from adjacent soil, and upward from a shallow water table (Figure 3.1).

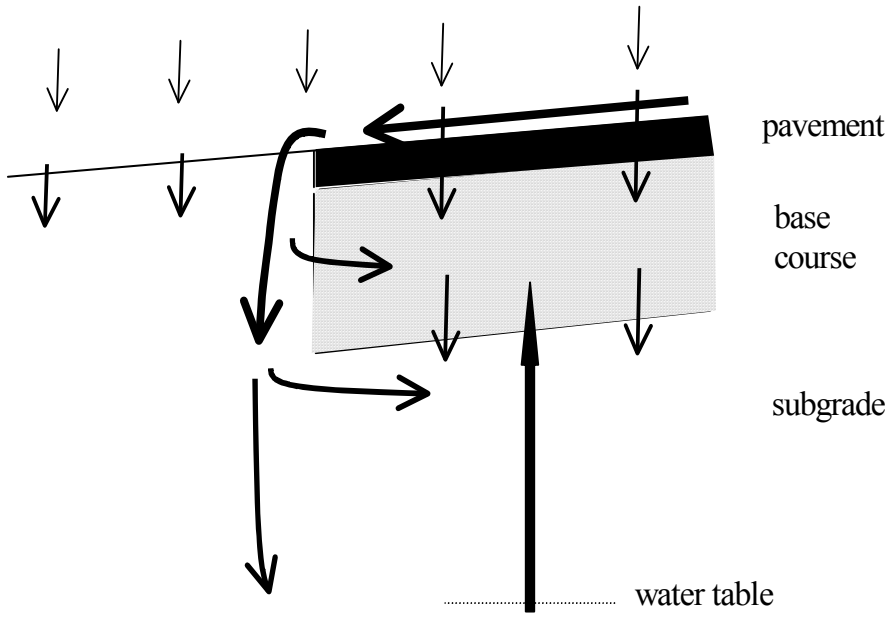

Figure 3.1 – Schematic illustration of sources of water in pavement layers.

Infiltration into the base course from infiltration has long been considered a source of water in pavement sections, and is generally treated as infiltrating uniformly through the pavement or through discrete cracks. Water that infiltrates can, in general, increase the saturation of the base course, laterally drain, or move downward into the subgrade.

A shallow water table is another source of water. Water is drawn up through the subgrade and into the base course. Water movement is in response to suction differences above the water table. Water can also move laterally from the adjacent soil into the base course and underlying subgrade. This water moves largely in response to suction differences. The adjacent soil can be wetted from precipitation events, including the additional wetting from pavement surface run-off that is concentrated at the shoulder.

3.1.2 Material and climate parameters

Four base course materials were selected for these calculations. These materials represent a wide range of potential base courses that may be used depending on material availability and cost, pavement design, drainage considerations, and design precedent. These materials were selected

principally to provide a range of material properties, and are not meant to define the full spectrum of possible base course properties.

The four base course materials are referred to as dense graded, conventional, permeable and stone. The hydraulic properties of the dense graded material are those determined for Class 5 base course from Minnesota. The properties of the conventional base course were those measured on a well-graded sand base course from New Hampshire (reported in Stormont and Zhou, 2005). The permeable base course properties were those of coarse sand (reported in Stormont and Zhou, 2005), and has a saturated hydraulic conductivity in the range of permeable base course materials intended to be readily drainable (Richardson, 1997; Elyasyed and Lindly, 1996; Rudolph et al., 1996). The stone base course corresponds to a clean, uniform gravel or stone (Stormont, 1995), and has hydraulic properties that are comparable to AASHTO 57 stone.

A typical means to quantify a base course is to calculate the "time-to-drain," which specifies a time to drain to an allowable saturation. According to AASHTO, classification of "excellent" results if the time-to-drain to 50% saturation is less than 2 hours, "good" for less than one day, and so on (Mallela et al., 2000). Although this approach is concerned with "de-saturation" of the base course, the equations are based solely on saturated flow. Shown in Table 1 are the classifications with respect to the "time-to-drain" for base course materials that are 15 cm thick and have a drainage length of 400 cm: the stone and permeable bases are classified as "excellent," the conventional base is classified as "good," and the dense graded material is "poor."

Hydraulic properties are tabulated below for each base course material, including the porosity (ϕ) and the saturated hydraulic conductivity (Ksat). The unsaturated hydraulic properties are described by the van Genuchten model (1980). The volumetric water content, θ, and suction head, h, are related by

$$\theta = \theta_r + (\theta_s - \theta_r)\left[1 + (\alpha h)^n\right]^{-m} \qquad (1)$$

where the subscripts s and r indicate the saturated and residual values of the water content, α,, m and n are fitting parameters, and $m = 1\text{-}1/n$. The fitting parameters can be determined from moisture characteristic curve data.

By adopting the model for hydraulic conductivity proposed by Mualem (1976), the hydraulic conductivity as a function of either water content or suction head can be predicted using the van Genuchten fitting parameters and the saturated hydraulic conductivity.

Table 3.1 – Base course material properties

Base course material	θr	θs	ϕ	α (1/cm)	N	Ksat (cm/s)	Time to drain classification (50% saturation)
dense graded	.067	.212	.40	.054	2.42	2.8e-4	Poor
conventional	.078	.239	.38	.031	2.75	1.3e-2	Good
permeable	.02	.25	.375	.043	3.1	.46	Excellent
stone	.0005	.25	.42	1	2.19	10	Excellent

The moisture characteristic curves for the base course materials are given in Figure 3.2. These curves indicate the amount of water the material retains at different values of suction. The base course materials are all coarse-grained materials, and they tend to not retain significant water at low to modest suctions. The stone base course in particular retains very little water under almost all values of suction.

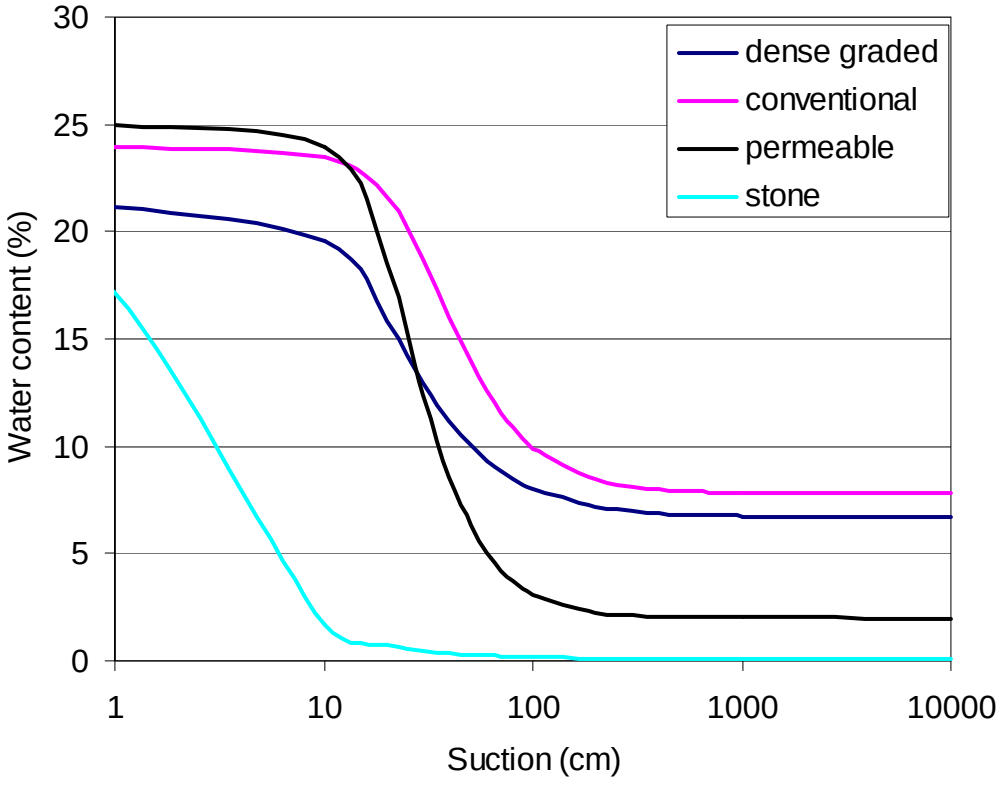

Figure 3.2 –Moisture characteristic curves for base course materials.

The GCBD is assumed to have a transport layer on top, a geonet, and a separator geotextile on the bottom. The transport layer is a very heavy, woven, multifilament material with a mass per unit area of 2370 g/m^2, a thickness of 3.2 mm, and an O_{95} size of 0.075 mm. The hydraulic properties of the transport layer are given by Stormont and Ramos (2004), and are given in Table 3.2. The GCBD is assumed to have a breakthrough head of 2 cm.

Table 3.2 – Transport layer properties

	θr	θs	α (1/cm)	N	Transmissivity, saturated (cm^2/s)
transport layer	.00	.83	.211	1.39	1e-1

Three subgrades types were included in the calculations: clay, clay loam and silt. These materials were selected to encompass a range of possible subgrade materials that a pavement section may be constructed upon. Fine-grained subgrades (e.g., clay and clay loam) can be problematic due to volume change that accompanies saturation changes. The silt is more likely to be a soil that experiences less volume change, but its strength and deformation characteristics will change with changing saturation.

The hydraulic properties of the subgrade materials are given in Table 3.3. The moisture characteristic curves for these materials are given in Figure 3.3.

Table3.3 – Subgrade material properties.

Subgrade material	θr	θs	α (1/cm)	N	Ksat (cm/s)
clay	.07	.36	.005	1.09	1e-7
clay loam	.095	.41	.019	1.31	2e-6
silt	.10	.38	.027	1.23	3.3e-5

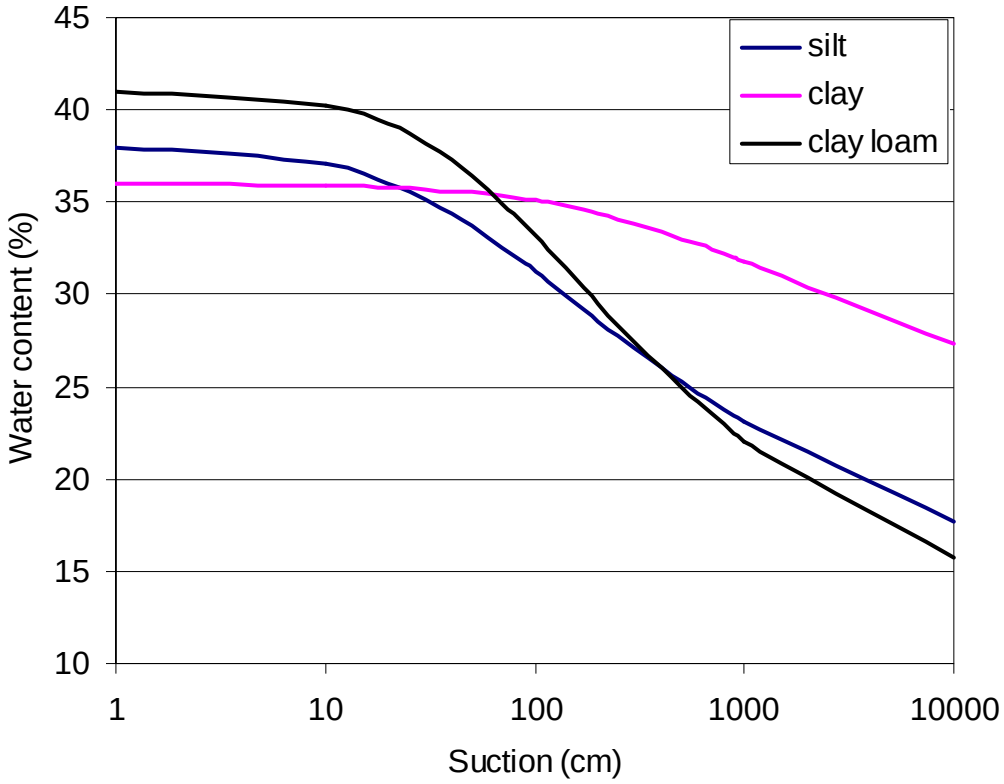

Figure 3.3 –Moisture characteristic curves for subgrade materials.

3.1.3 Climate

Three precipitation inputs were considered: Minneapolis, Albany and Albuquerque. Cumulative precipitation for the year 2006 is shown in Figure 3.4. The cumulative precipitation for these three locations provides a wide range that encompasses the annual precipitation of majority of locations within the US.

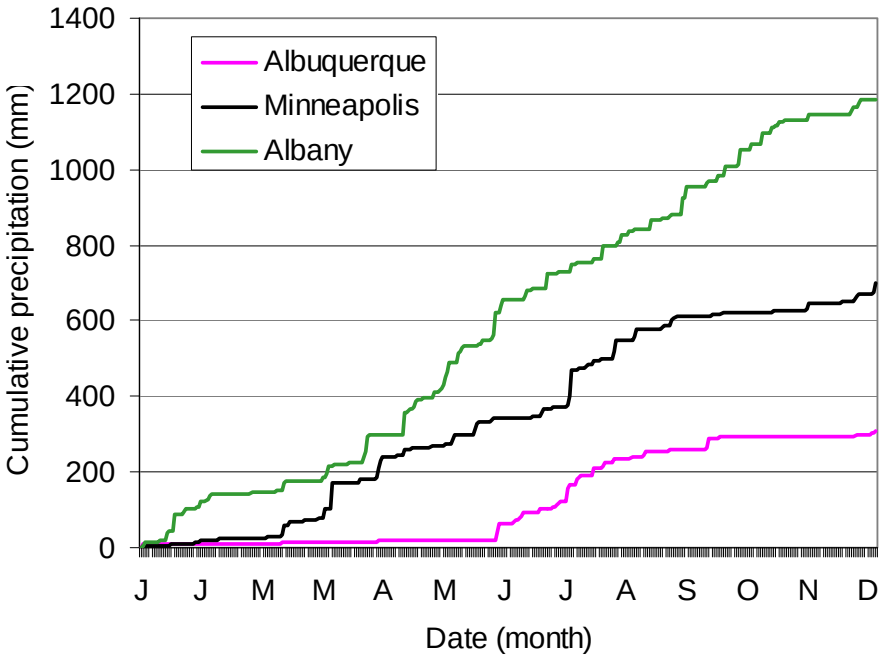

Figure 3.4 –Cumulative precipitation for three climates used in design calculations.

3.2 Infiltration, lateral drainage and flow into subgrade

Design calculations that considered infiltration from above, lateral drainage out of the base course and flow into the subgrade were conducted with a daily water balance model implemented in a spreadsheet. The purpose of the calculations is to provide a quantitative measure of the impact of the GCBD on the amount of water in the base course and subgrade for various conditions. Calculations were conducted for the case that includes a GCBD between the base course and subgrade, and the case without a GCBD (Figure 3.5). Four different base course layers, three subgrade soils, and four climates were considered in the calculations. This model only considers downward infiltration in response to precipitation, and does not address upward flow from a shallow water table. In this way, the benefit of the GCBD can be estimated.

In this model, a fraction of the daily precipitation (if any) is allowed to infiltrate into the base course. The pavement layer is not included in this model. The water is allowed to drain laterally in the base course. Without a GCBD, water in the base course can move vertically downward into the subgrade. In the case when the pavement system includes a GCBD, water movement from the base course to the subgrade is prevented until the water entry suction head of the GCBD is reached. If the amount of water in the base course is sufficient to reduce the suction in the base course to the water entry head of the transport layer, water is drained laterally in the transport layer. If the transport layer capacity is exceeded, water will move downward into the subgrade (breakthrough). If the bottom of the base course becomes saturated, water can also laterally drain in the geonet layer of the GCBD.

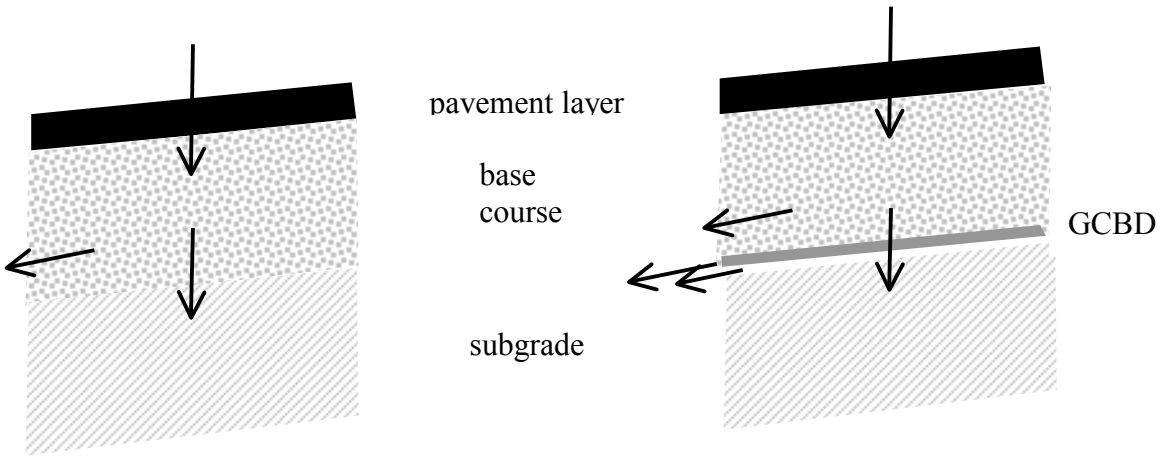

Figure 3.5 – Schematic illustration of water balance model without (left) and with GCBD (right).

3.2.1 Infiltration and water distribution within the GCBD

For both the cases with and without the GCBD, water from precipitation enters the base course. This water is assumed to distribute itself within the base course to result in an equilibrium suction profile. Thus, the suction at the bottom of the base course will be lower than the suction at the top of the base course. To satisfy equilibrium, the suction varies linearly with depth in the base course. For example, if the suction at the bottom of the base course is 10 cm, the suction at the top of a 15 cm thick base course would be 25 cm. The model determines the appropriate suction profile for the amount of water in the base course after any precipitation is added. If the water from a daily precipitation event exceeds the saturation of the base course, precipitation is assumed to run-off rather than enter the base course.

3.2.2 Lateral flow in the base course

Lateral flow within the base course is estimated by assuming daily steady-state flow driven only by the lateral grade of the base course. These calculations divided the base course into 5 sub-layers. The unsaturated hydraulic conductivity for each sub-layer is determined using the suction head at the mid-point of each sub-layer. The effective lateral hydraulic conductivity of the base course is then calculated by averaging these values. The lateral flow (cm^3/sec per cm of pavement length) is then calculated as

$$Q = k_{eff} * i * th$$

where i is the lateral gradient or grade, and th is the thickness of the base course.

3.2.3 Water movement into subgrade for the case without GCBD

Flow of water into the subgrade and the subsequent saturation changes in the subgrade is calculated based on the first 60 cm of the subgrade below the base course. Flow from the base course to the subgrade is limited by the hydraulic conductivity of the subgrade material. The unsaturated hydraulic conductivity is calculated for the suction head at the base course – subgrade interface. The gradient that drives flow is calculated from the suction at the base course interface and the average suction in the first 60 cm of the subgrade. Water flow out of the 60 cm layer to lower portions of the subgrade is calculated based on an unsaturated hydraulic conductivity of the 60 cm layer, and a unit gradient (gravity flow).

For the case of no GCBD, flow into the subgrade is calculated under all suction conditions at the base course – subgrade interface. With the GCBD, flow is only calculated when the breakthrough head of the GCBD is exceeded.

3.2.4 Water movement in GCBD

The transport layer will laterally drain water based on its transmissivity. The transmissivity (cm^2/sec) is calculated as a function of the suction at the base course-subgrade interface (Stormont and Ramos, 2004). Drainage (cm^3/sec per cm of pavement length) in the transport layer is calculated from

$$Q = tran * i$$

where tran is the GCBD transmissivity and i is the lateral gradient or grade.

The water in the base course on a given day is updated after subtracting the combined lateral drainage in the base course and the transport layer. If the updated suction head at the bottom of the base course exceeds the breakthrough head of the transport layer, water will move downward into the subgrade.

The amount of water in the base course is updated, and the suction head at the interface is calculated. If this value exceeds the breakthrough head, the excess water is removed laterally by flow in the geonet.

3.2.5 Calculation inputs

The material properties of the base course and subgrade materials as well as the precipitation data have been previously described. The calculations assume the 43% of the daily precipitation infiltrates into the base course. This value is the mean value of the range of infiltration amounts for asphalt pavement that the DRIP program uses (Malella et al., 2002), and is a long-standing traditional estimate of the amount of infiltration that may pass through an asphalt pavement (Ridgeway, 1982).

The calculations assume a constant lateral slope or grade of 2%. Most of the calculations assume the base layer is 15 cm thick, and has a lateral drainage length of 400 cm (nominally one traffic lane). Thicker base course and a longer lateral drainage length are also considered. The base course and the subgrade are assumed to begin at 50% saturation for all calculations.

3.2.6 Results and discussion

Results of 24 model simulations are presented in a series of figures that follow this section (Figures 3.6 to 3.53). Results are included from model simulations using 4 different base course, 3 different subgrades, 3 different climates, and different pavement geometries. Results from each set of conditions were used to produce two figures. In one figure, the saturations of the base course and subgrade layer both with and without the GCBD are presented for the year-long simulation. The other figure is an annual water balance for the model with and without the GCBD.

The results are consistent with the GCBD functioning as a capillary barrier: the capillary barrier effect of the GCBD prevents water from moving from the base course to the subgrade until the base course gets very wet. In contrast, without a GCBD, there is no barrier to water movement from the base course to the subgrade.

The consequence of the capillary barrier effect of the GCBD is that the subgrade is largely isolated from downward infiltrating water. This is quantified by the change in subgrade saturation and the amount of subgrade vertical flow shown in annual water balance figures. In every case, the GCBD results in less water in the subgrade compared to the same conditions but without a GCBD. In many cases, the 60 cm of the subgrade immediately below the base course saturates without a GCBD, whereas with a GCBD. For an example, see Figure 3.14.

Water that is retained in base course above the GCBD due to the capillary barrier effect can drain laterally either in the base course itself or in the transport layer of the GCBD. The amount that drains in the transport layer vs. the base course depends principally on the base course properties. If the base course has a relatively low conductivity, it will not be effective in laterally draining water. This is the case with the dense graded base course (see Figures 3.12 through 3.17). If the base course retains little water, then water in the base course tends to reside at the bottom of the base course. The majority of the base course will have a low water content and a corresponding low conductivity, and consequently will not divert much water. The transport layer will be in contact with the wet portion of the base course, and will have the opportunity to remove this water. This is why the stone base course removes less water laterally than the GCBD transport layer (see Figures 3.24 through 3.29). In contrast, if the base course retains enough water to be conductive through much of its thickness, then most of the water will be laterally diverted in the base course. This is condition for the permeable base (see Figures 3.18 through 3.23). The conventional base response is intermediate between that of the dense graded and permeable base.

The capillary barrier effect often results in somewhat more water being retained in the base course compared to the case of no GCBD. The differences in saturation tend to be modest, usually less than 10%. When the base course is not an effective drainage medium such as the case of the dense graded base, then the saturation of the base course without the GCBD can be substantially greater than that of in the GCBD configuration (see Figures 3.12, 3.14, and 3.16).

The results indicate that the GCBD permits breakthrough into the subgrade under some conditions. Breakthrough is generally in response to large precipitation events. The amount of

water that moves into the base course depends on the hydraulic conductivity of the base course. For example, contrast the results obtained with a conventional base course but three different subgrade soils exposed to the Minneapolis climate (Figures 3.6, 3.8 and 3.10 for clay, clay loam and silt, respectively). In all cases, there is breakthrough in response to precipitation input around day 100 and day 220. The change in saturation in response to breakthrough is imperceptible for the clay, barely detectable for the clay loam, and noticeable for the silt. This is because subgrade soils with greater hydraulic conductivity will accept more water. If the subgrade does not accept much water, then the bottom of the base course may saturate and water will drain laterally in the geonet. Note that the silt has no geonet drainage, whereas there is geonet drainage for the clay and clay loam subgrades (Figure 3.7, 3.9, and 3.11).

The GCBD is restored after breakthrough. Water is removed from the base course through lateral drainage in the base course, transport layer and geonet, as well as any flow into the subgrade. After breakthrough, the GCBD is restored. In this way, the subgrade is once again isolated from the base course. This can be observed in results where there is a noticeable increase in saturation of the subgrade due to breakthrough, and then a reduction in the saturation as water in the subgrade moves downward (for example, see Figure 3.16).

The drainage length was increased from 400 to 800 cm for the case of dense graded and permeable base courses with the clay loam subgrade. The 800 cm length corresponds to a two-lane configuration. For the dense graded base course, more breakthrough into the subgrade occurs with the longer drainage length. This is because the lateral diversion capacity of the transport layer is exceeded more often for the case of the longer lateral drainage distance. Contrast the results for the 400 cm length given in Figures 3.14 and 3.15 with those with the 800 cm length given in Figures 25 and 26. For the permeable base course, there is virtually no difference between the results with the two different lengths (see Figures 3.20, 3.21, 3.34, and 3.35). This is because the majority of the lateral drainage occurs in the base course and not in the transport layer for these conditions.

Results with a thicker base course indicate little difference in the water balance. Refer to Figures 3.30 through 3.33 for results with a dense graded base and Figures 3.34 through 3.37 for results with a permeable base.

GCBD performance depends on precipitation stress, both the amount and timing. Most often, the greater precipitation, the more water is laterally diverted by the transport layer and the less breakthrough there is. Exceptions to this generality occur with the conventional and stone base course: the Albany climate results in less breakthrough than the Minneapolis climate even though there is substantially more precipitation (compare Figures 3.8 and 3.9 with Figure 3.46 and 3.47 for the conventional base course and Figure 3.28 and 3.29 with Figures 3.52 and 3.53 for the stone base course). This result is a consequence of the timing and magnitude of specific precipitation events.

The permeable base with a GCBD prevents any breakthrough for all climates (Figures 3.20, 3.21, 3.42, 3.43, 3.50 and 3.51). The dense graded base course performance, both in terms of how much water is diverted in the transport layer and how much breaks through into the subgrade, is dependent on the climate (Figure 3.14, 3.15, 3.40, 3.41, 3.48, and 3.49).

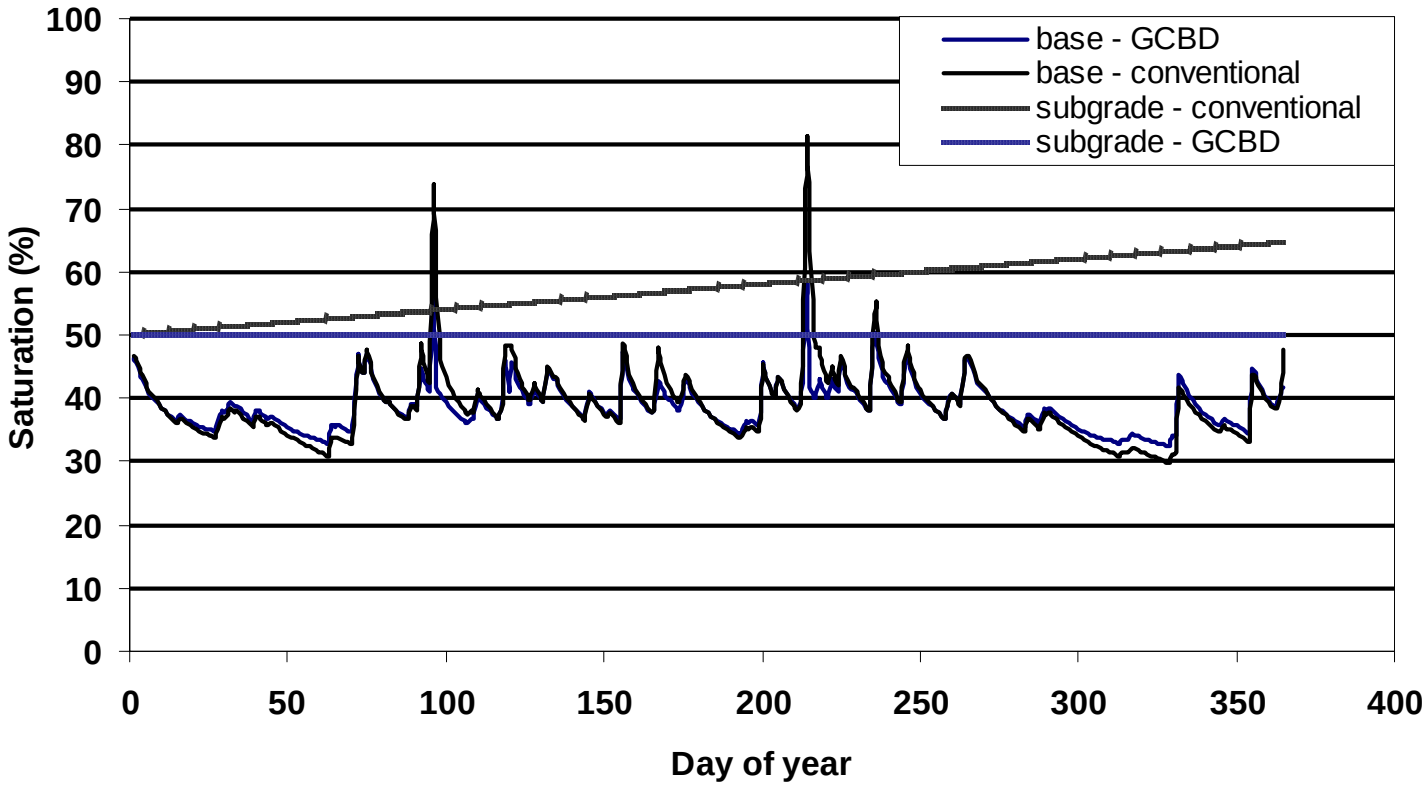

Figure 3.6 – Saturations of base course and subgrade for case with and without GCBD. Conditions: conventional base course 15 cm thick, 400 cm width, clay subgrade, and Minneapolis climate.

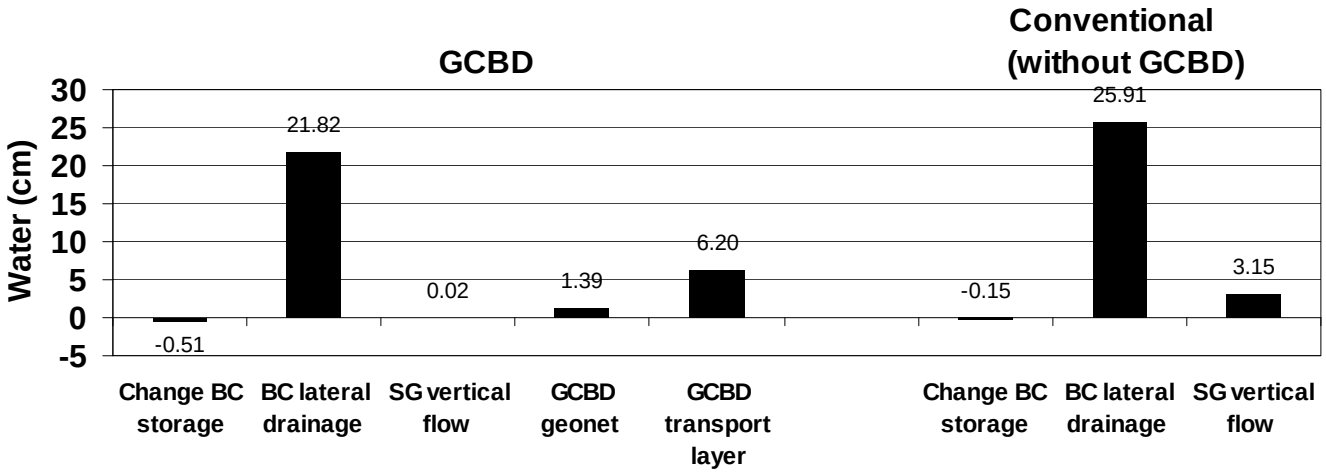

Figure 3.7 – Annual water balance results. Conditions: conventional base course 15 cm thick, 400 cm width, clay subgrade, and Minneapolis climate.

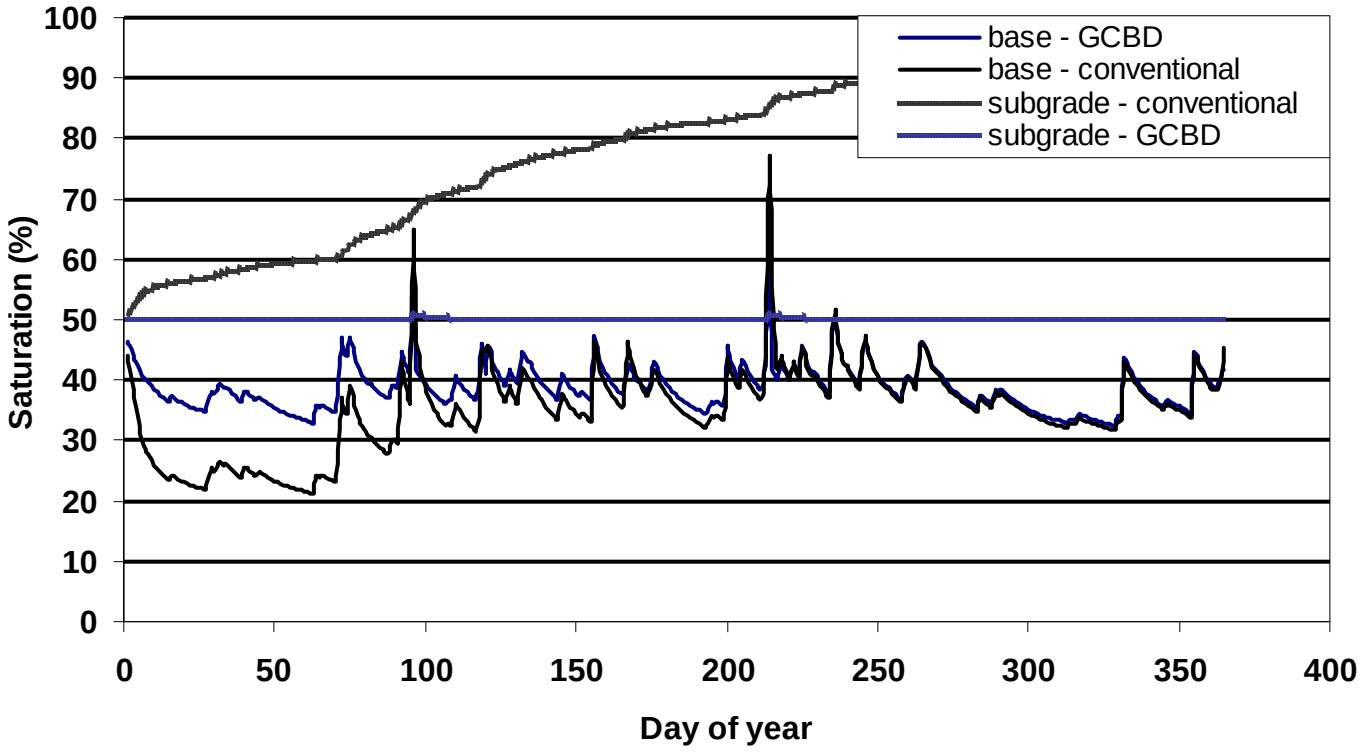

Figure 3.8 – Saturations of base course and subgrade for case with and without GCBD. Conditions: conventional base course 15 cm thick, 400 cm width, clay loam subgrade, and Minneapolis climate.

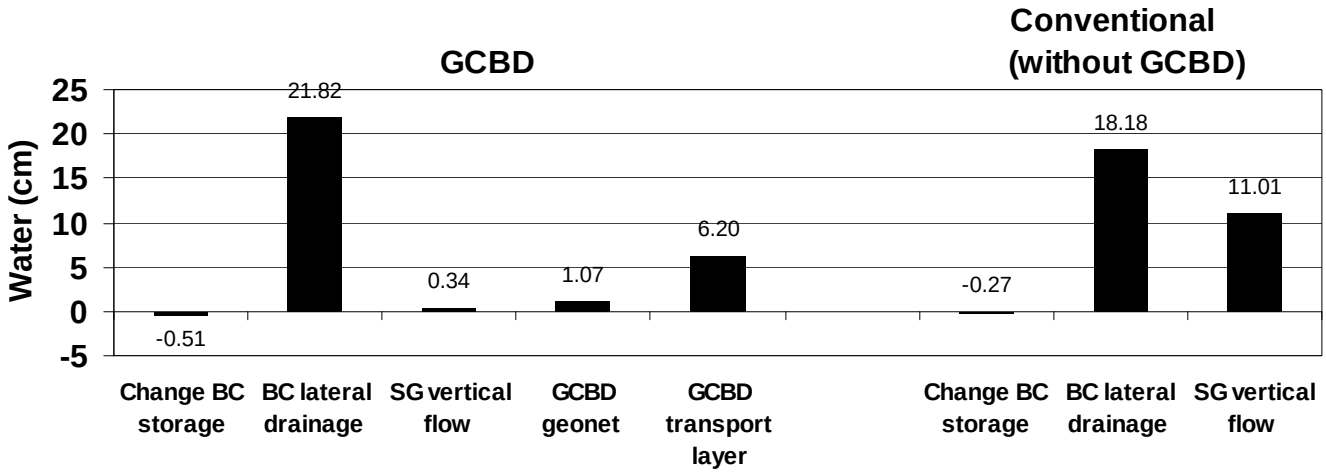

Figure 3.9 – Annual water balance results. Conditions: conventional base course 15 cm thick, 400 cm width, clay loam subgrade, and Minneapolis climate.

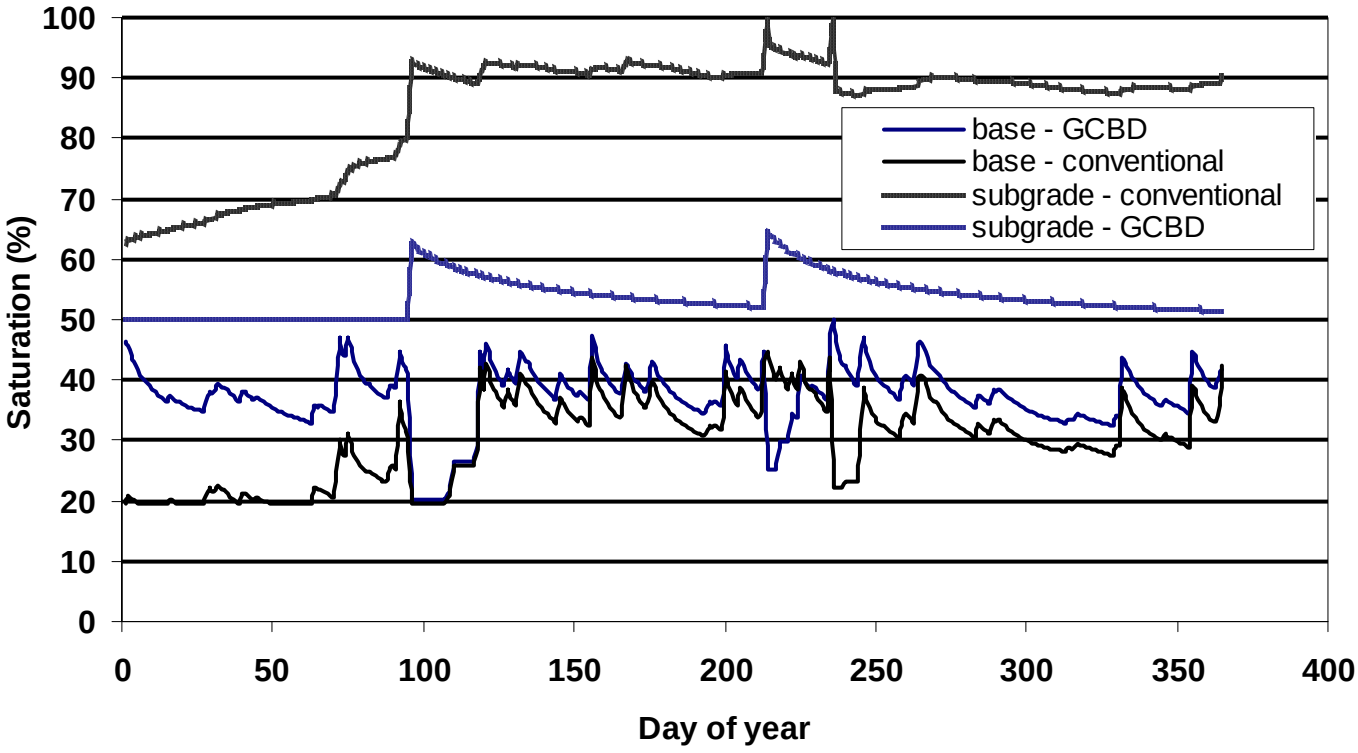

Figure 3.10 – Saturations of base course and subgrade for case with and without GCBD. Conditions: conventional base course 15 cm thick, 40 cm width, silt subgrade, and Minneapolis climate.

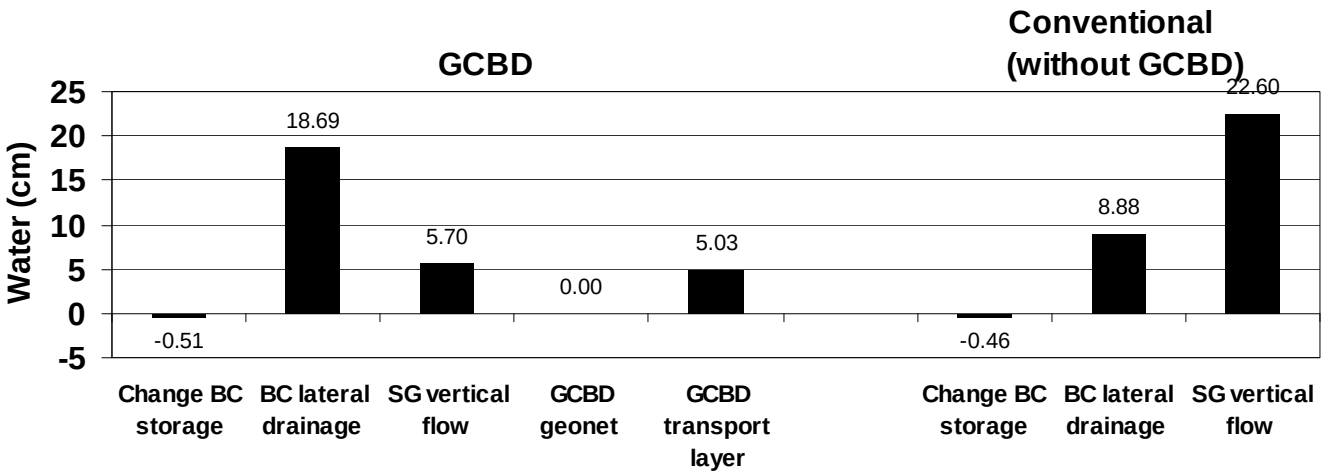

Figure 3.11 – Annual water balance results. Conditions: conventional base course 15 cm thick, 400 cm width, silt subgrade, and Minneapolis climate.

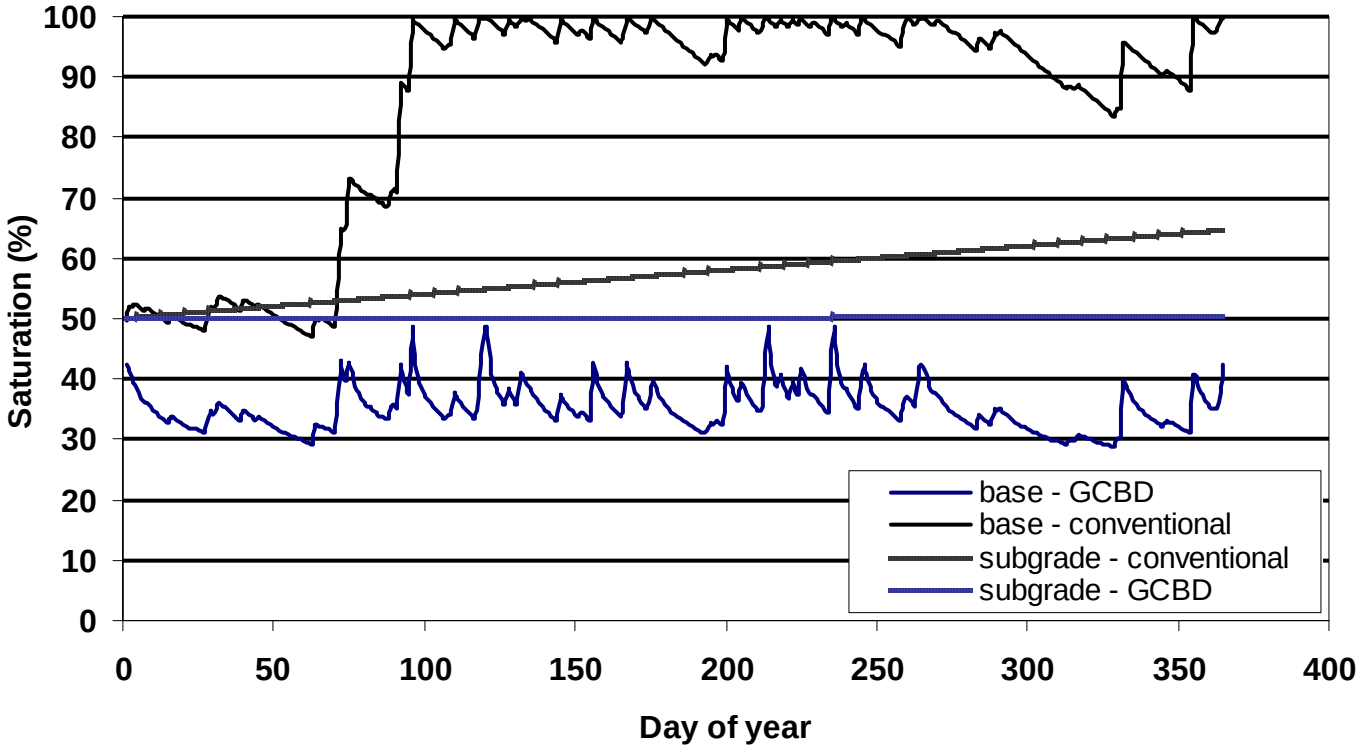

Figure 3.12 – Saturations of base course and subgrade for case with and without GCBD. Conditions: dense graded base course 15 cm thick, 400 cm width, clay subgrade, and Minneapolis climate.

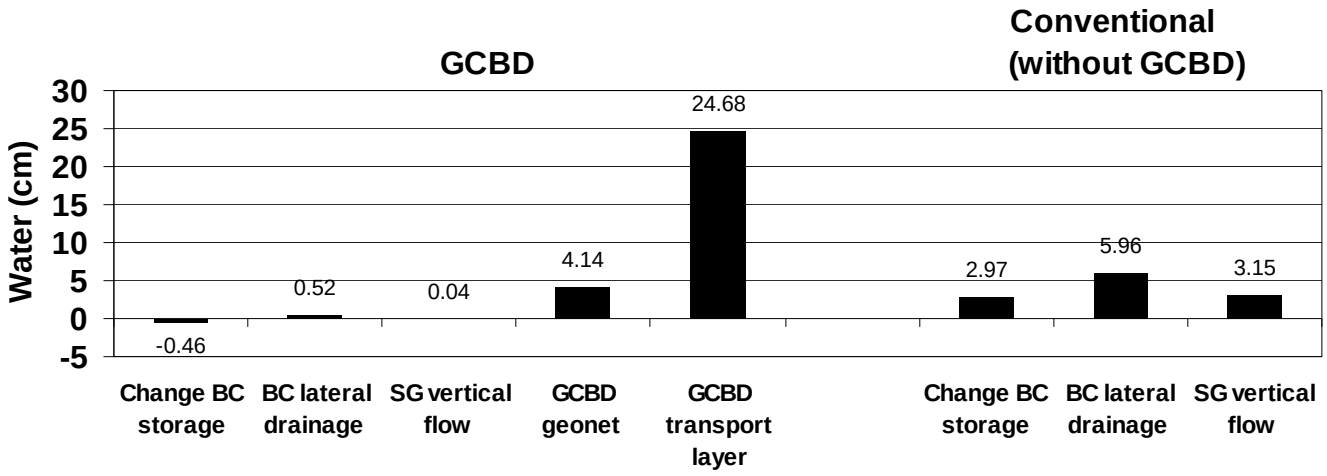

Figure 3.13 – Annual water balance results. Conditions: dense graded base course 15 cm thick, 400 cm width, clay subgrade, and Minneapolis climate.

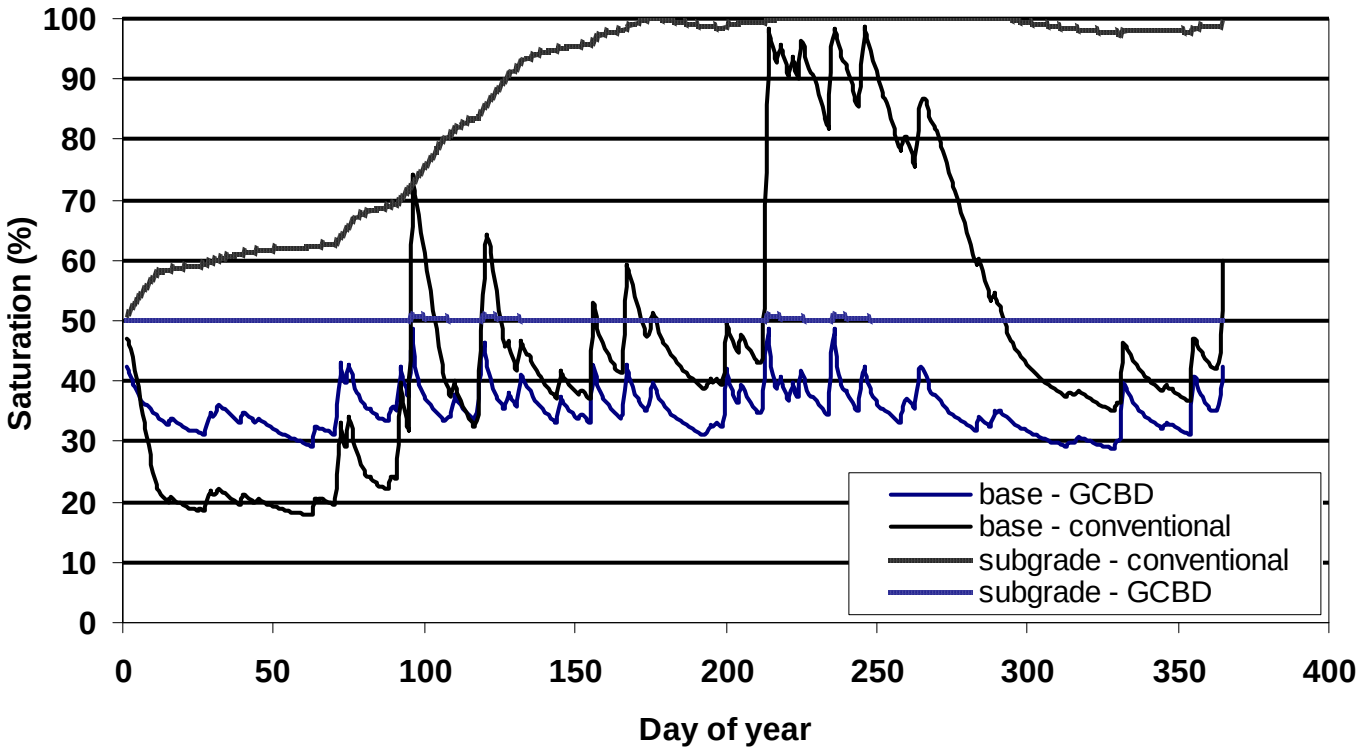

Figure 3.14 – Saturations of base course and subgrade for case with and without GCBD. Conditions: dense graded base course 15 cm thick, 400 cm width, clay loam subgrade, and Minneapolis climate.

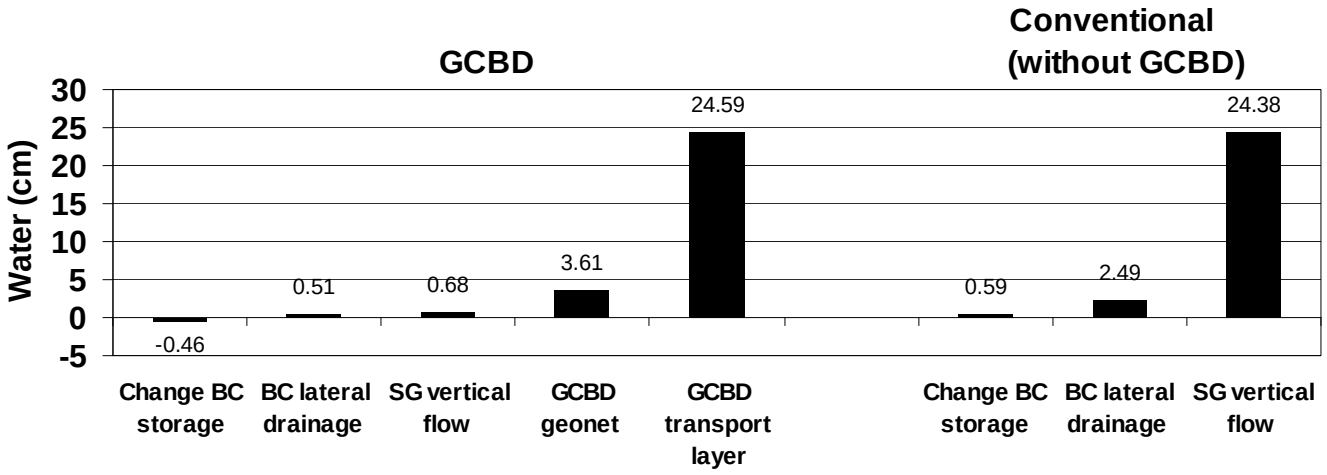

Figure 3.15 – Annual water balance results. Conditions: dense graded base course 15 cm thick, 400 cm width, clay loam subgrade, and Minneapolis climate.

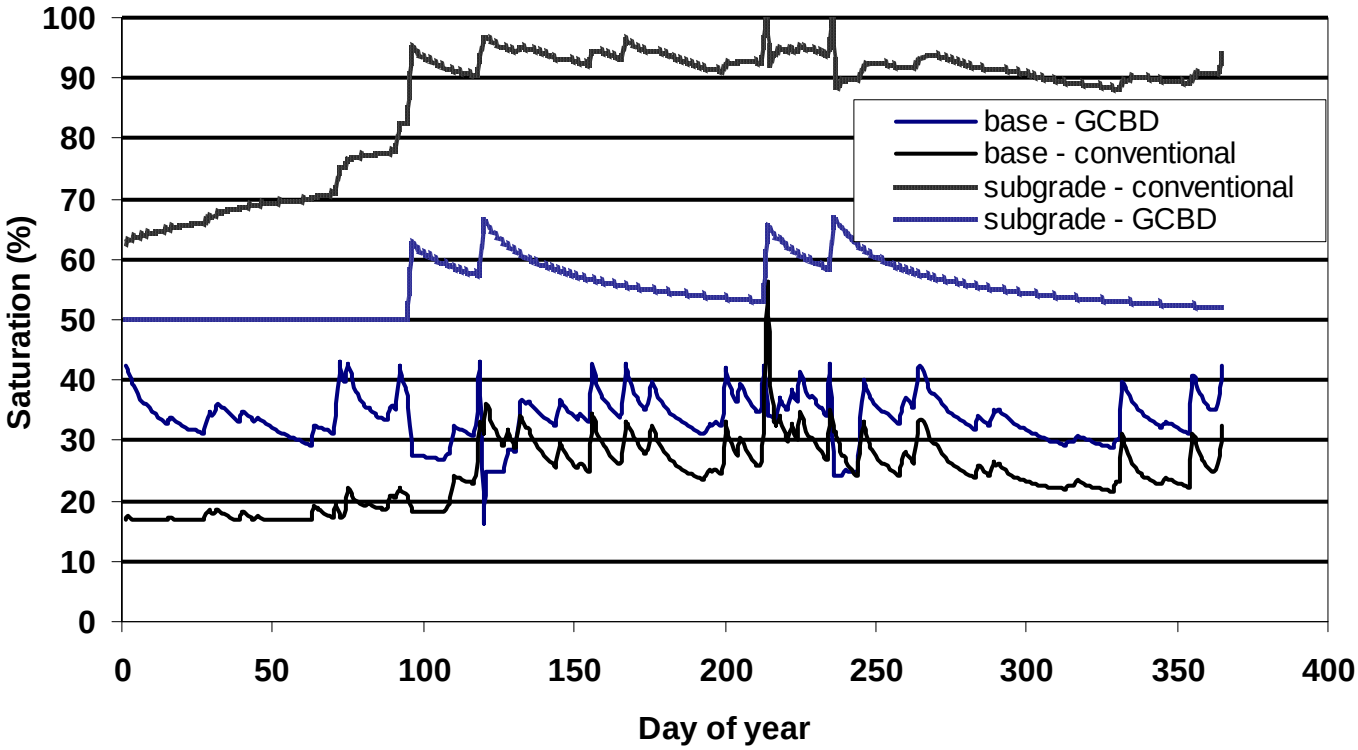

Figure 3.16 – Saturations of base course and subgrade for case with and without GCBD. Conditions: dense graded base course 15 cm thick, 400 cm width, silt subgrade, and Minneapolis climate.

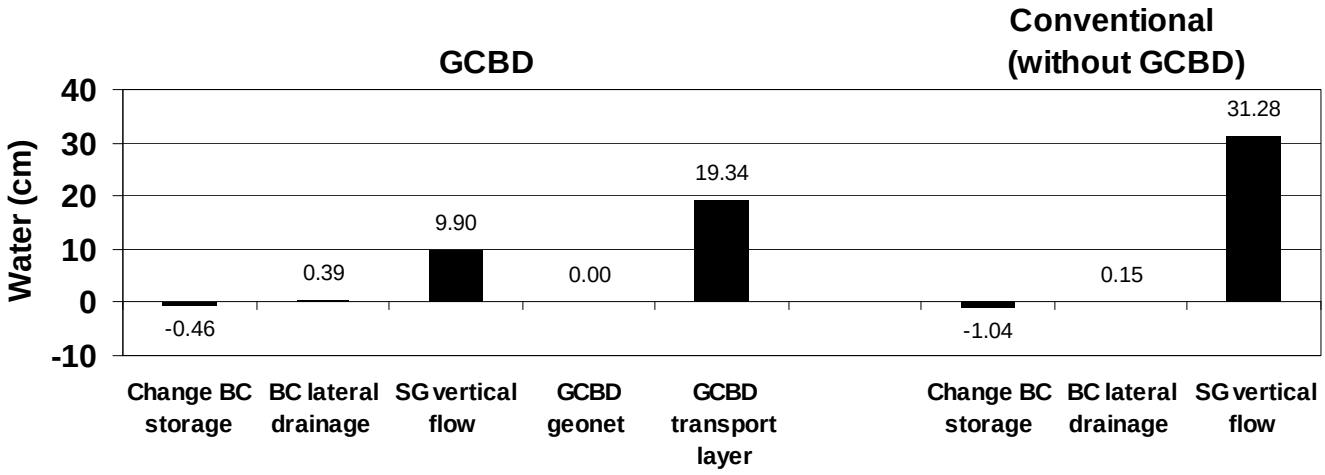

Figure 3.17 – Annual water balance results. Conditions: dense graded base course 15 cm thick, 400 cm width, silt subgrade, and Minneapolis climate.

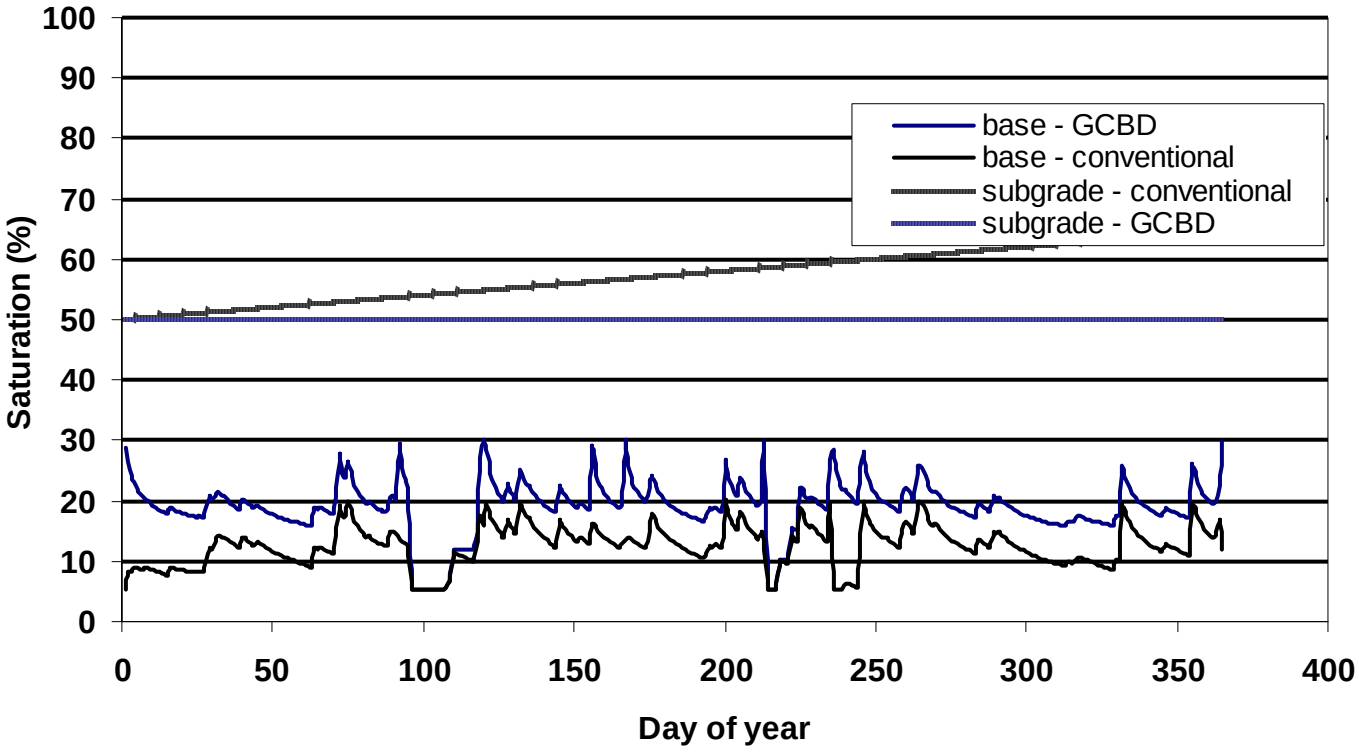

Figure 3.18 – Saturations of base course and subgrade for case with and without GCBD. Conditions: permeable base course 15 cm thick, 400 cm width, clay subgrade, and Minneapolis climate.

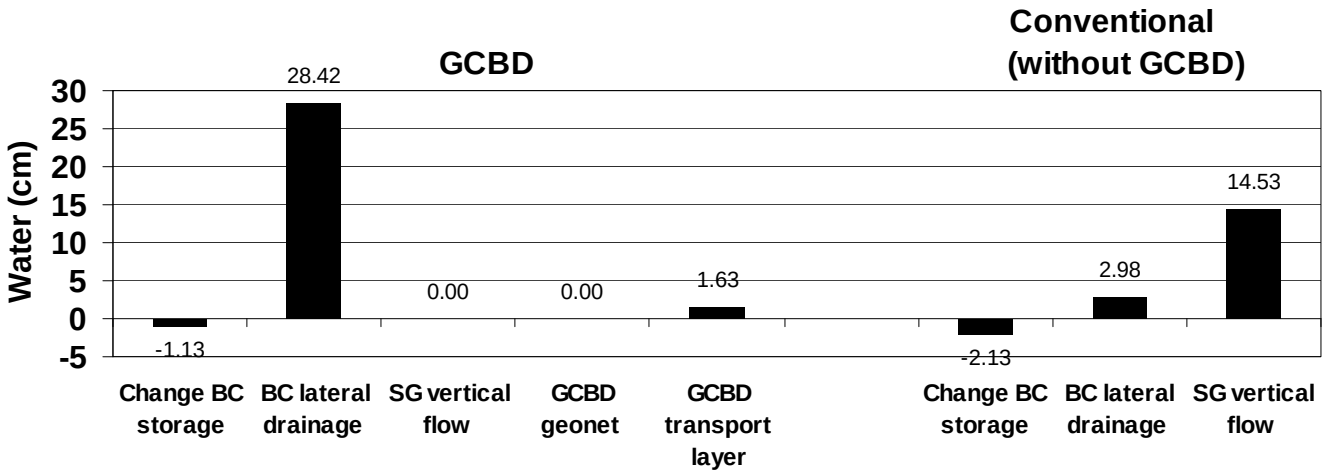

Figure 3.19 – Annual water balance results. Conditions: permeable base course 15 cm thick, 400 cm width, clay subgrade, and Minneapolis climate.

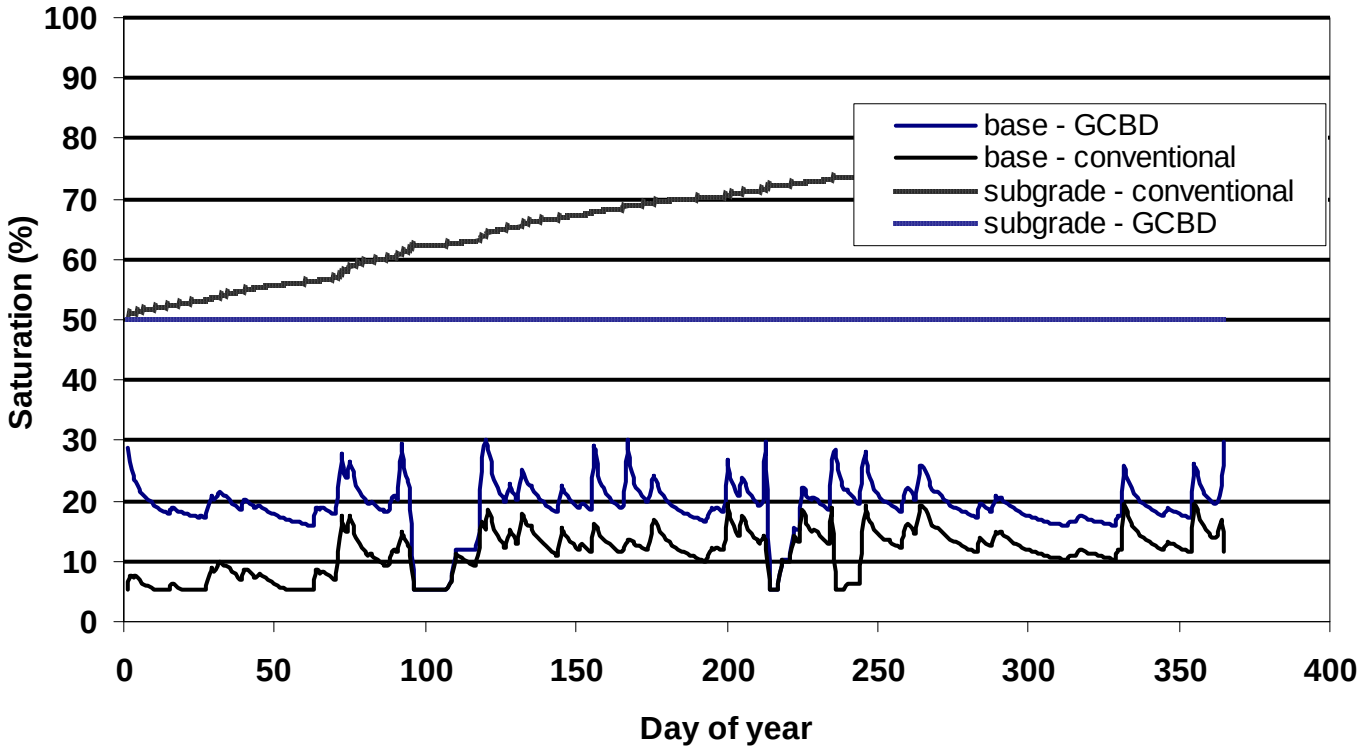

Figure 3.20 – Saturations of base course and subgrade for case with and without GCBD. Conditions: permeable base course 15 cm thick, 400 cm width, clay loam subgrade, and Minneapolis climate.

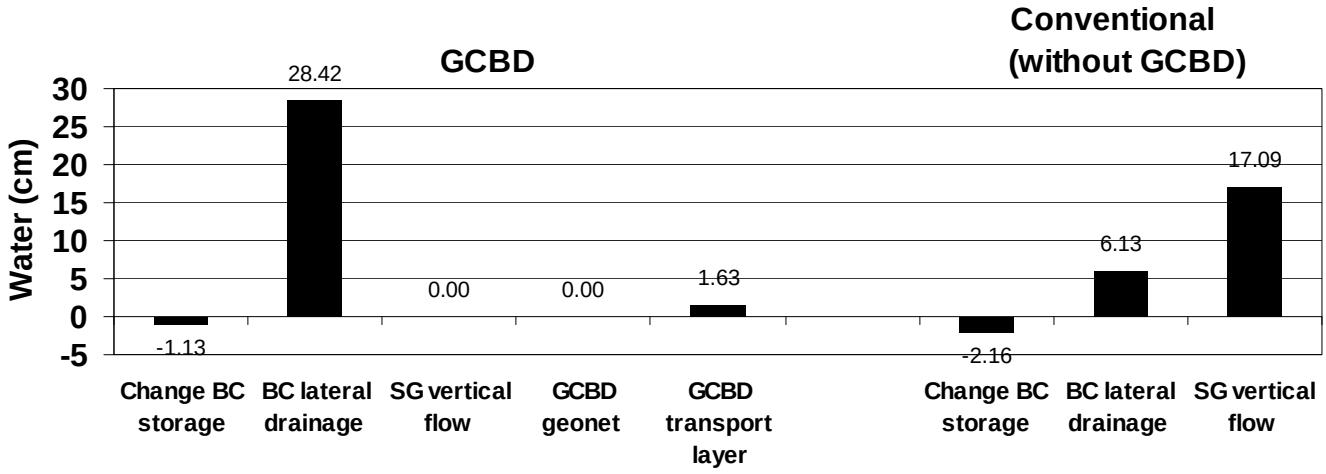

Figure 3.21 – Annual water balance results. Conditions: permeable base course 15 cm thick, 400 cm width, clay loam subgrade, and Minneapolis climate.

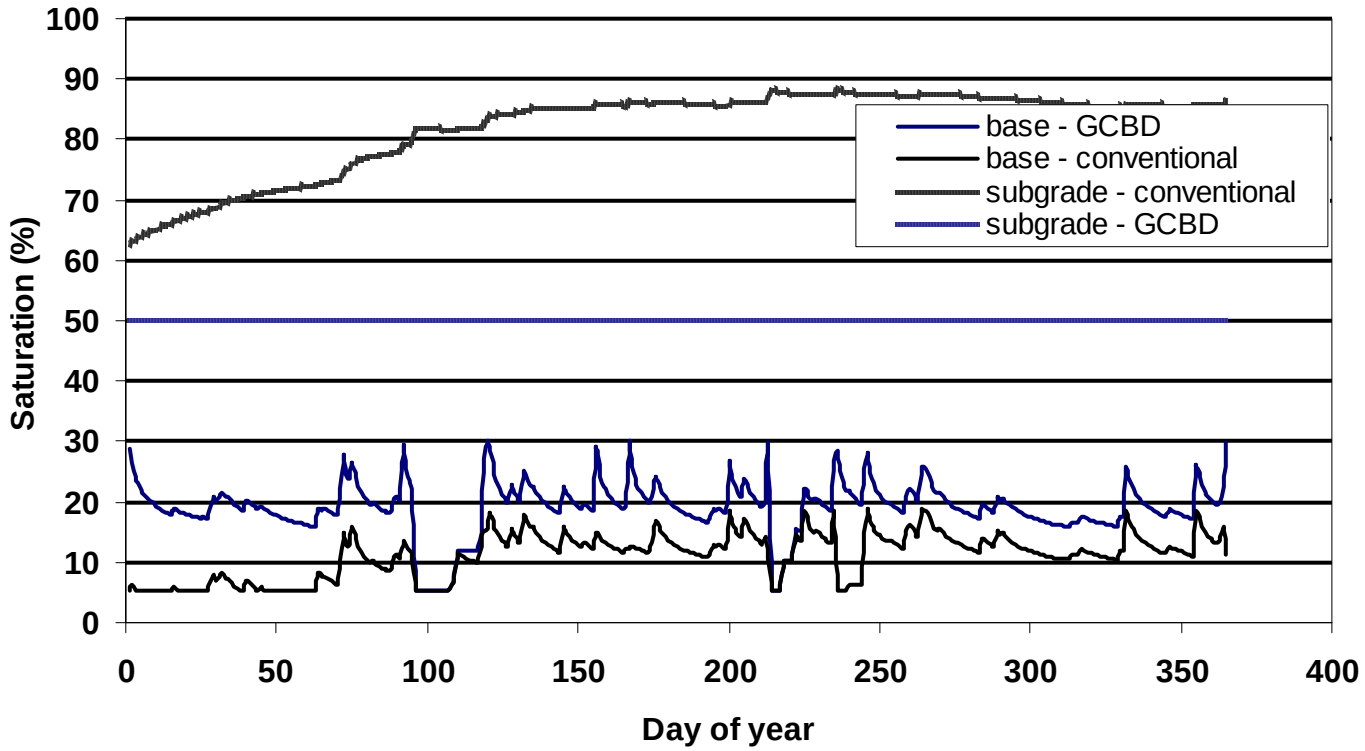

Figure 3.22 – Saturations of base course and subgrade for case with and without GCBD. Conditions: permeable base course 15 cm thick, 400 cm width, silt subgrade, and Minneapolis climate.

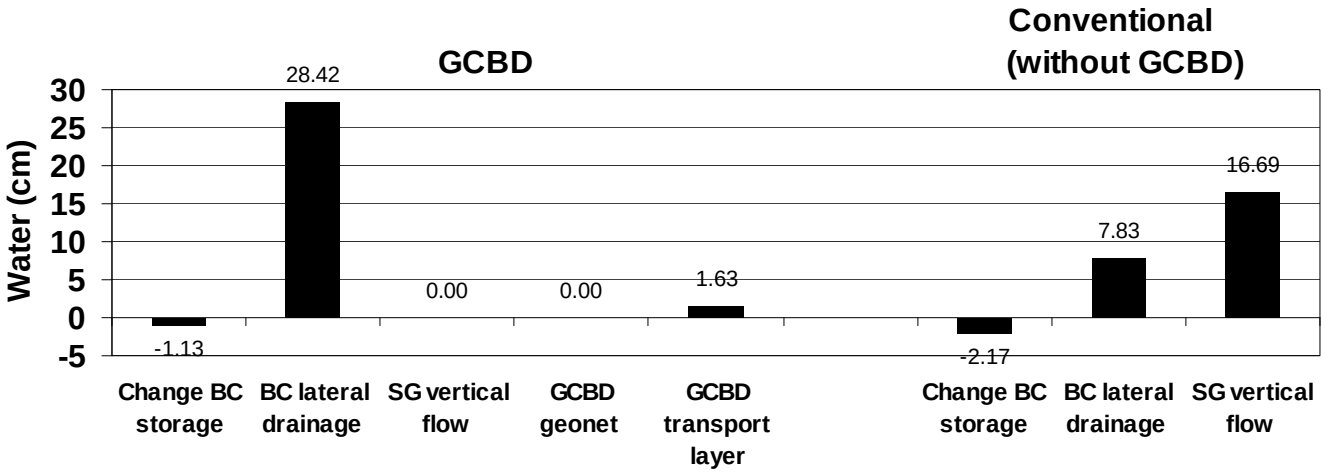

Figure 3.23 – Annual water balance results. Conditions: permeable base course 15 cm thick, 400 cm width, silt subgrade, and Minneapolis climate.

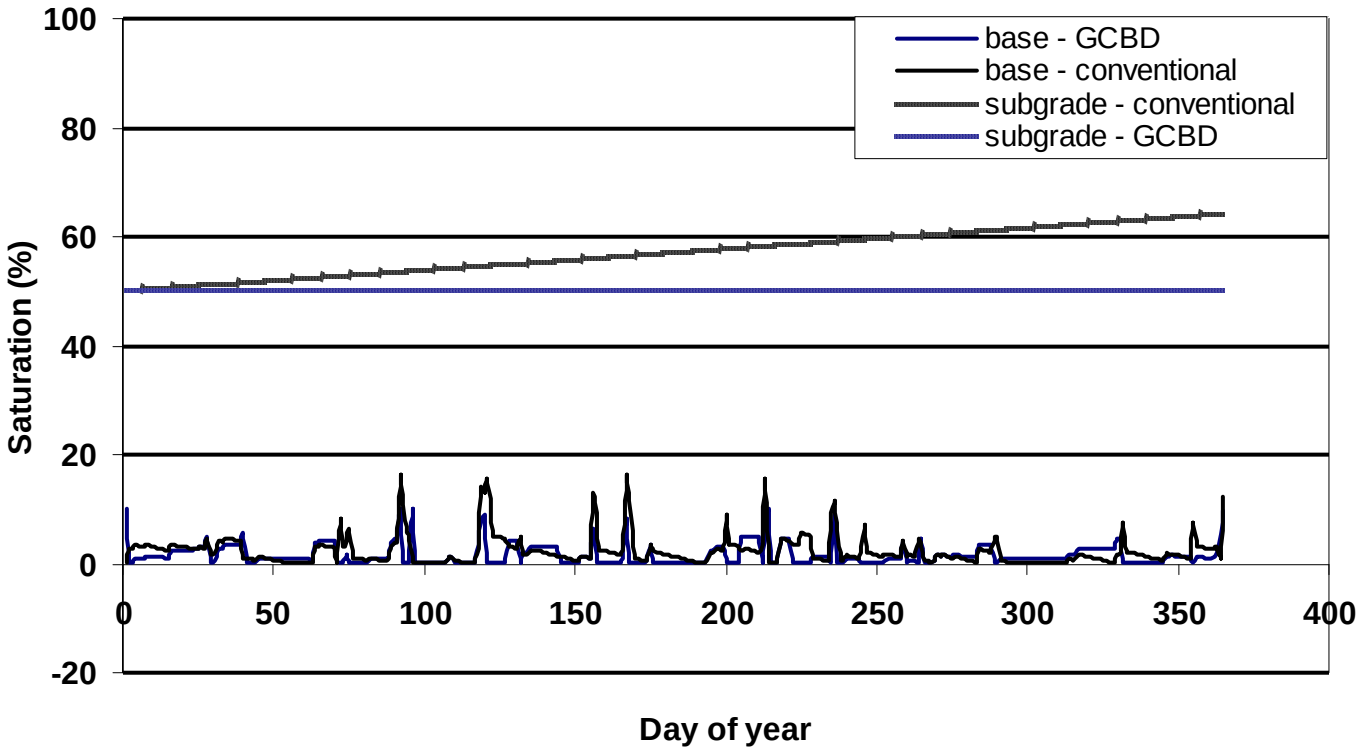

Figure 3.24 – Saturations of base course and subgrade for case with and without GCBD. Conditions: stone base course 15 cm thick, 40 cm width, clay subgrade, and Minneapolis climate.

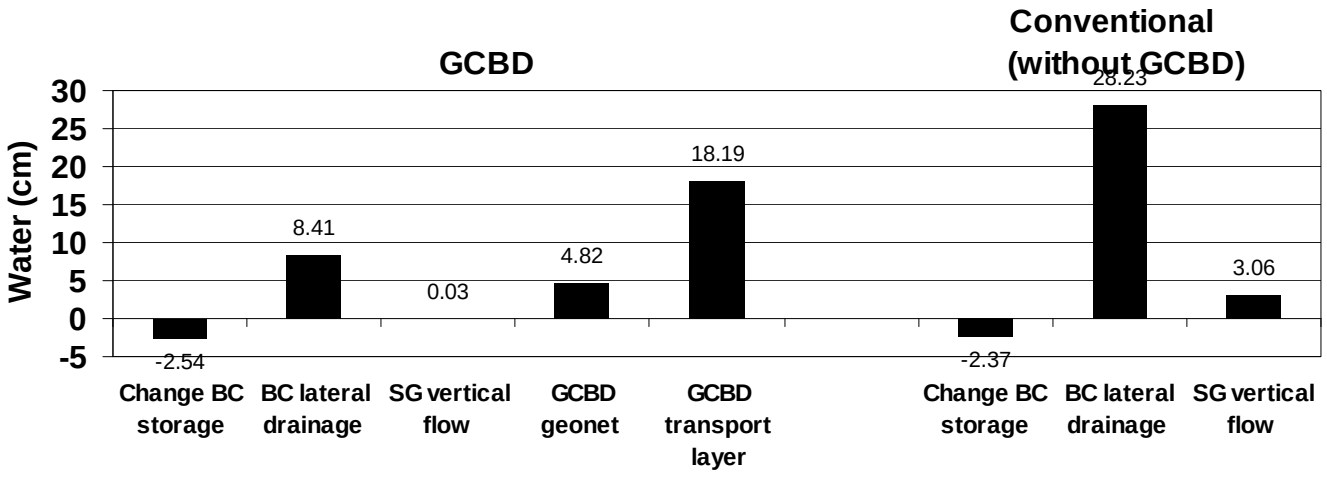

Figure 3.25 – Annual water balance results. Conditions: stone base course 15 cm thick, 400 cm width, clay subgrade, and Minneapolis climate.

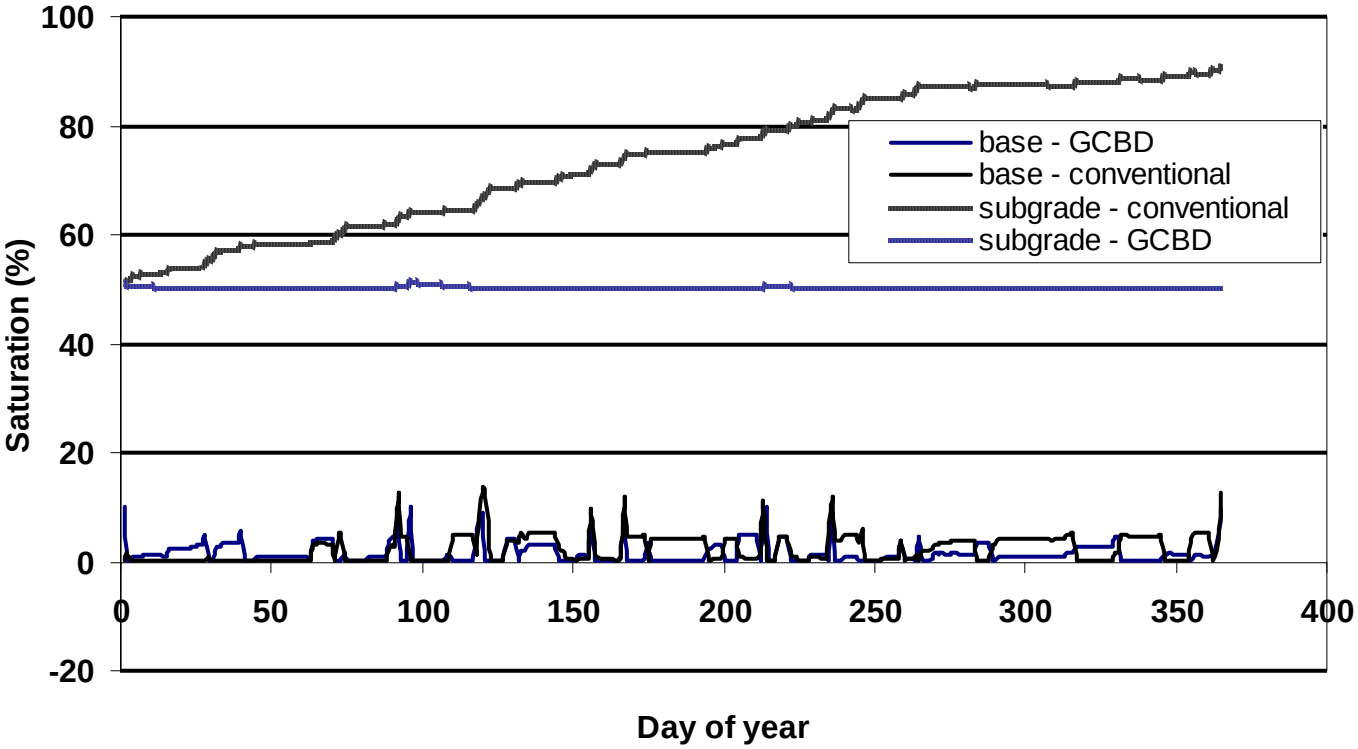

Figure 3.26 – Saturations of base course and subgrade for case with and without GCBD. Conditions: stone base course 15 cm thick, 400 cm width, clay loam subgrade, and Minneapolis climate.

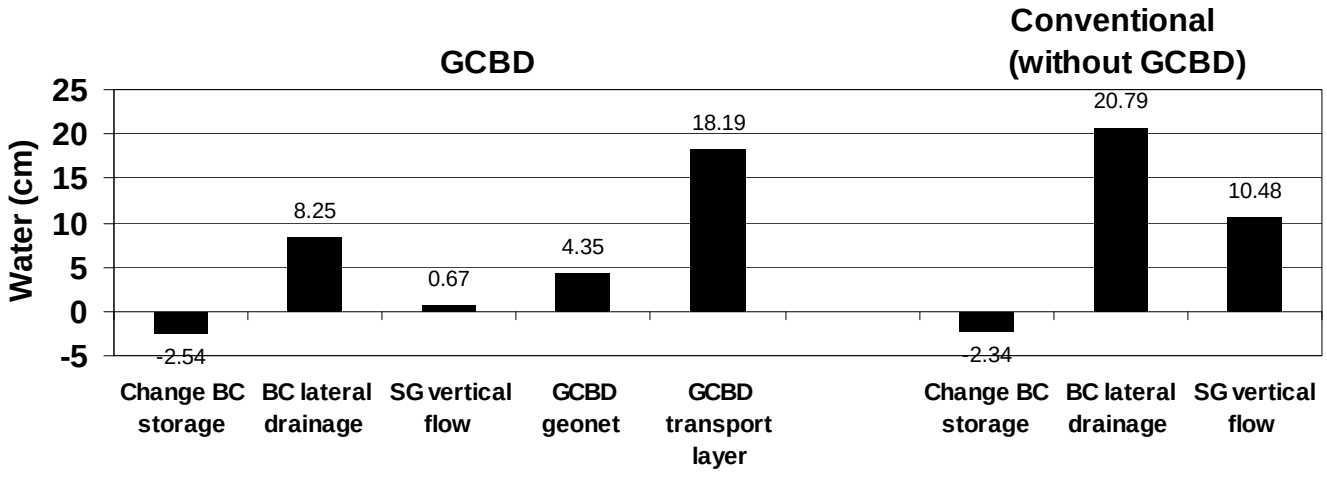

Figure 3.27 – Annual water balance results. Conditions: stone base course 15 cm thick, 400 cm width, clay loam subgrade, and Minneapolis climate.

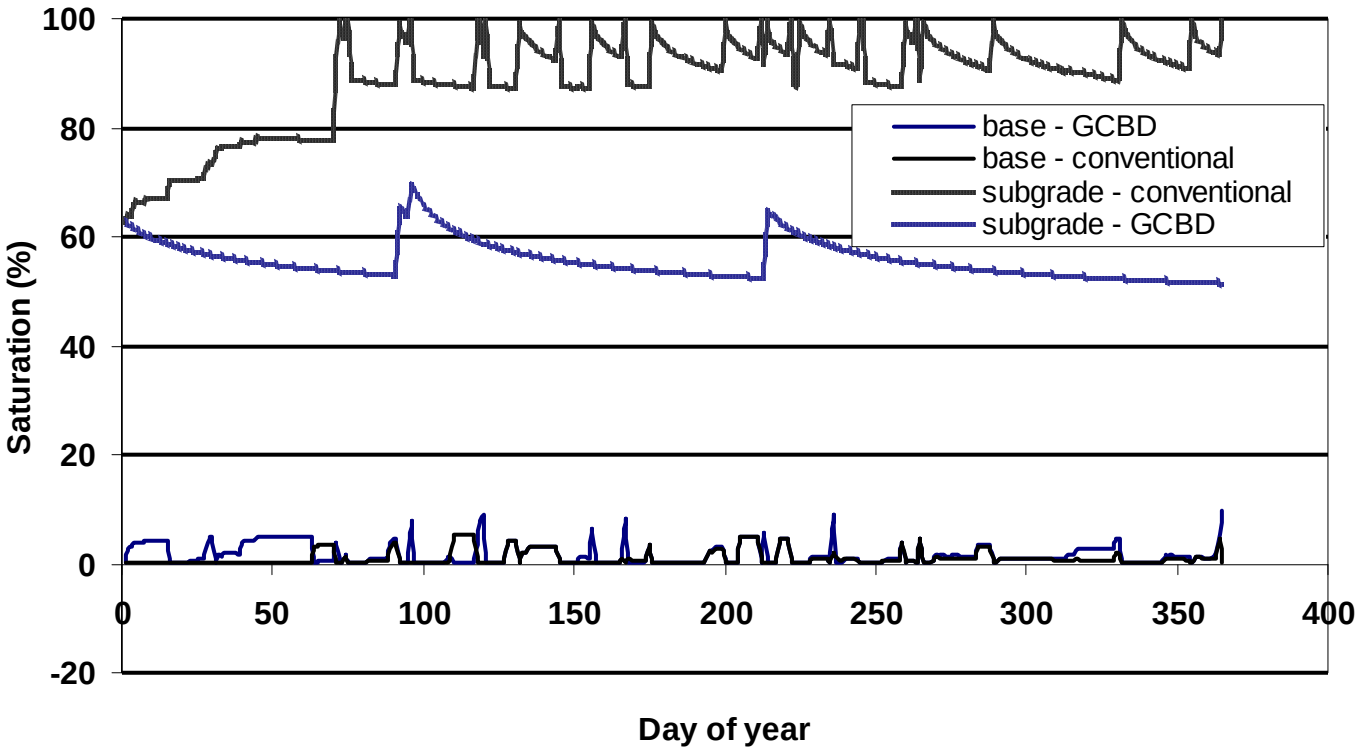

Figure 3.28 – Saturations of base course and subgrade for case with and without GCBD. Conditions: stone base course 15 cm thick, 400 cm width, silt subgrade, and Minneapolis climate.

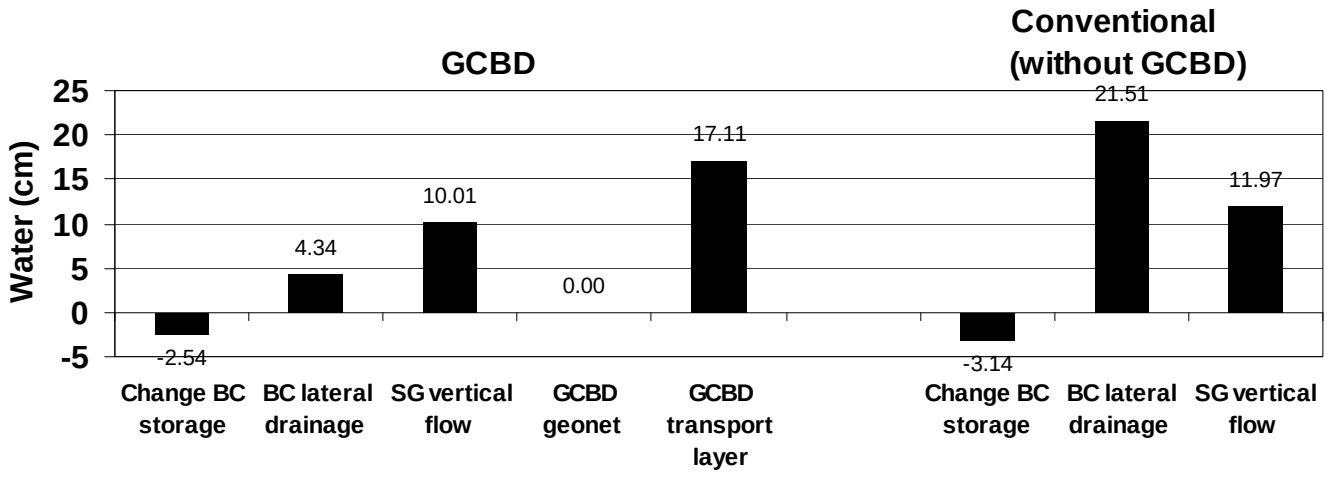

Figure 3.29 – Annual water balance results. Conditions: stone base course 15 cm thick, 400 cm width, silt subgrade, and Minneapolis climate.

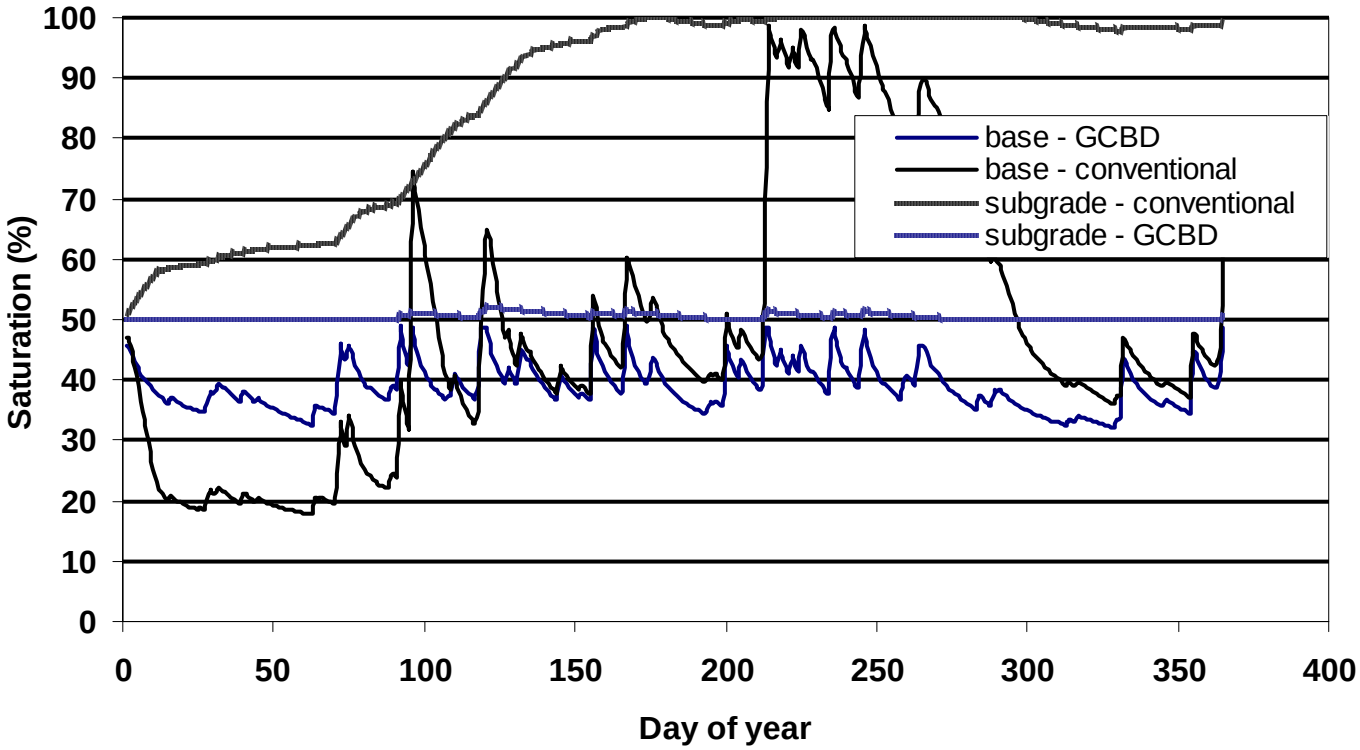

Figure 3.30 – Saturations of base course and subgrade for case with and without GCBD. Conditions: dense graded base course 15 cm thick, 800 cm width, clay loam subgrade, and Minneapolis climate.

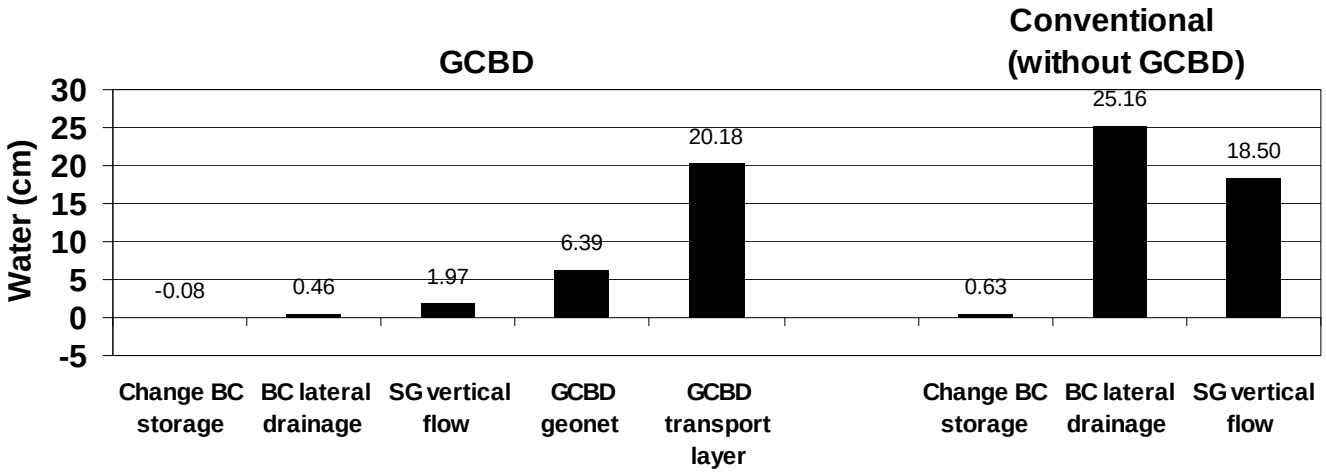

Figure 3.31 – Annual water balance results. Conditions: dense graded base course 15 cm thick, 800 cm width, clay loam subgrade, and Minneapolis climate.

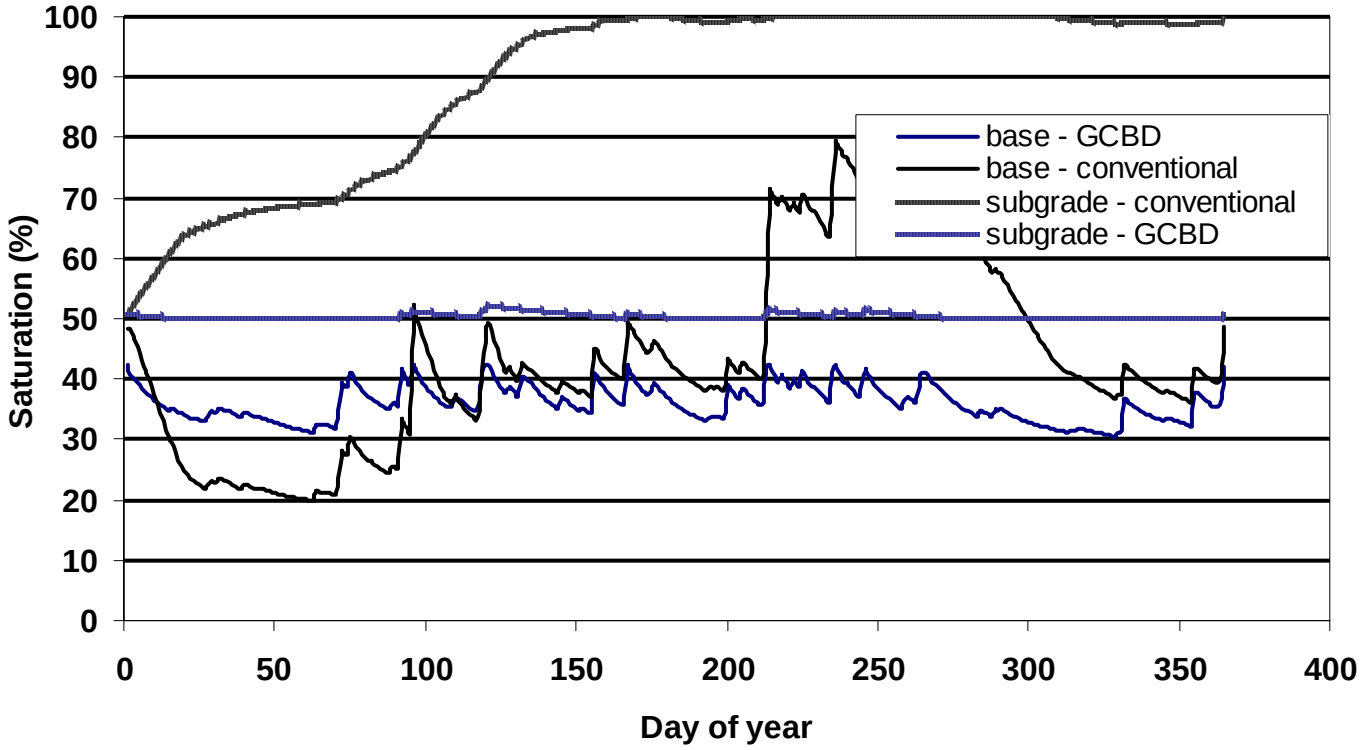

Figure 3.32 – Saturations of base course and subgrade for case with and without GCBD. Conditions: dense graded base course 30 cm thick, 800 cm width, clay loam subgrade, and Minneapolis climate.

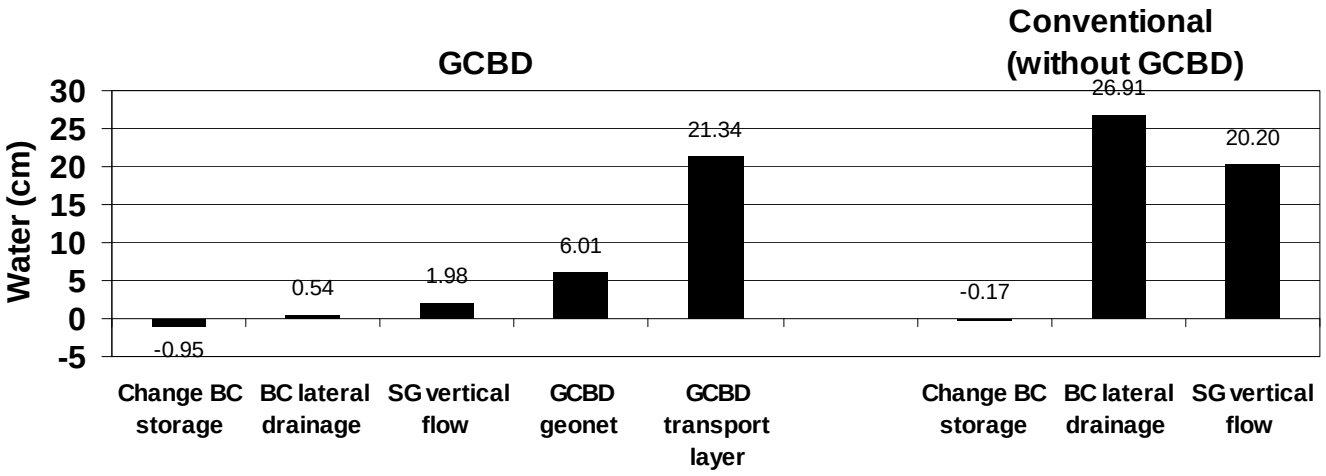

Figure 3.33 – Annual water balance results. Conditions: dense graded base course 30 cm thick, 800 cm width, clay loam subgrade, and Minneapolis climate.

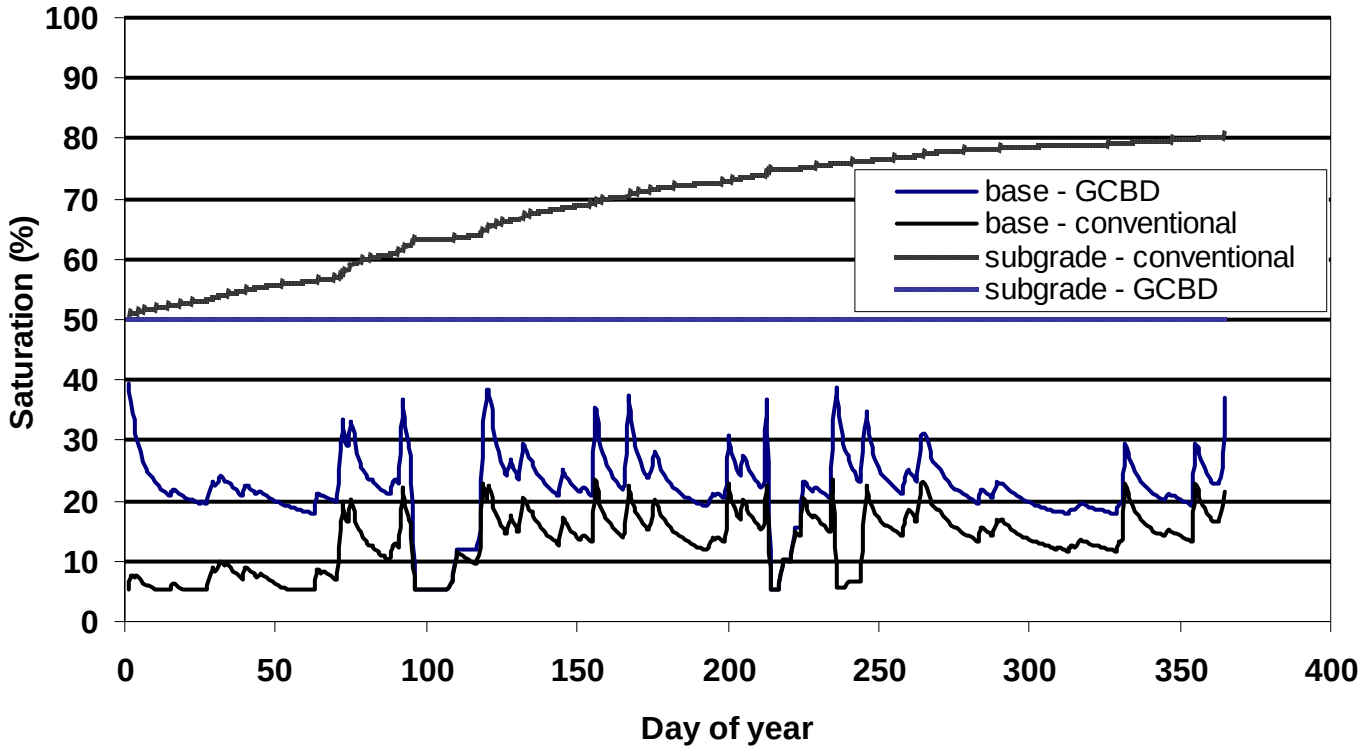

Figure 3.34 – Saturations of base course and subgrade for case with and without GCBD. Conditions: permeable base course 15 cm thick, 800 cm width, clay loam subgrade, and Minneapolis climate.

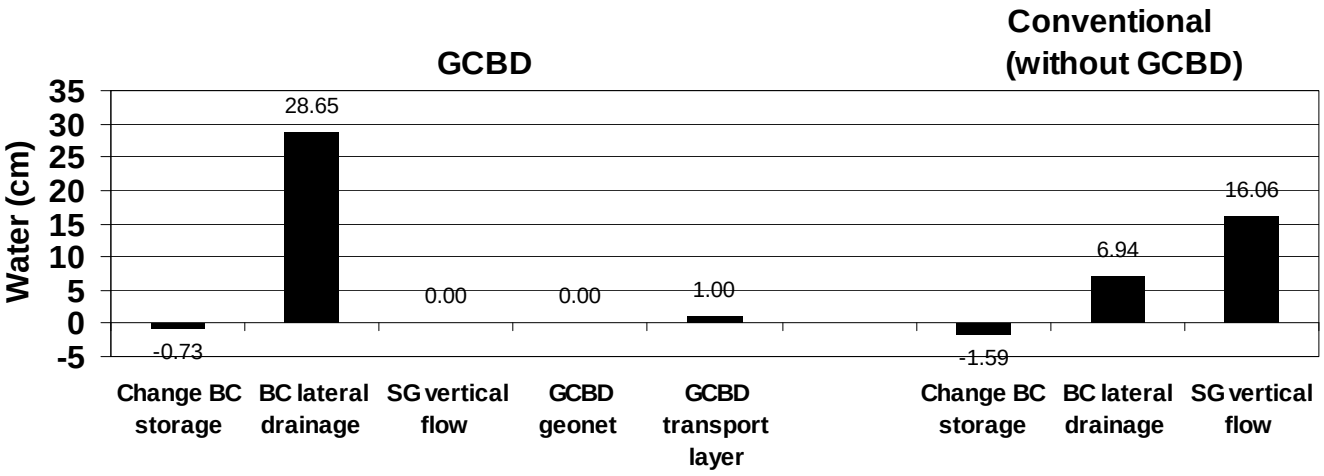

Figure 3.35 – Annual water balance results. Conditions: permeable base course 15 cm thick, 800 cm width, clay loam subgrade, and Minneapolis climate.

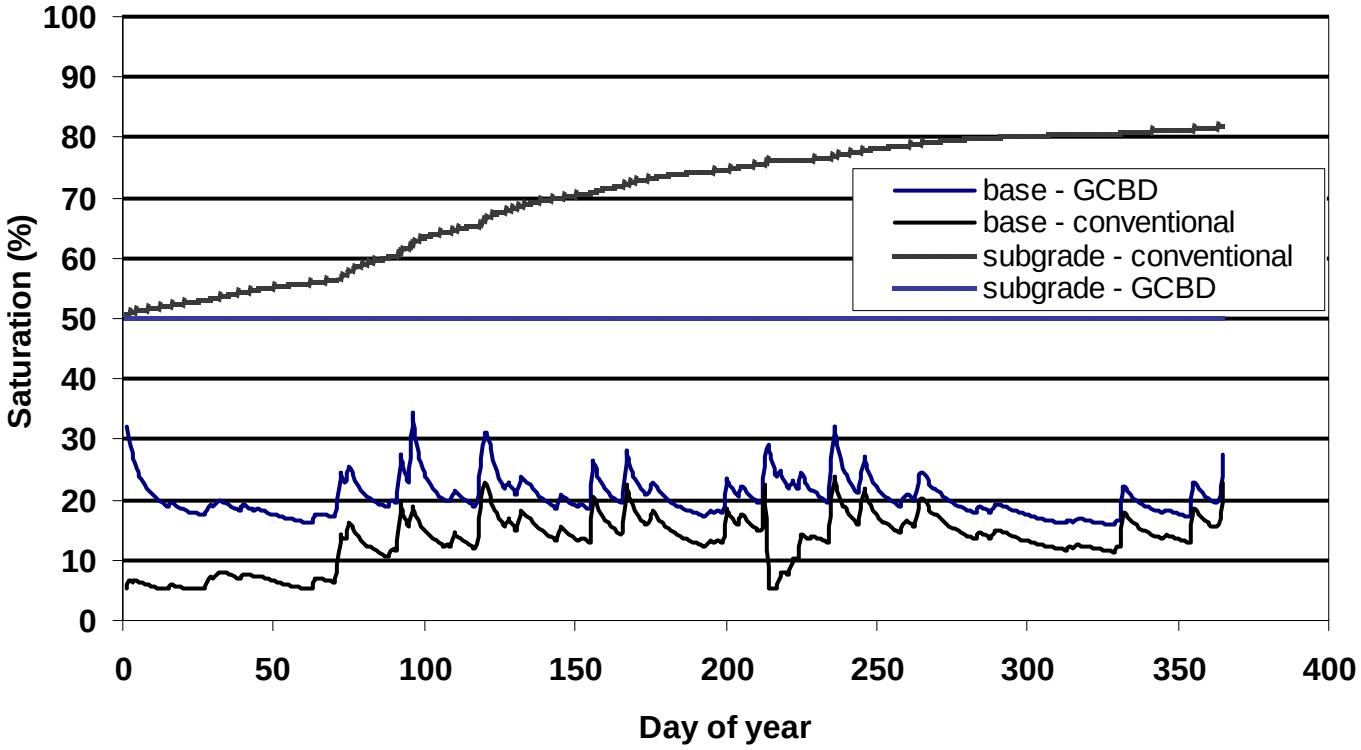

Figure 3.36 – Saturations of base course and subgrade for case with and without GCBD. Conditions: permeable base course 30 cm thick, 800 cm width, clay loam subgrade, and Minneapolis climate.

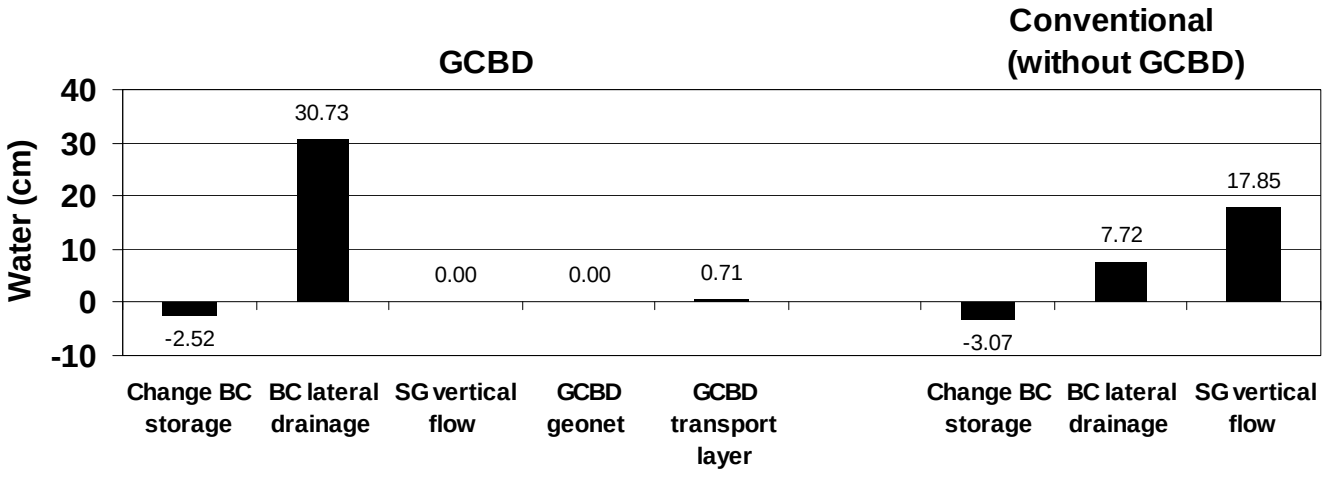

Figure 3.37 – Annual water balance results. Conditions: permeable base course 30 cm thick, 800 cm width, clay loam subgrade, and Minneapolis climate.

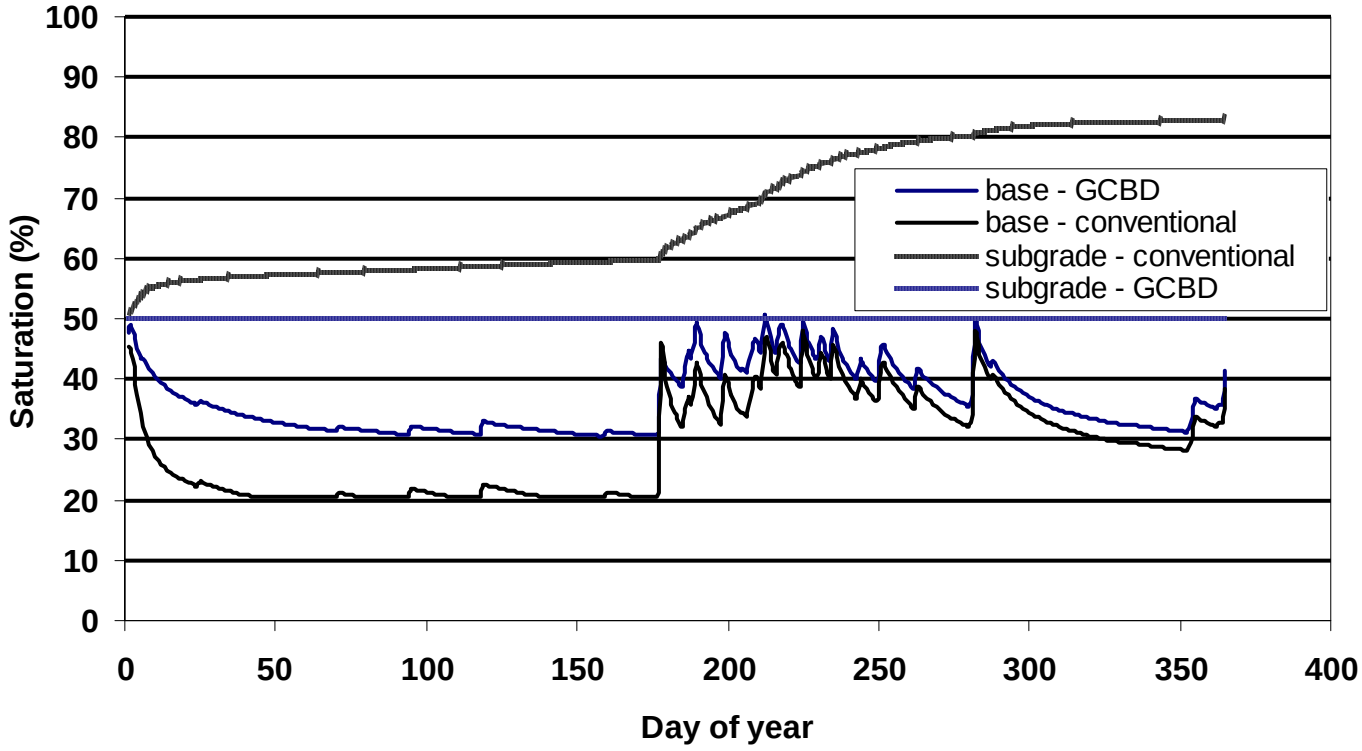

Figure 3.38 – Saturations of base course and subgrade for case with and without GCBD. Conditions: conventional base course 15 cm thick, 400 cm width, clay loam subgrade, and Albuquerque climate.

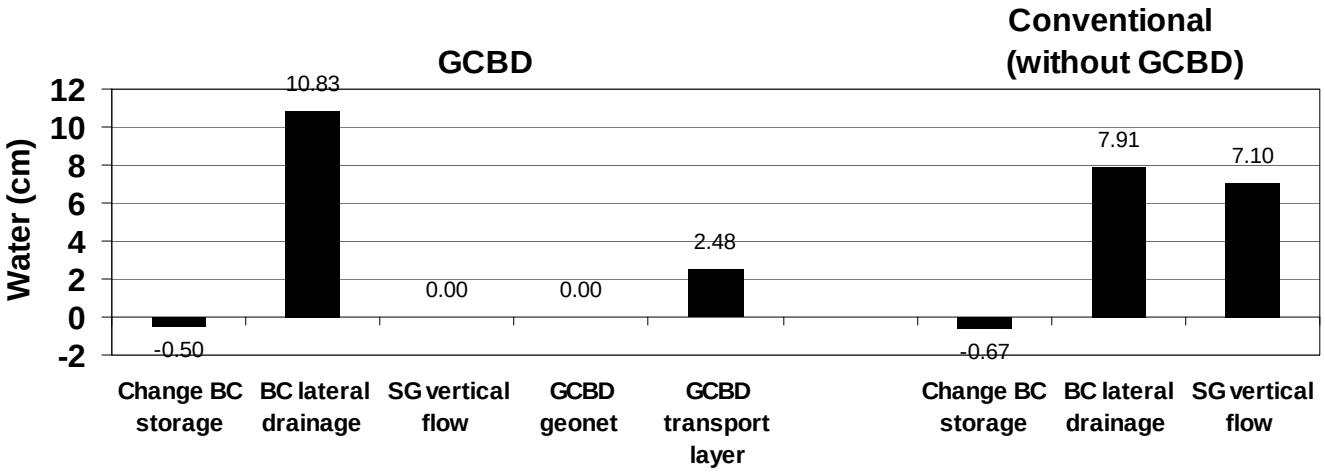

Figure 3.39 – Annual water balance results. Conditions: conventional base course 15 cm thick, 400 cm width, clay loam subgrade, and Albuquerque climate.

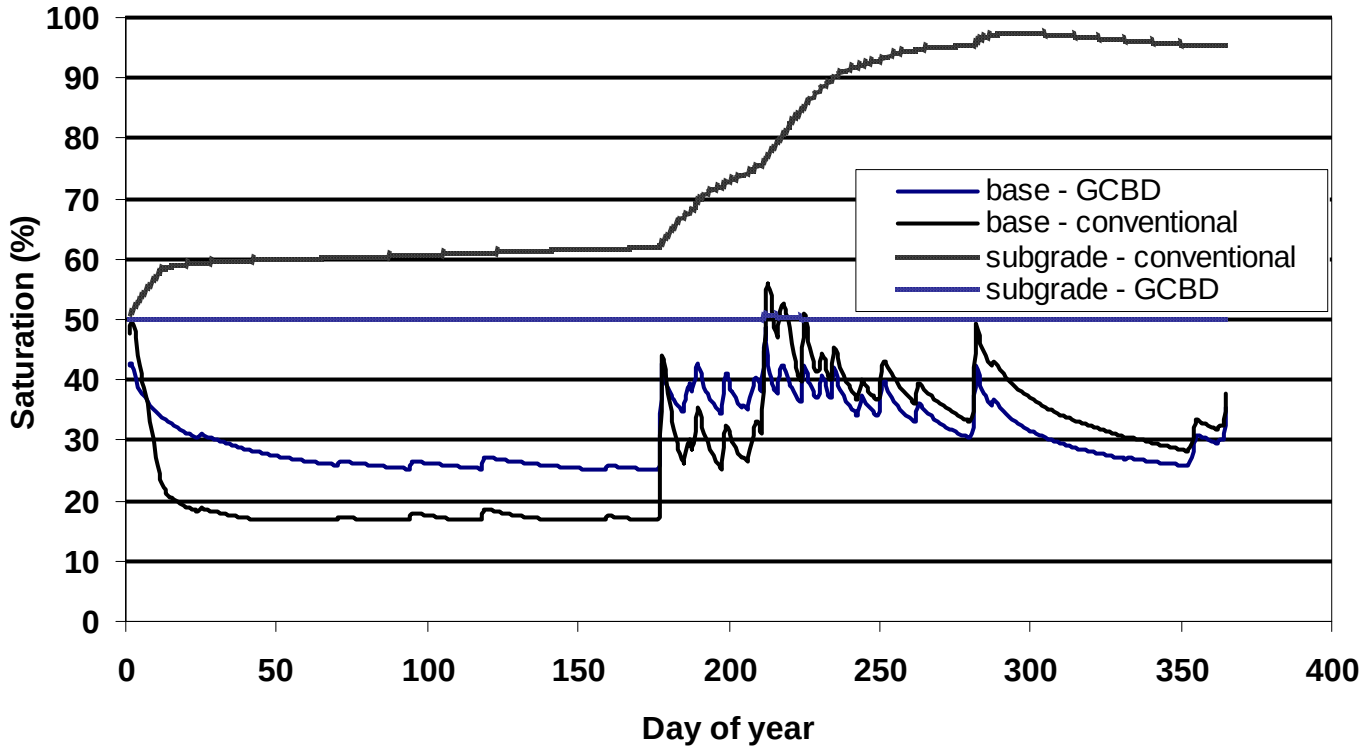

Figure 3.40 – Saturations of base course and subgrade for case with and without GCBD. Conditions: dense graded base course 15 cm thick, 400 cm width, clay loam subgrade, and Albuquerque climate.

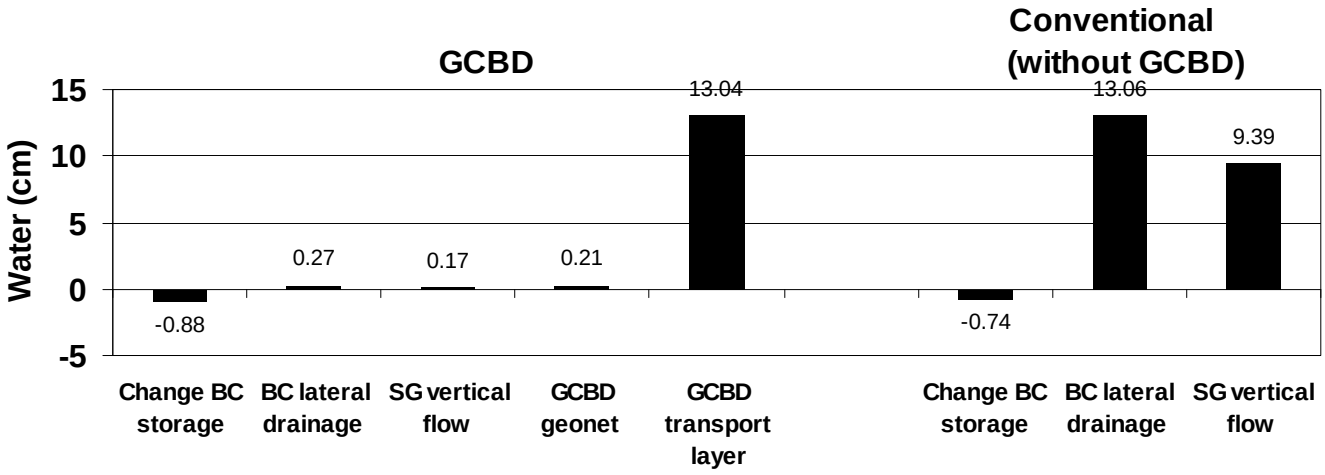

Figure 3.41 – Annual water balance results. Conditions: dense graded base course 15 cm thick, 400 cm width, clay loam subgrade, and Albuquerque climate.

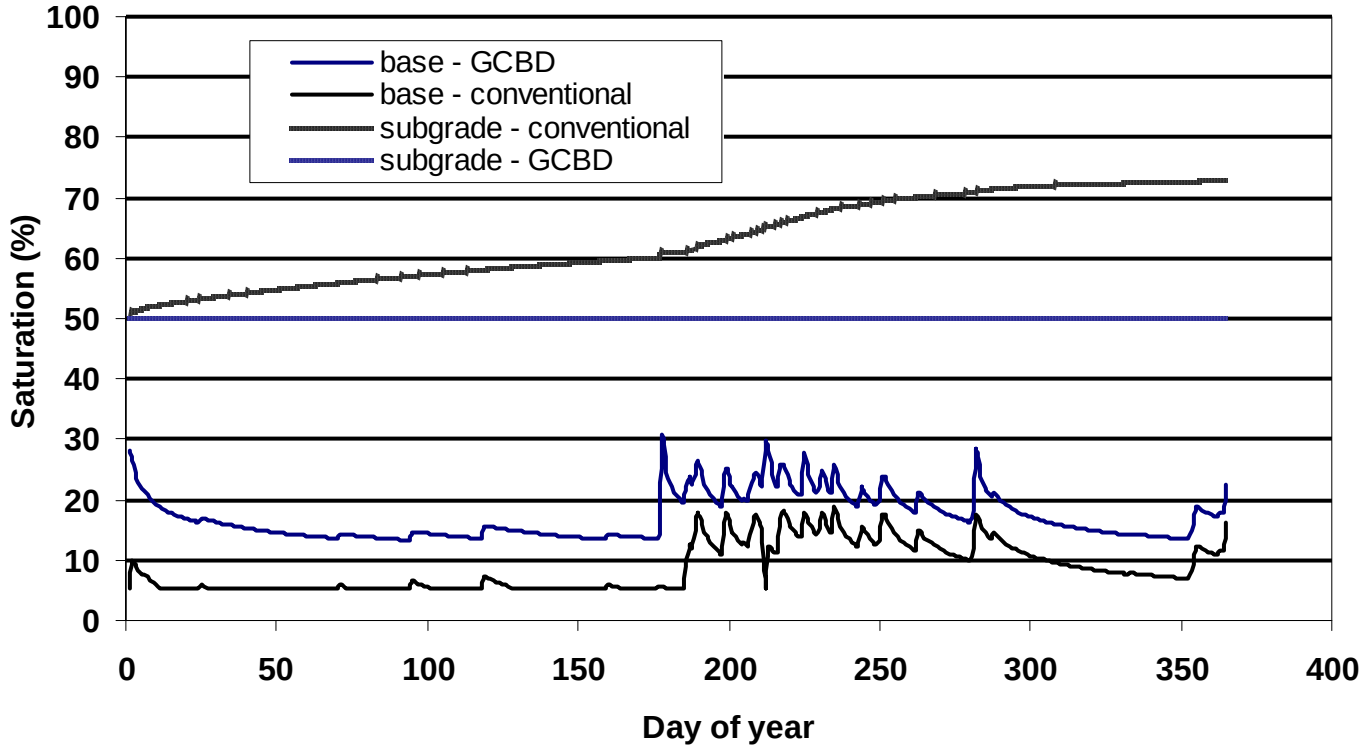

Figure 3.42 – Saturations of base course and subgrade for case with and without GCBD. Conditions: permeable base course 15 cm thick, 400 cm width, clay loam subgrade, and Albuquerque climate.

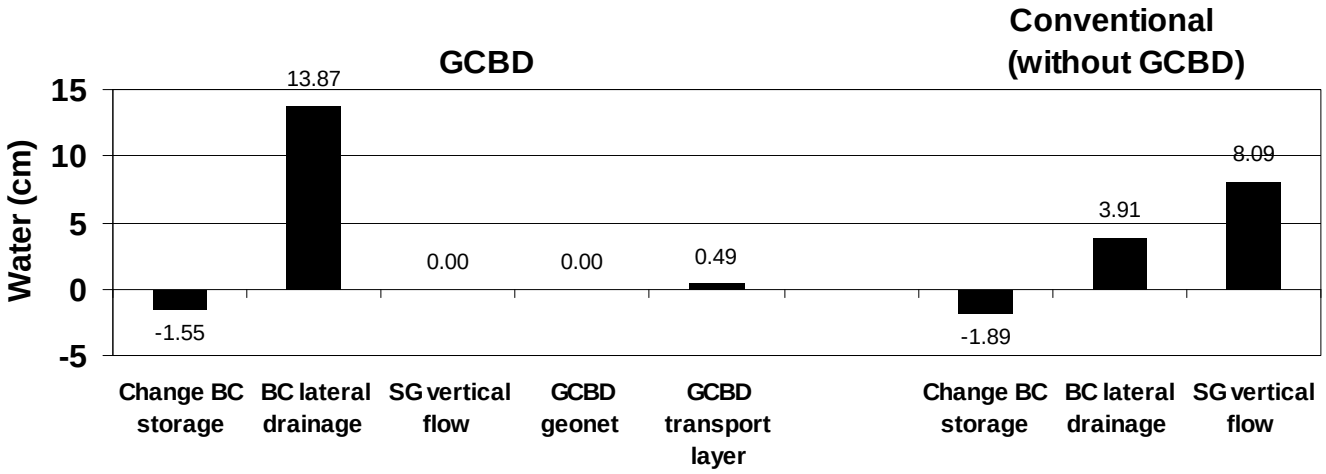

Figure 3.43– Annual water balance results. Conditions: permeable base course 15 cm thick, 400 cm width, clay loam subgrade, and Albuquerque climate.

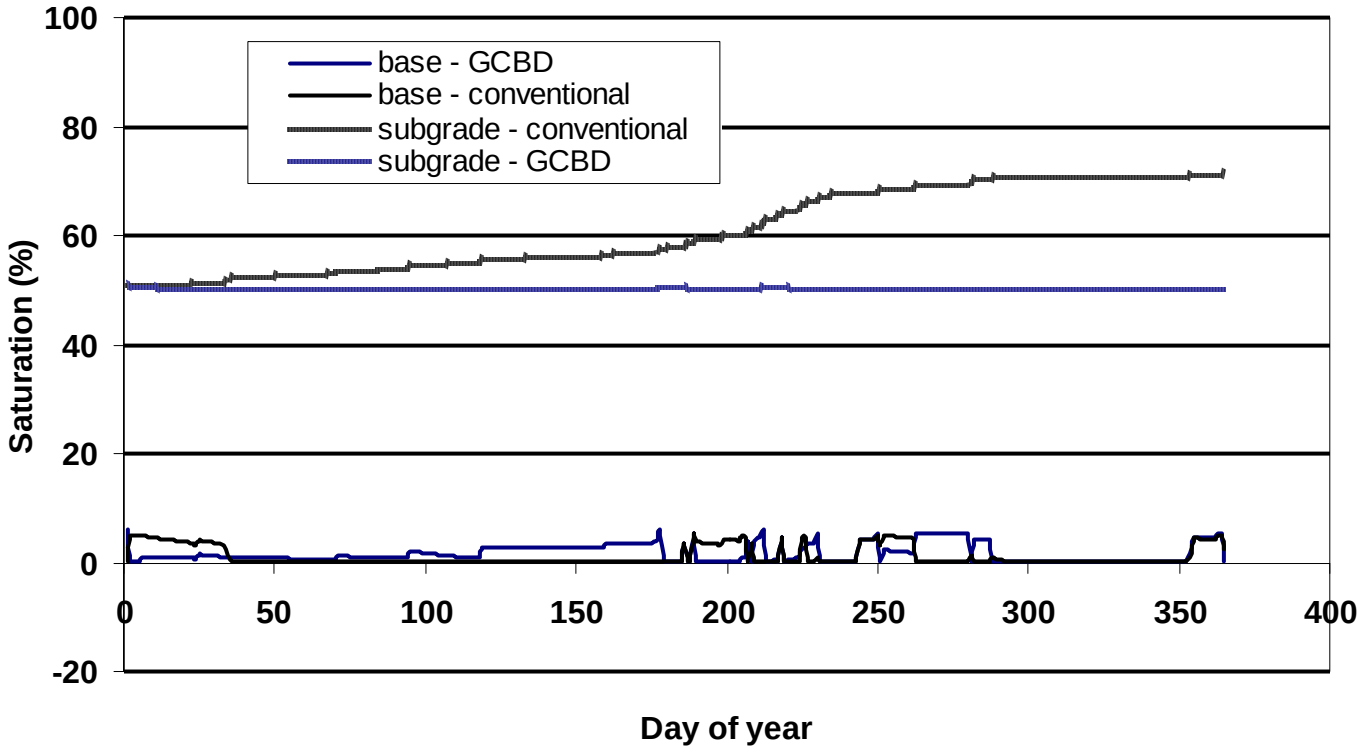

Figure 3.44 – Saturations of base course and subgrade for case with and without GCBD. Conditions: stone base course 15 cm thick, 400 cm width, clay loam subgrade, and Albuquerque climate.

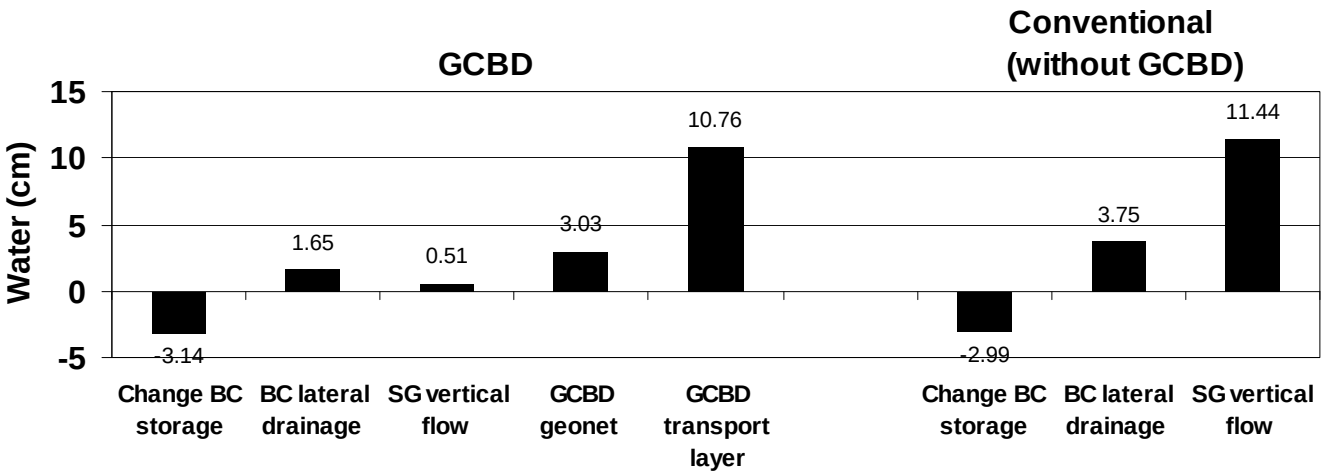

Figure 3.45 – Annual water balance results. Conditions: stone base course 15 cm thick, 400 cm width, clay loam subgrade, and Albuquerque climate.

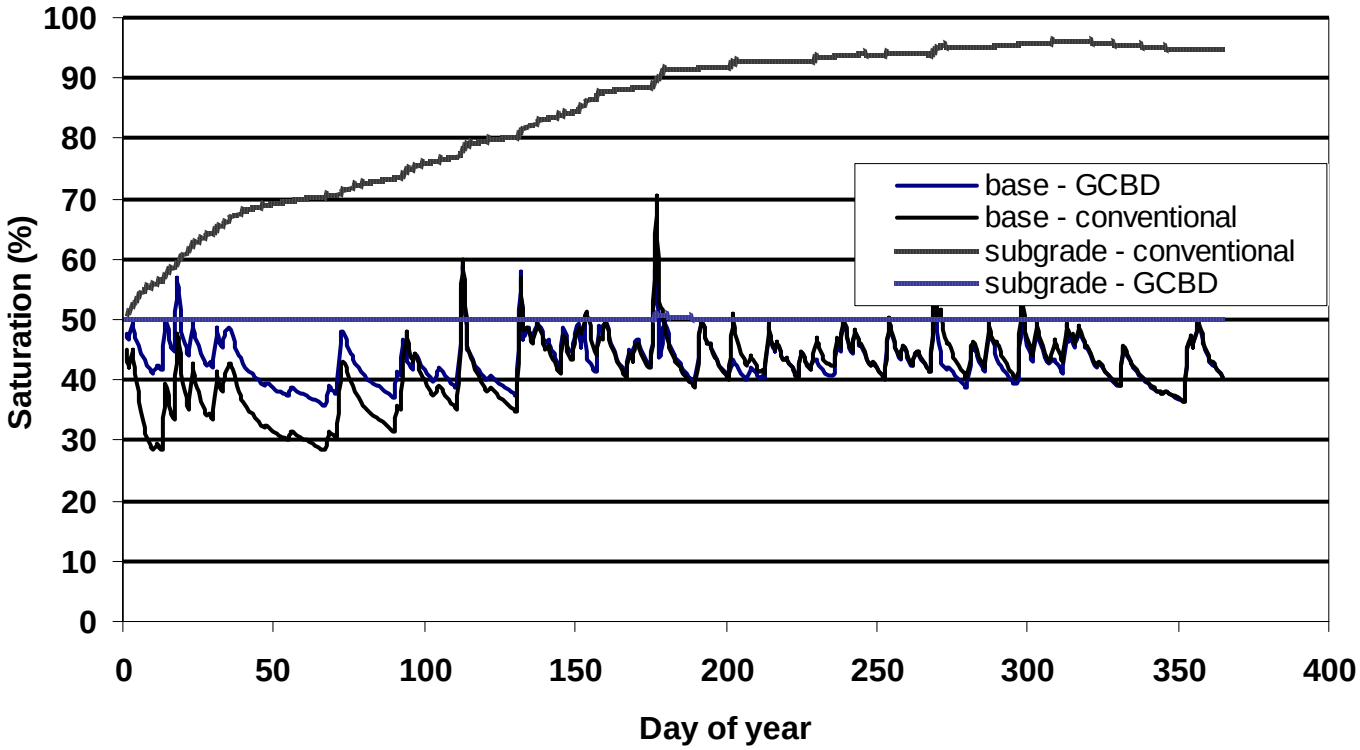

Figure 3.46 – Saturations of base course and subgrade for case with and without GCBD. Conditions: conventional base course 15 cm thick, 400 cm width, clay loam subgrade, and Albany climate.

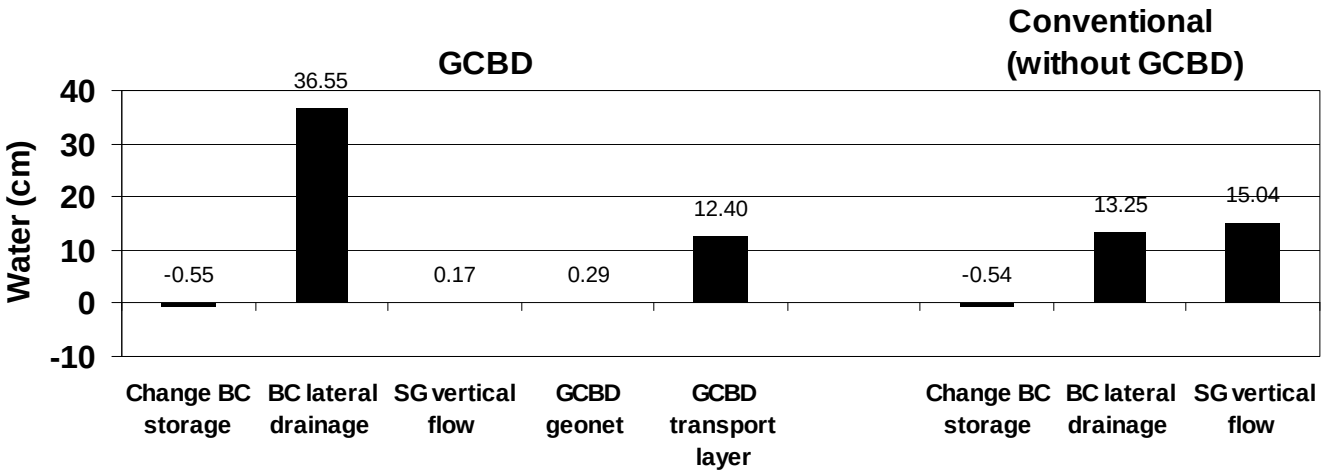

Figure 3.47 – Annual water balance results. Conditions: conventional base course 15 cm thick, 400 cm width, clay loam subgrade, and Albany climate.

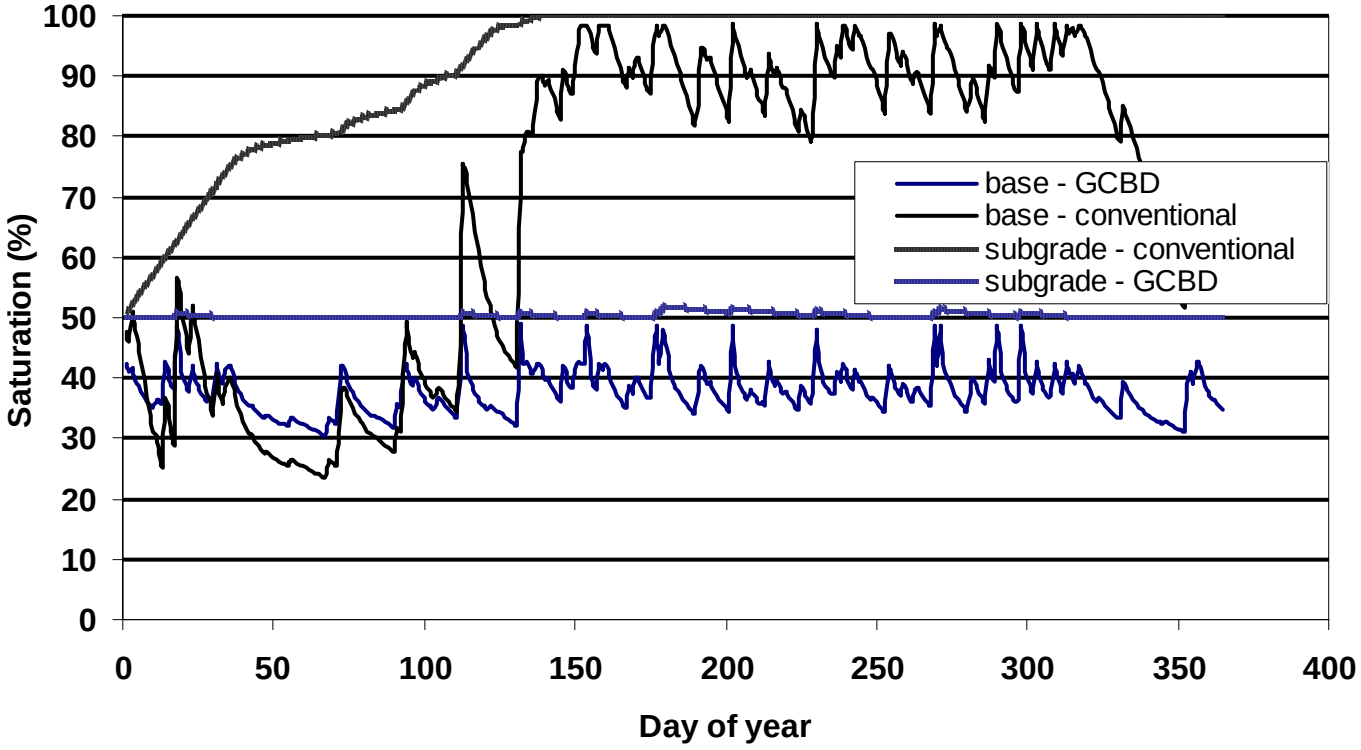

Figure 3.48 – Saturations of base course and subgrade for case with and without GCBD. Conditions: dense graded base course 15 cm thick, 400 cm width, clay loam subgrade, and Albany climate.

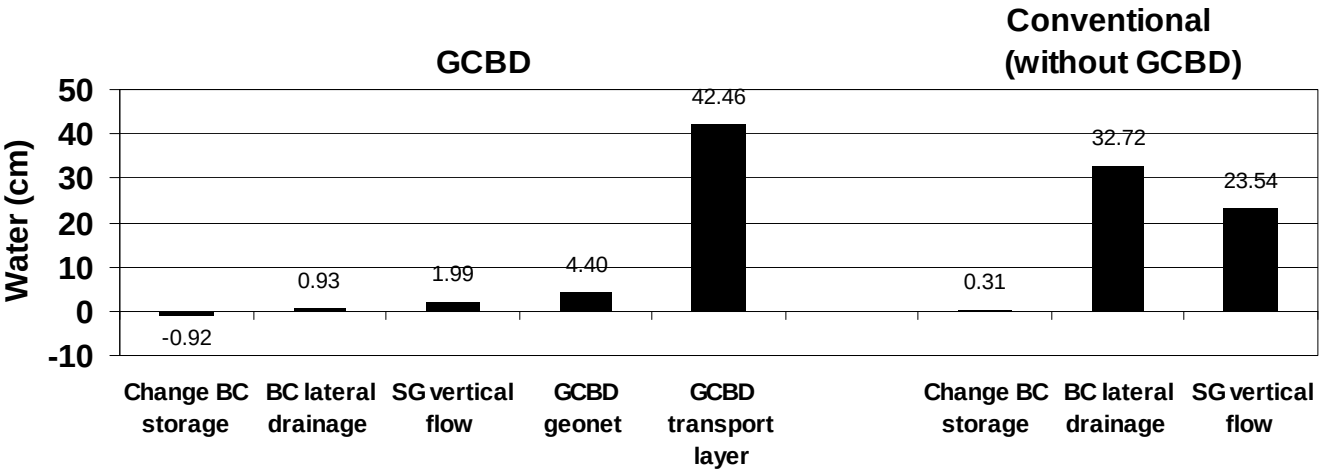

Figure 3.49 – Annual water balance results. Conditions: dense graded base course 15 cm thick, 400 cm width, clay loam subgrade, and Albany climate.

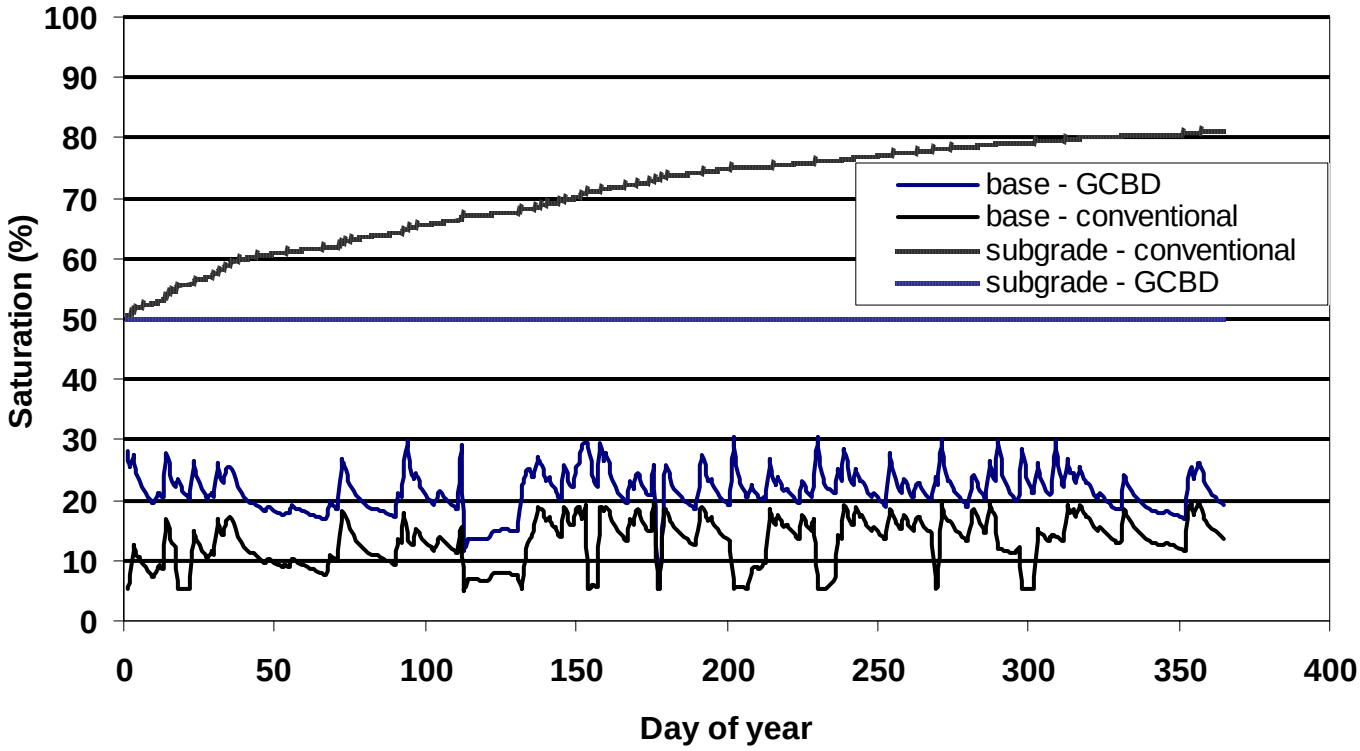

Figure 3.50 – Saturations of stone base course and subgrade for case with and without GCBD. Conditions: permeable base course 15 cm thick, 400 cm width, clay loam subgrade, and Albany climate.

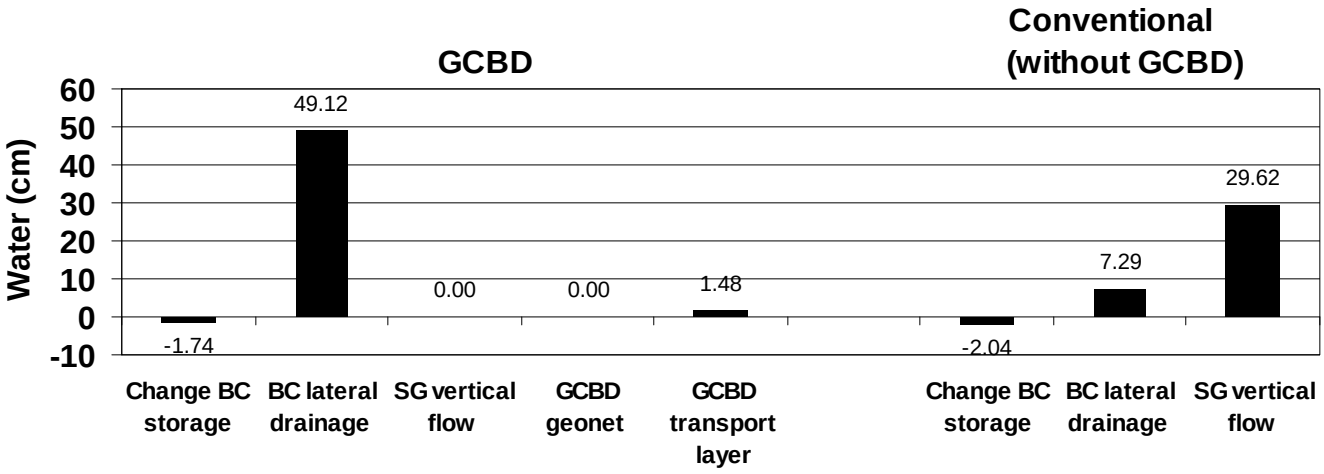

Figure 3.51 – Annual water balance results. Conditions: permeable base course 15 cm thick, 400 cm width, clay loam subgrade, and Albany climate.

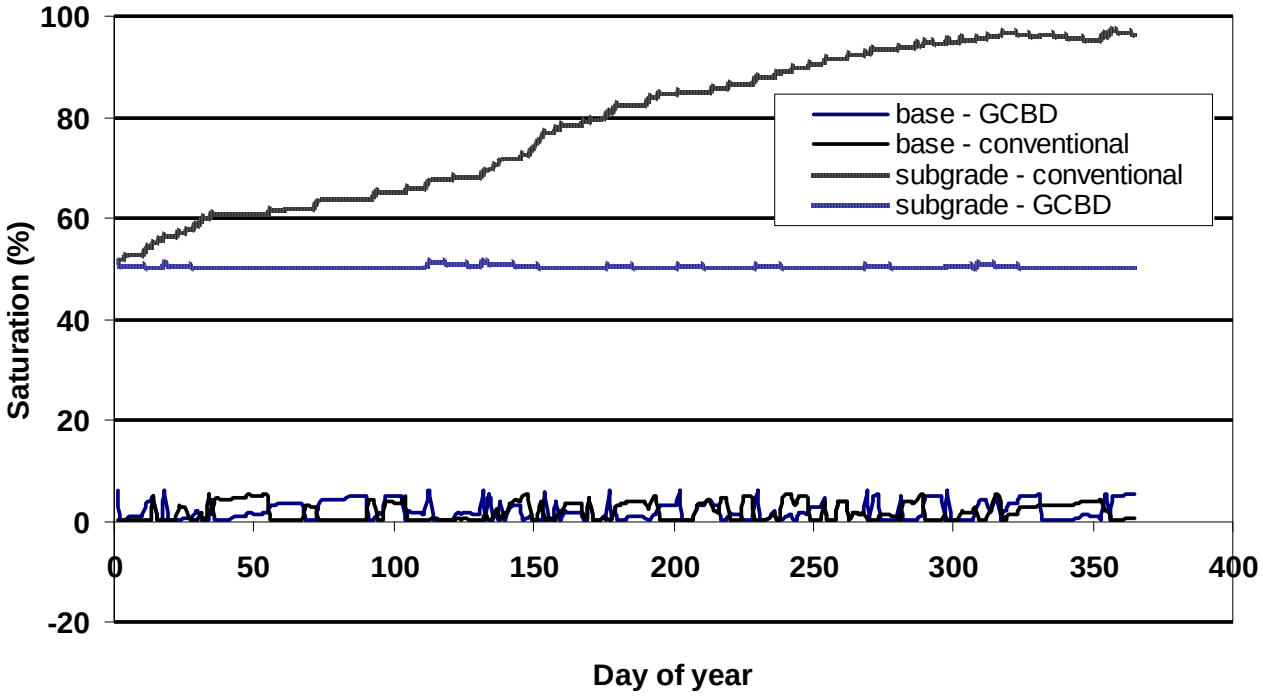

Figure 3.52 – Saturations of base course and subgrade for case with and without GCBD. Conditions: stone base course 15 cm thick, 400 cm width, clay loam subgrade, and Albany climate.

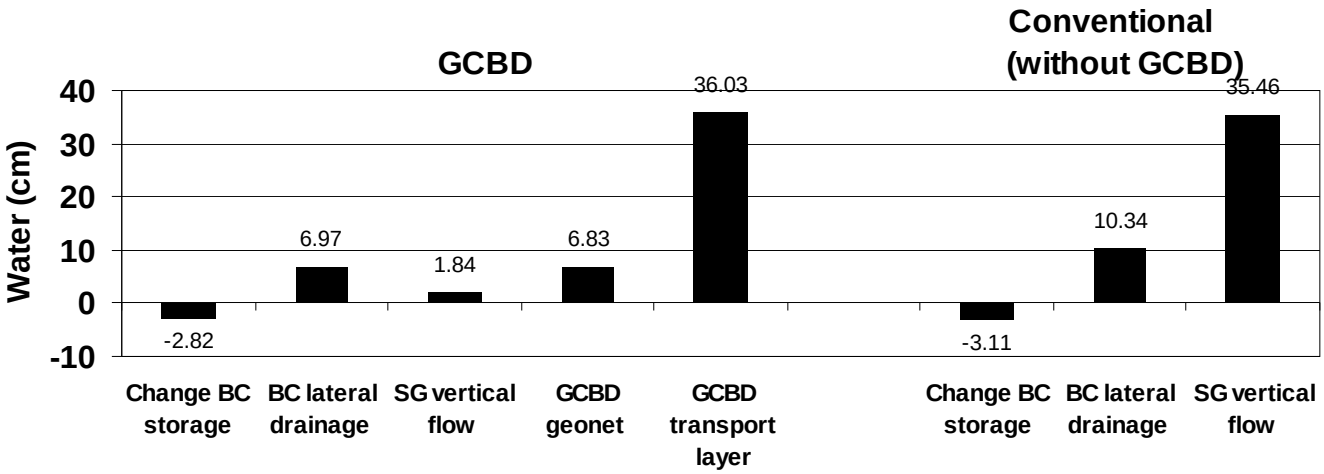

Figure 3.53 – Annual water balance results. Conditions: stone base course 15 cm thick, 400 cm width, clay loam subgrade, and Albany climate.

3.3 Upward and lateral flow

3.3.1 Upward flow

The GCBD serves as a capillary break, interrupting upward or lateral flow from the subgrade into the base course. Consequently, a base course that has a GCBD beneath it may have a lower saturation than a comparable configuration without a GCBD. The significance of the GCBD in terms of limiting upward flow is expected to be greatest in the presence of a shallow water table.

For the case with no GCBD, the amount of water in the base course is calculated assuming the base course is in hydraulic equilibrium with a water table. Assuming equilibrium allows the suction head to be determined - it is simply the distance above the water table. From its moisture characteristic curve, the water content and saturation of the base course can be estimated.

It is useful to compare the saturation of the base course with and without a GCBD. With a GCBD, the base course will be isolated from the water table, and the amount of water will be independent of the water table. The amount of water in the base course is estimated from the infiltration model. No precipitation is applied to the base course, rather, the base course and the GCBD are allowed to equilibrate for one year. In this way, any excess construction or initial water drains from the base course.

The difference in saturation with and without a GCBD for 3 base course materials is given in Figure 3.54. The base course layers are assumed to be 15 cm thick. Because a stone base course forms a capillary barrier comparable to that of the GCBD, no benefit is gained with a GCBD for this situation and thus the stone base course was not included in the calculations.

The capillary barrier effect of a GCBD for upward flow is significant when the water table is within 1 m. The increase in base saturation increases greatly as the depth to the water table decreases. When the water table is less than 50 cm, large differences in saturation are expected. Because the difference in saturation is principally a result of the moisture characteristic curve of the base course material, each base course material should be evaluated individually.

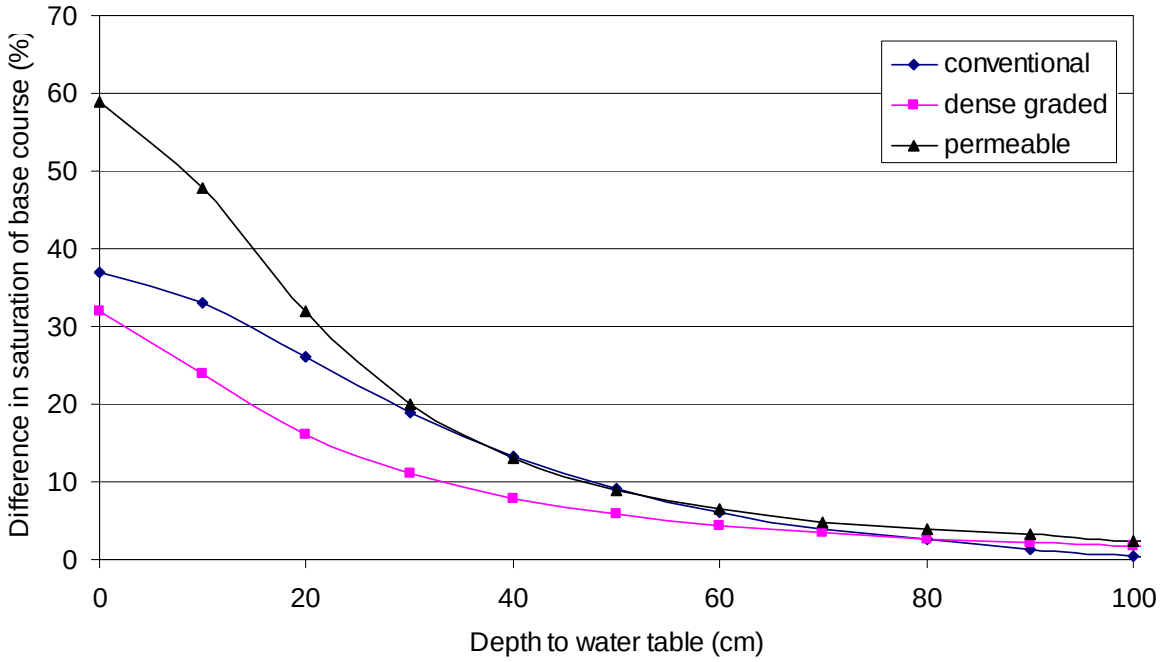

Figure 3.54 – Increase in base course saturation for pavement section without a GCBD compared to one with a GCBD.

3.3.2 Lateral flow

The capillary barrier effect also applies to limiting lateral flow into the base course. This scenario could be envisioned in response to a precipitation event where there is considerable infiltration in the adjacent native soils (Figure 3.55). Such infiltration may be increased from the contribution of pavement run-off. The protection the GCBD offers depends on the details of the infiltration event. The extreme case would be a large precipitation event in which the ground adjacent to the pavement gets very wet and approaches saturation. In this case, the difference in saturation of the base course due to the presence of the GCBD would correspond to the case of zero suction or zero water table depth.

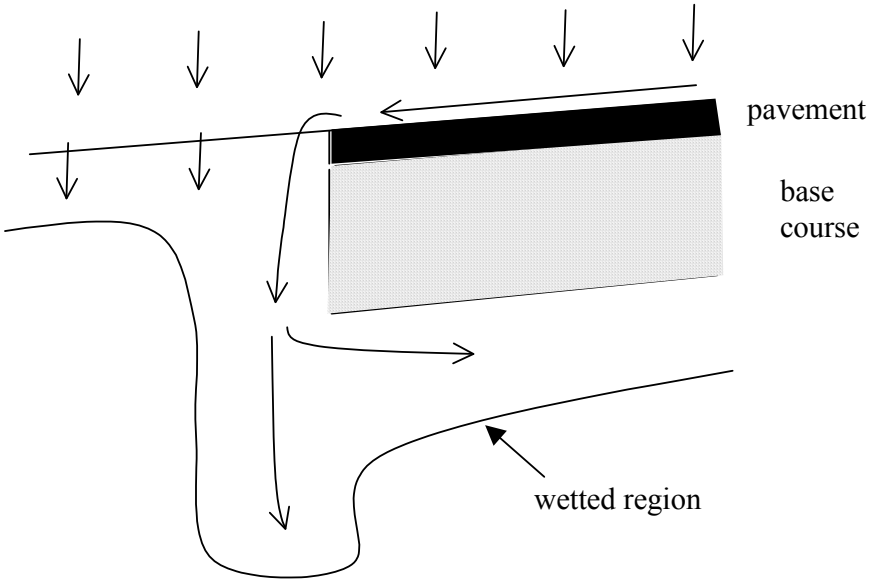

Figure 3.55 – Schematic illustration of wetting of soil adjacent to pavement section in response to precipitation and pavement run-off.

Although these results are based on very idealized and approximate conditions, they suggest that the GCBD may have a very significant impact on the saturation within a base course when the adjacent soil wets. With no barrier to unsaturated water movement, the base course will nearly saturate if it is exposed to and equilibrates with fully wetted soil. A GCBD will isolate the base course from the surrounding wet soil.

3.4 Summary

The design calculations indicate that less of the water that infiltrates through the pavement will reach the underlying subgrade soil if the pavement includes a GCBD at the bottom of the base course. This result is true for all base courses, climates, and subgrade soils that were considered in this study. The significance of less water in the subgrade depends on the strength and modulus reduction that the subgrade will experience due to an increased saturation.

For base course materials that are not good drainage materials, the GCBD will provide a drainage mechanism that can substantially limit the saturation of the base course. In this way, materials that are desirable for cost or availability considerations but do not drain well can be used in conjunction with a GCBD with a substantially increased performance as inferred by a lower saturation.

The GCBD limits base course saturation of the base course when there is a shallow water table. For water tables within 1 m of the base course, there is always less water in the base course with a GCBD compared to the case without a GCBD. This effect is diminished with the coarseness of the base course material. A base course may also be isolated from adjacent soil that wets due to infiltration. Including a GCBD in a pavement system will always result in less water in the base course compared to the case of without it.

A schematic that summarizes the applicability of the GCBD for different design conditions is shown in Figure 3.56.

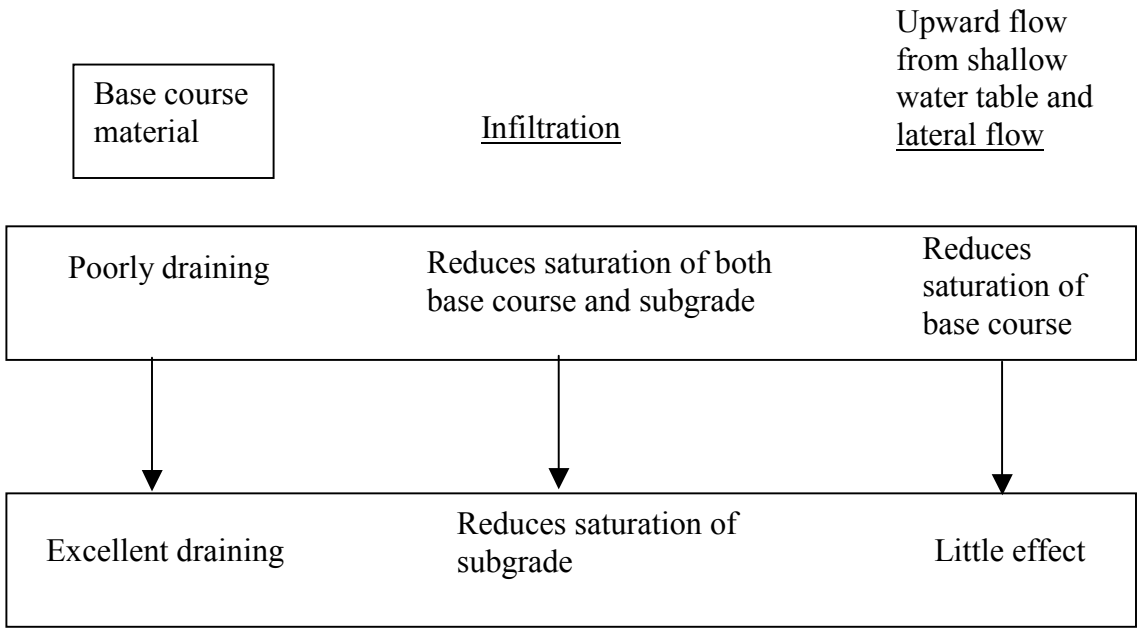

Figure 3.56 – Schematic of benefits of GCBD in pavement configuration as a function of the drainage characteristics of the base course.

4. Recommendations

The results of laboratory and field demonstrations indicate that the GCBD has provided the following benefits:

- Reduced equilibrium water content in base
- Prevent positive pressures in base
- Prevent wetting of underlying subgrade due to infiltration
- Prevent capillary rise of water from subgrade into base

Further, practical issues related to the contructability of the GCBD have been resolved, including how to tie the GCBD into a conventional edgedrain system.

The following efforts are recommended to continue the development of the GCBD toward full-scale commercial deployment:

- Continued monitoring of the MnROAD test cells will provide water content data that will allow ongoing evaluation of the GCBD performance to be estimated.

- Numerical modeling of GCBD performance. To date, sophisticated numerical models to predict the detailed response of the GCBD have not produced useful results due to numerical stability issues.

- Development of additional applications. There are other applications for use of the GCBD that can be developed, including retaining wall and foundation drainage.

- Presentation of results of laboratory, field and numerical studies at conferences.

- Pursue commercial development with manufacturers and distributions of geosynthetic products. There is serious interest in the technology, especially if a less costly alternative to the transport layer can be found.

References

Barna, L. A.; K.S. Henry, D. M. Solano Velez and J.C. Stormont (in review) "Estimating modulus values for layers in a flexible pavement incorporating Geocomposite Capillary Barrier Drain," Draft Report, Prepared for FHWA Pooled fund program Project TPF-5(126).

Elsayed, A. S. and Lindly, J.K. (1996) "Estimating permeability of untreated roadway bases." *Transp. Res. Rec. 1519*, TRB, National Research Council, Washington, D.C., 11-18.

Mallela, J., Titus-Glover, L. and Darter, M. (2000). "Considerations for Providing Subsurface Drainage in Jointed Concrete Pavements." *Transp. Res. Rec.1709,* TRB, National Research Council, Washington, D.C., 1-10.

Mallela, J., G. Larson, T. Wyatt, J. Hall and W. Barker (2002). *"User's Guide for Drainage Requirements for Pavements – DRIP 2.0 Microcomputer Program,"* Federal Highway Administration.

Mualem, Y. (1976). "A New Model for Predicting the Hydraulic Conductivity of Unsaturated Porous Media," *Water Resources Research*, Vol. 12, pp. 513-522.

Randolph, B.W., E. P. Steinhauser, E.P., Heydinger, A.G. and Gupta, J.D. (1996). "In Situ Tests for Hydraulic Conductivity of Drainable Bases," *Transp. Res. Rec. 1519*, TRB, National Research Council, Washington, D.C., 36 – 40.

Richardson, D. N. (1997). "Drainability Characteristics of Granular Pavement Base Material." *J. Transp. Engrg*., ASCE, 123(5), 385-392.

Ridgeway, H.H. (1982). "Pavement Subsurface Drainage System." *NCHRP Synthesis of Highway Practice 96*. TRB, National Research Council, Washington, D.C.

Stormont, J.C. (1995). "The Performance of Two Capillary Barriers During Constant Infiltration." *Geotech. Spec. Pub. No. 53: Landfill Closures*. ASCE, 77-92.

Stormont, J.C. and R. Ramos, (2004). "Characterization of a Fiberglass Geotextile for Unsaturated In-Plane Water Transport," *Geotechnical Testing Journal*, Vol. 27, No. 2, pp. 214-219.

Stormont, J.C. and S. Zhou (2005). "Impact of Unsaturated Flow on Pavement Edgedrain Performance," *J. Trans. Engng*., Vol. 131, No. 1, pp 46-53.

van Genuchten, M. Th. (1980). "A Closed –form Equation for Predicting the Hydraulic Conductivity of Unsaturated Soils." *Soil Sci. Soc.Am. J.,* 44, 892-899.

Level Survey Measurements for GCBD-IDEA Project conducted on MnRoad in Albertville, MN

Karen S. Henry, June, 2008

The level survey measurements reported below were taken at the locations indicated in Table 1.

Table 1. Frost pin location by station and cell number.

Station	Cell	Description	Frost Pin	Offset (m/ ft)
175+80	27	Control	2711	2.7/ 9.0
			2712	0.9/ 3.0
			2713*	0.0/ 0.0
			2714	-0.9/ -3.0
177+00	27	GCBD	2721	2.7/ 9.0
			2722	0.9/ 3.0
			2723*	0.0/ 0.0
			2724	-0.9/ -3.0
			2725	-2.7/ -9.0
178+30	27	GCBD	2731*	2.7/ 9.0
			2732*	0.9/ 3.0
			2733*	-0.9/ -3.0
			2734*	-2.7/ -9.0
179+80	27	GCBD	2741*	2.7/ 9.0
			2742*	0.9/ 3.0
			2743*	-0.9/ -3.0
			2744*	-2.7/ -9.0
181+51	28	Control	2811	2.7/ 9.0
			2812	0.9/ 3.0
			2813	-0.9/ -3.0
			2814	-2.7/ -9.0
182+51	28	Control	2821	2.7/ 9.0
			2822	0.9/ 3.0
			2823	-0.9/ -3.0
			2824	-2.7/ -9.0
183+51	28	Control	2831	2.7/ 9.0
			2832	0.9/ 3.0
			2833	-0.9/ -3.0
			2834	-2.7/ -9.0
184+51	28	Control	2841	2.7/ 9.0
			2842	0.9/ 3.0
			2843	-0.9/ -3.0
			2844	-2.7/ -9.0

* Indicates that no elevations were taken on 12/20/06.

The ‘frost pins’ installed in the pavement as points on which to take level survey measurements are fabricated from black rebar and are 16 mm (5/8 in.) in diameter and were 50 mm (2 in.) high prior to installation.

Figures 1-6 below show the elevation changes measured in 2006-07 winter for stations which had an initial elevation reading taken on 20 December 2006. On 20 December 2006, the subgrade was not frozen; however, it was frozen earlier in the month, with frost penetrating the subgrade between approximately 3 December and 14 December 2006.

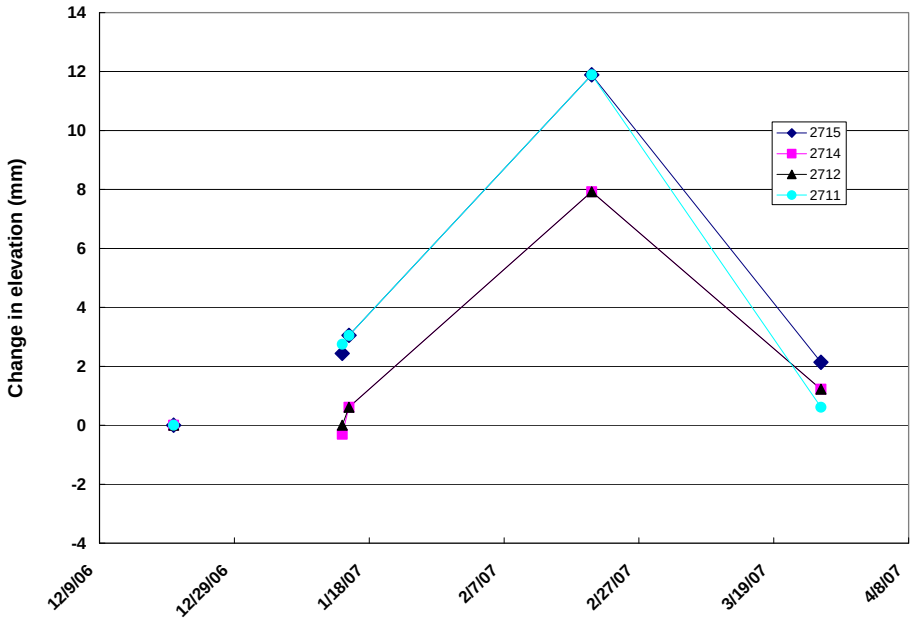

Figure 1. Elevations changes in 2006-07 according to level survey for frost pins located in Cell 27, Station 175+80. This isa control portion of Cell 27, with no GCBD (see Table 1 for offsets).

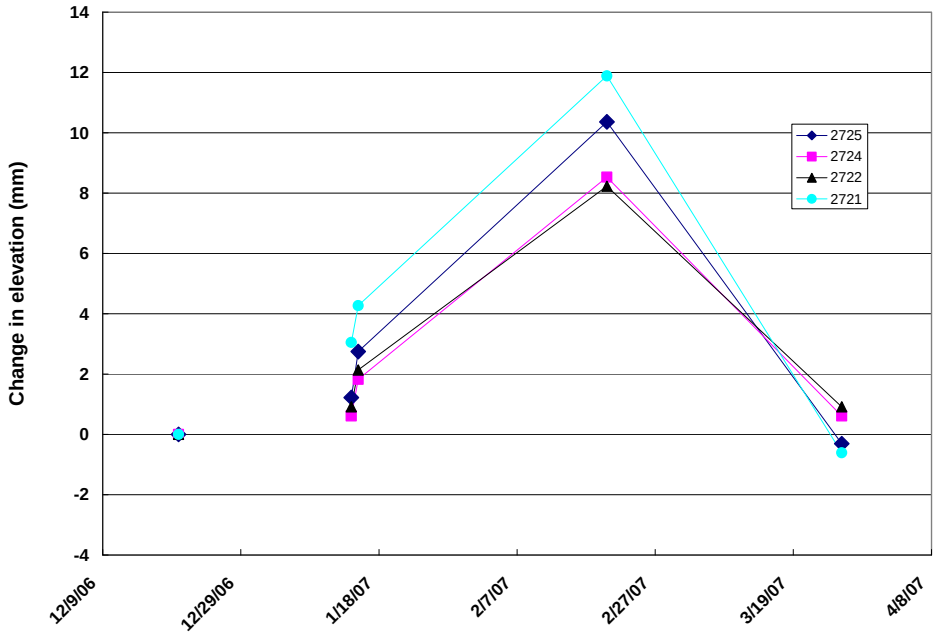

Figure 2. Elevations changes in 2006-07 according to level survey for frost pins located in Cell 27, Station 177+00. This is Cell 27, with GCBD (see Table 1 for offsets).

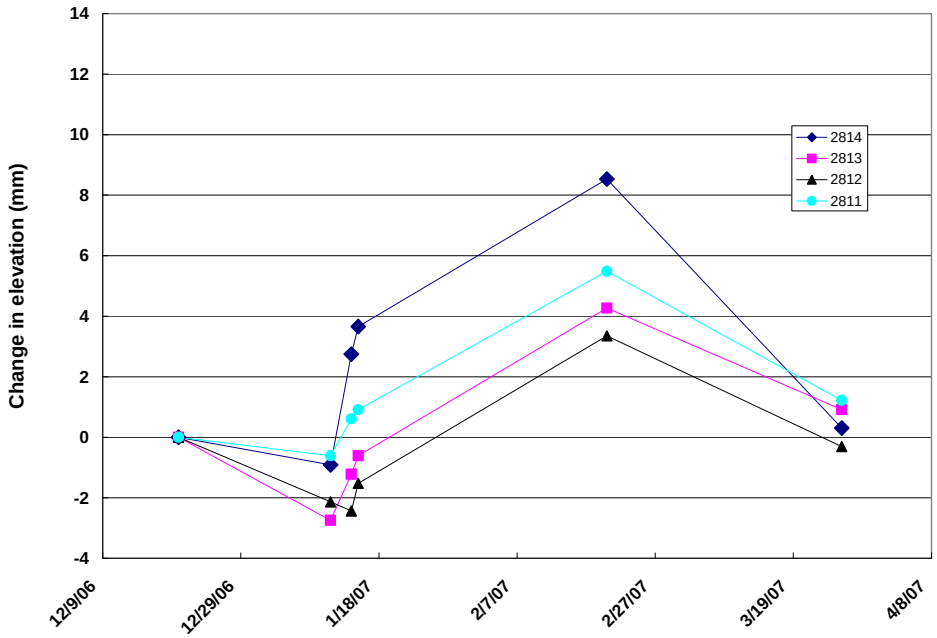

Figure 3. Elevations changes in 2006-07 according to level survey for frost pins located in Cell 28, Station 181+51. This is the control cell, with no GCBD (see Table 1 for offsets).

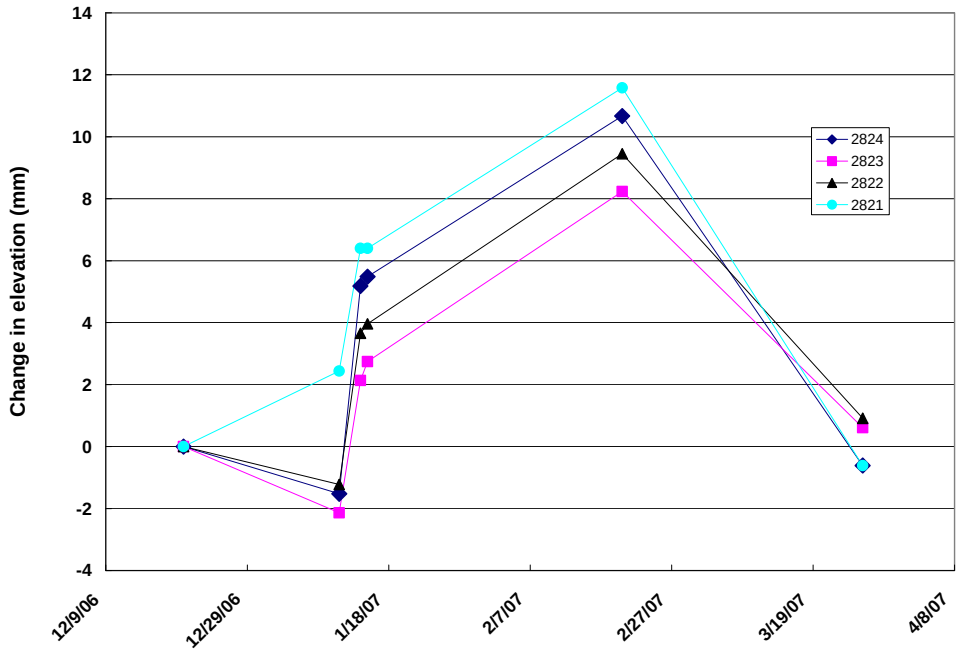

Figure 4. Elevations changes in 2006-07 according to level survey for frost pins located in Cell 28, Station 182+51. This is the control cell, with no GCBD (see Table 1 for offsets).

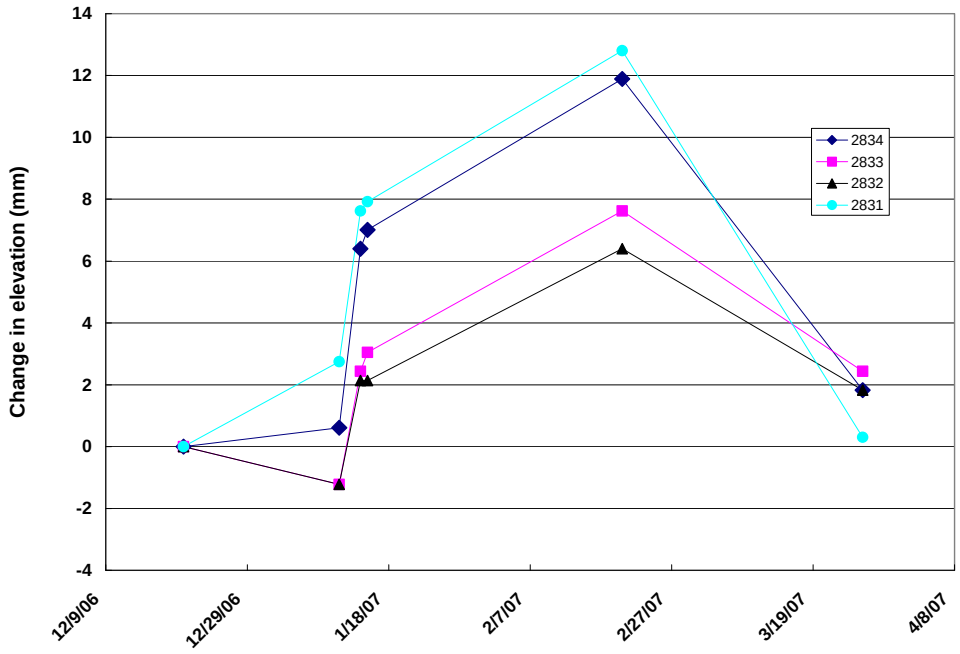

Figure 5. Elevations changes in 2006-07 according to level survey for frost pins located in Cell 28, Station 183+51. This is the control cell, with no GCBD (see Table 1 for offsets).

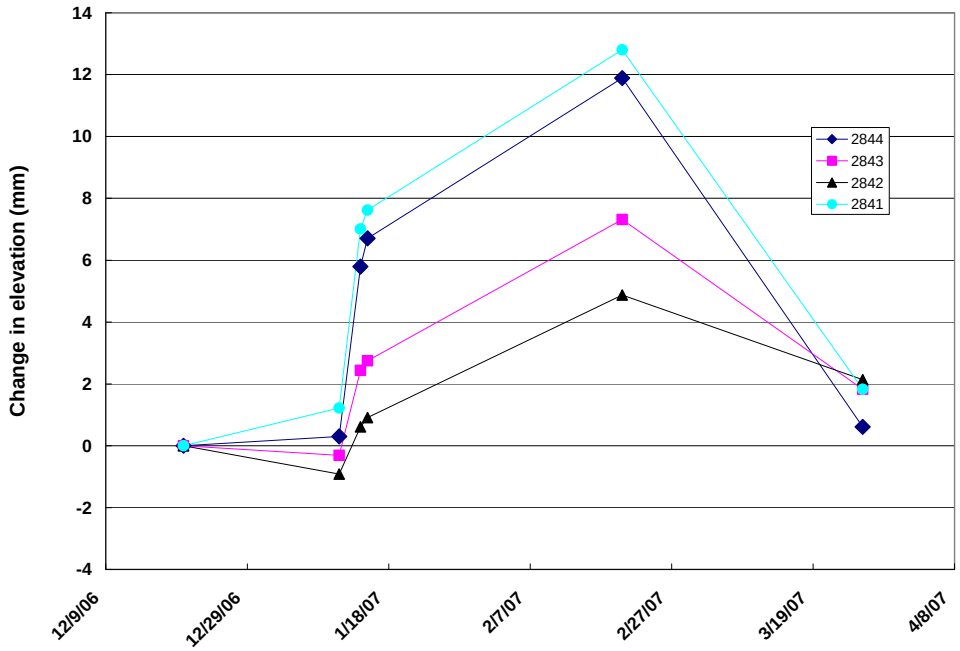

Figure 6. Elevations changes in 2006-07 according to level survey for frost pins located in Cell 28, Station 184+51. This is the control cell, with no GCBD (see Table 1 for offsets).